THE EFFECT OF ENVIRONMENT ON CORROSION KINETICS WITH PARTICULAR REFERENCE TO TEMPERATURE AND PRESSURE

Submitted for the degree of

Ph.D. in The University of London

by

MUHAMMAD ZAFAR ULLAH

Department of Metallurgy

Royal School of Mines

Imperial College of Science and Technology

London

1968

ABSTRACT

The aqueous corrosion of zirconium has been studied as a function of various environmental conditions, e.g. temperature, pressure, hydrogen activity and the solution pH. An autoclave was designed to permit measurements at temperatures above 100°C, and an optical method was used for recording the rate of corrosion. The experimental technique not only permitted control of various test conditions but allowed rates to be measured continuously during the reaction without removal of the specimen from its environment.

The results of the present investigation emphasise the importance of the protective oxide film formed during corrosion. It has been shown that hydrogen in some circumstances greatly increases the corrosion rate and this is attributed to enhanced electronic conductivity and consequently, in turn, to increased diffusion rates in the oxide. The results have also shown that, if the growth of a film can be characterized by a sequence of rate laws, then the exponents calculated for all but the initial law will be liable to error unless the effect of the transition point co-ordinates is taken into consideration when interpreting data.

CONTENTS

INTRODUCTORY REMARKS

Corrosion may be defined as the reaction of a metal with its environment and, therefore, a study of the effects of various environmental conditions on the corrosion behaviour of a metal is very important. The majority of metals react spontaneously with oxygen-containing species in gaseous or aqueous environments and the slow oxidation of some of the metals is due to the formation of papyraceous films which shield the metal and reduce the rate of further attack. Under these circumstances, therefore, the rate of the corrosion reaction would decrease and it is generally accepted that the diffusion of ions through this protective layer is the rate controlling factor.

The development of nuclear technology in the last two decades has brought about a great deal of research to establish the corrosion character of zirconium because of its usefulness as a structural material in this industry. One of the corrosion products, hydrogen, is known to have a major effect in increasing the corrosion rate of oxide-covered metals and, therefore, the role of hydrogen in changing the properties of corrosion oxide of zirconium has been considered. Zirconium absorbs hydrogen and it has been found that, under certain conditions, hydrogen content in zirconium as little as 25 ppm can cause serious embrittlement and, hence, mechanical failure of the metal. The higher corrosion rates resulting from the drastic conditions of service increase this problem and, therefore, an investigation of the effects of hydrogen

on corrosion rate bears direct relationship with the practical problems encountered in industry.

In order to extrapolate from the conditions of the research programme to industrial conditions, the kinetic data and laws must be established. The method of plotting the results which appeared most frequently in the literature can lead to different characterization and an improved method is required which will eliminate some of the uncertainties.

The scheme adopted in presentation of this thesis is that the first chapter includes a brief description of electrochemical kinetics and thermodynamics; detailed derivations appear in appendices. In the second chapter the laws of kinetics of oxidation with kinetics of zirconium are considered, while the third chapter deals with the method of rate measurements in which the basic principle of various methods are considered with relative advantages and disadvantages. The chapters four, five and six are respectively concerned with the experimental technique, the results and the discussion of these results.

CHAPTER 1

ELECTRODE PROCESSES

When a metal is immersed in an electrolyte, an equilibrium tends to be established in which a steady difference of electric potential exists across the region of the interface between metal and solution. This equilibrium electrode potential arises because the atoms of the metal ionize until the displacement of the electric charges produced exactly balances the tendency for more metallic atoms to ionize. The solution acts as the medium for the equilibrium reaction

$$M \rightleftharpoons M^{+z} + Ze \qquad (1)$$

Since the system involves the transfer of charge, the reaction, therefore, is electrochemical in nature. There are two different approaches to electrochemical reactions, i.e. the thermodynamic and the kinetic. The electrochemical thermodynamics is concerned with the behaviour and the magnitude of these equilibrium potential differences in analogy to the chemical equilibrium in reactions of purely chemical nature, whereas the electrochemical kinetics explain the individual processes and their rates in analogy to chemical reaction kinetics. The word "potential" used here has the same connotation as "tension" recommended by Commission No. 2 of the International Committee for Electrochemical Thermodynamics and Kinetics (CITCE); but the word potential has been used here because of the popularity of the conventional terminology in the English

speaking countries. Detailed electrochemical derivations based on the CITCE nomenclature have been given by Rysselberghe. (1)

From electrochemical thermodynamics one may derive Pourbaix diagrams which are qualitatively considered here. Fig. (1) shows a typical diagram which particularly refers to pure iron in contact with water at 25°C, and it describes the most stable phases for this system under equilibrium conditions for given values of electrode potential and of solution pH. The terms corrosion, immunity and passivity used in this diagram have precise definition (2) which are as follows:

Corrosion: The reaction of a metal with its non-metallic environment that results in the continuing destruction of metal.

Immunity: The state of a metal in which corrosion is thermodynamically impossible in a particular environment.

Passivity: The state of metal in which corrosion in a particular environment is much reduced by modification of its surface, for instance, by the formation of a thin protective layer of oxide.

Some quantitative measure is required to be taken as the specific amount of reaction that will be considered to be corrosion. Any smaller extent of reaction will then be considered to be the absence of corrosion, i.e. immunity. This critical amount of reaction for these definitions is chosen to be a concentration of reaction product equal to 10^{-6} moles per litre, indeed, a negligible value for practical purposes. Consider, for example, the reaction of iron with water according to the equation

$$Fe \longrightarrow Fe^{++} + 2\bar{e}$$

the corrosion of iron would be assessed on the concentration (Fe^{++}) of Fe^{++} ions in the solution after the reaction had come to equilibrium. Fig. (1) shows that, for acidic solutions, at a value of $(Fe^{++}) = 10^{-6}$ is obtained only when the electrode potential is - 0.62 volt. In practice, this is achieved by applying ~~the~~ a negative potential to iron. With increase in negative potential the concentration of ferrous ions would decrease, but with decrease in negative potential, the equilibrium value of (Fe^{++}) would increase rapidly. The region of the diagram where the concentration of ferrous ions is greater than 10^{-6} is, therefore, the region of corrosion.

When the point determined by the conditions of solution pH and electrode potential is such that it lies in the immunity region, it is certain (thermodynamically) that the metal cannot corrode dangerously because at equilibrium the concentration of the corrosion product will be negligible. Similarly, if the point describing the pH potential conditions lies in the corrosion region, corrosion will occur. The region labelled passivity, however, needs some special interpretations because here the metal is envisaged as being put into a relatively unresponsive state as a result of the formation of solid protective layer of oxidation product, Fe_2O_3 in this case.

The regions labelled as corrosion, immunity and passivity have been summed up by Evans (3) as the regions in which corrosion

"can, cannot and does not" occur respectively. The diagram gives a panoramic view of various reaction possibilities predicted on a thermodynamic basis. In view of the important information obtainable from such diagrams, the construction of Pourbaix diagram is described at greater length in App. I. A brief discourse of uses and limitations of these diagrams is given below:

(1) It is possible to predict the corrosion behaviour of metals under various conditions of solution pH and potential. Conversely, a knowledge of the corrosion characteristics can be used in controlling corrosion, e.g. by applying a negative potential, the system can be moved into the domain of immunity. An alternative means of corrosion control is anodic protection and consists of applying the potential in a direction to cause the system to move into the region of passivity. (2) When an effective inhibitor is added to a solution, it reacts in a way such that the thermodynamic boundaries of the passivity domain are broadened but the modified situation can be equally well predicted (not shown in diagram). (3) Apart from the obvious uses of Pourbaix diagrams in the electrochemical field, these diagrams have also been found useful in geochemical work (4). The limitations are (a) the diagrams represent thermodynamic information about the equilibrium between the metal and its environment whereas the practical corrosion problems, however, often shown considerable deviation from equilibrium; (b) the diagrams represent the pure systems and not their alloys;

(c) Since the passivity of the metals depends on the protective property of film which is itself dependent on its composition. Any change in the surface film will, therefore, change the thermodynamic domain of stability and consequently, the theoretical prediction will not be possible. Also it is not possible to show whether passivity will practically occur because of the nature of the corrosion product which may not form a continuous surface film; (d) Information on the corrosion rate is not given by the diagrams. Decreases in the corrosion rate, e.g. parabolic law would not be predictable from these diagrams. It has been reported previously and also supported by present work that, under certain circumstances, the corrosion rate increases with increase in negative potential. This is contradictory to the basic postulates of electrochemical thermodynamics because the effect is brought about by influencing the kinetic processes. Therefore, for the comprehensive understanding of the electrode processes, the principles of electrochemical thermodynamics and kinetics should be applied in conjunction with each other.

Consider, then, eq. (1) again representing a reaction in reversible equilibrium. It may be noted that, in principle, no equilibrium can be measured to be thermodynamically reversible because the application of an external device can only measure the reaction current which would, then be disturbed from its equilibrium value.

As mentioned before, the development of an electrochemical

potential difference between two phases requires the movement of electrically charged species, ions or electrons, in either direction. When the equilibrium potential has been reached, the reaction apparently ceases macroscopically. However, considered kinetically, the forward rate does not become zero when equilibrium potential is reached, but is compensated by the reverse reaction of identical rate. From the molecular point of view, there is a constant exchange in both directions, even though the reaction has macroscopically come to a complete standstill at the equilibrium potential.

The charge transfer takes place by the simultaneous transport of species through the electrical double layer in both directions. This is briefly considered here; a detailed review of the theory of double layer is given by Grahame (5). In order to develop the potential difference, one phase must carry a positive charge and the other phase a negative charge at the phase boundary, as with the plates of a charged condenser. At the phase boundary, the positively and negatively charged layers appear at a certain distance from each other, and together form the electrical double layer. This definition of the double layer was given by Helmholtz (cf. Ref. No. 5).

Guy and also Chapman (Ref. No. 5) extended this idea by showing that the solution side of the Helmholtz double layer would attract unlike charges causing a more extensive disturbance of the charge distribution, with the result that the compact double

layer would be destroyed. They therefore suggested that the solution side of the double layer has a diffuse structure in which there would be a non-linear fall in potential away from the interface. However, it was found that by applying the Gouy-Chapman theory, the calculated variation in the double layer capacity with concentration is much greater than is observed. Stern (cf. Ref. No. 5) has further analysed these theories and has shown that the ionic adsorption could play an important role at the interface. Accordingly, he has shown that the potential gradient in the entire double layer is generally composed of a large component in the compact double layer (Helmholtz layer) and a component in diffuse layer (Gouy-Chapman layer).

After considering the mechanism of potential formation, it is relevant to study the effect of various conditions on the development of associated potentials. Consider, then the application of an external current on the reversible system represented by example (1). The equilibrium will be disturbed and a net reaction in the direction which will sustain this current will take place. Accordingly, the equilibrium potential will change, and this change is called the overpotential and the system is said to have undergone polarization. The equations relating to the overpotential and current were originally given by Julius Tafel (6) who theoretically derived them by assuming the transfer co-efficient as two (cf. App. II) for the case of rate control by hydrogen atom recombination (see below). However, a more

rigorous theoretical derivation in accordance with the practically observed value of the transfer co-efficient as 0.5 has been attributed to Erdey-Gruz and Volmer (7). Horiuti and Ikusima (8) have derived similar relationships by assuming that an elementary system, a set of elementary particles involved in elementary reaction, at the critical state of transition, is charged. They have shown that the transfer co-efficient is 0.56 for the higher negative polarization.

In view of the importance of the potential-current relationships in understanding and interpreting the phenomena associated with the electrochemical kinetics, it is considered necessary to include an "ab initio" derivation of Tafel equation in App. II and a critical appraisal of the salient points in Discussion.

Consider some of the main accepted causes of irreversibility which were first systematically reported by Bowden and Agar (9,10). When a dissolved ion reaches the electrode surface, it will be evolved as an atom or a molecule after undergoing complete discharge. The overall reaction may take place in several steps, each requiring a definite activation energy but the reaction requiring the highest energy of activation (the slowest reaction) will be ~~the~~ rate controlling. The type of overpotential arising from the sluggish reaction and requiring high activation energy is called Activation Overpotential. The overpotential of hydrogen and oxygen are of this type. The various stages in the evolution of hydrogen are briefly given (11) here without considering the

mechanistic details.

$$(H_3O^+)_B \xrightarrow[\text{Convection}\ \text{Diffusion}]{\text{Migration}} (H_3^+O)_E$$

Hydrated ion in Bulk of Soln

Hydrated ion at electrode surface

$$(H_3O^+)_E + e \xrightarrow[\text{Dehydration}]{\text{Discharge}} M\text{–}H$$

electron from Metal M

H atom adsorbed on Metal M.

$$2MH \xrightarrow{\text{Combination}} H_2$$

$$MH + (H_3O^+)_E + e \xrightarrow[\text{Discharge}]{\text{Secondary}} H_2$$

According to this scheme, therefore, the hydrated ions first arrive at the electrode surface, then undergo discharge and adsorption before molecular evolution takes place.

Another major cause of irreversibility is due to concentration polarization; an expression introduced by Bowden and Agar (9, 10) and is briefly explained here. When a discharge reaction takes place at the surface of an electrode, the ionic concentration in the immediate vicinity of the electrode must fall to accomplish this reaction. The ionic concentration in the bulk of the electrolyte does not appreciably change and, in fact, it is assumed to remain constant. If, now, the rate of replenishment of ions which undergo discharge is equal to the discharge rate, then, the reaction will continue indefinitely. In practice, however, it has been noted at higher currents, i.e. at discharge rates

higher than the rates at which the ions are brought at the surface of the electrode, the potential of the electrode changes and is called the concentration overpotential. The cause of such a potential is the concentration gradient near the electrode surface due to higher discharge rate. When steady state is reached, a dynamic equilibrium between the ionic transport and the ionic discharge would exist. Three important processes, in this connection, have been considered (9, 10).

(1) Migration: The process of the movement of ions towards the electrode surface under the influence of an electric field. It may be pointed out here that any environmental variation, such as stirring, etc., would not influence the actual charge transfer reaction and, therefore, the relationship of migration process with concentration overpotential appears not to be completely clear.

(2) Convection: The process of bulk movement of the electrolyte containing the dischargeable ions. This can either be caused externally by mechanical stirring or by the self-generated convective currents due to the differential changes in density at various points in the solution.

(3) Diffusion: The most important phenomenon causing concentration overpotential is the diffusion process and this is considered at some length here. Agar and Bowden (10) supposed that the electrode surface is covered by a "diffusion layer" of thickness δ. Outside this layer, the concentration is constant,

and is that of the bulk of the solution. They assumed that convection is negligible inside the layer, and that the reactant is supplied to the electrode by diffusion (and migration) alone.

However, a certain concentration equalization will always occur by convection in the outer layer of this diffusion layer. Thus, the concept of a liquid which is stationary through a thickness δ, which abruptly and discontinuously becomes an electrolyte having a certain movement by convection, outside this layer constitutes a gross simplification. Fortunately, however, experiments have demonstrated that such a concept serves well for calculations. Theoretically a sharp delineation between a static diffusion layer and the stirred electrolyte solution cannot occur, since finite viscosity always causes a finite gradient of flow rate. Therefore, the transition between the mass transport by diffusion in the interior of the diffusion layer and by convection in the stirred electrolyte solution cannot be sharp. Rather there exists an overlapping of both types of transport in the outer areas of the diffusion layer.

The actual variation of concentration as a function of the disturbance from the surface, therefore, cannot be represented by a straight line but by a curved line. From the linear extrapolation of the concentration in the interior of the diffusion layer and that of the main bulk of the solution would, thus, give an intersection at the interface of an ideal boundary layer.

The solution agitation would, therefore, affect the thickness of the diffusion layer depending upon whether it is low (stream line or laminar conditions) or high disturbance (turbulent conditions). Detailed analysis of the hydrodynamics of mass transfer is given by Eckert (12).

The third major cause of electrode irreversibility is the Resistance Overpotential which is due to the ohmic drop within the electrolyte and in surface films during current flow. Also the measured magnitude of the resistance overpotential depends on the experimental set-up, i.e. the distance of the reference electrode from the test specimen. When all these causes are contributing to the irreversible reaction, the Total Overpotential is equal to

= Activation Op. + Concentration Op + Resistance Op.

(Op = overpotential)

These somewhat simple but self consistent concepts of electrode processes expounded some thirty years ago by Agar and Bowden are satisfactory for the schematic understanding of the corrosion problem. More recent developments in this field are reported by Bockris (13) who has also given the controversal theories of Rysselberghe (1b.).

An electrochemical reaction can only be accomplished by the transference of electric charge. It is relevant, therefore, to consider the reactions in which electrons are involved. It may be noticed that there are only two possible reactions of this

nature: (1) the reactions in which electrons are produced; these are called anodic or oxidation reactions, and (2) the reactions in which electrons are consumed, these are called cathodic or reduction reactions. A few examples of these reactions are given below:

Anodic Reactions: (1) The metallic dissolution is an anodic reaction, e.g.

$$M \longrightarrow M^{+z} + Ze$$

(2) The anodic oxygen evolution is another important example and can be represented by the two different reactions

(i) $2H_2O \longrightarrow O_2 + 4H^+ + 4e$

(ii) $4OH^- \longrightarrow 2H_2O + O_2 + 4e$

However, the actual mechanism of the intermediate stages of these overall reactions are not defined by these equations. The anodic reactions are of great importance in industry and these processes either depend on the discharge of ions at inert anode, e.g. the production of gases like chlorine, oxygen, etc. or the actual dissolution of the anode for recovering precious metals from scrap.

Cathodic Reactions: (1) Any process associated with metallic deposition is a cathodic reaction.

$$M^{+z} + Ze \longrightarrow M$$

(2) The hydrogen evolution is an important reaction.

$$2H^+ + 2e \longrightarrow H_2$$

The intermediate stages of this overall reaction have already been considered. For corrosion to occur spontaneously the electrons produced in the anodic reaction must be absorbed by a cathodic reaction. The most common cathodic reaction leading to metallic corrosion is the reduction of dissolved oxygen as

$$O_2 + 2H_2O + 4\bar{e} \longrightarrow 4\bar{O}H$$

The cathodic reactions are immensely important in industry and these principles are applied in many processes, e.g. (1) electroplating of metals, (2) electrowining of metals, (3) electrorefining of these metals, (4) electroforming and electrotyping, (5) production of metallic powder, (6) electrolysis of fused salts, (7) electrocleaning, (8) production of hydrogen gas.

CHAPTER 2

1. Kinetics of oxidation

This section reviews the various theories related to the growth process of oxide films. It should be noted that although the fundamental relationships described here were originally conceived to account for the atmospheric oxidation, they are equally applicable to aqueous reactions in cases where solid state processes are rate controlling.

The growth of the oxide film is classified, at any given stage during the process, by obedience to a particular law. The most frequently encountered laws are the parabolic law, the logarithmic law and the linear law. The first two are responsible for the formation of protective films while the third is indicative of non-protective kinetics. The other less familiar laws are the cubic law and the inverse logarithmic law.

The parabolic law is obeyed by most metals in one way or the other. The law is derived from rate control by anion or cation migration through the growing oxide film. The rate of increase of thickness is proportional to the reciprocal of film thickness, i.e.

$$\frac{dx}{dt} = \frac{K}{X}$$

or

$$X^2 = K_p t$$

where K_p is called the parabolic rate constant. Since the thickness is proportional to the amount of oxide, i.e. gm/cm^2, the units of K_p are simplified as $(gm/cm^2)^2/Sec$.

The linear law is found for conditions other than the simple diffusion control:

$$X = Kt$$

Linear kinetics can result from one of the several causes. The following causes will be considered: non-coherency of the oxide, extreme mobility of the ions (reactants) and physical breakdown of the oxide layer and reaction rates controlled at interfaces.

The growth of non-protective films was considered in a classical work by Pilling and Bedworth (14). It was predicted that the linear law would apply to cases of oxidation which resulted in the formation of a surface layer of lesser specific volume than that of the parent metal. Under such conditions, coherency of the oxide is not possible and fresh metal surface is continuously exposed to the environment.

In the light of some recent work (15) the explanation by Pilling-Bedworth principle is doubtful and, furthermore, linear kinetics have been observed even in the presence of an intact, coherent surface oxide. In such instances, it has been concluded that the diffusion of reactants through the film is extremely rapid as compared to the interfacial reaction rate, and the rate of the process is, therefore, constant and independent of the oxide thickness.

Physical breakdown of a coherent film is often responsible for a transition from protective to non-protective kinetics (15). The faster reaction takes place because of the direct contact

between the attacking medium and the newly exposed metal surface.

The logarithmic law, which has been derived for thin films, has also been found to describe the kinetics of some thick films. However, in these cases, the origin of the law is quite different and has been derived by Evans (15) for the case of a growing layer which also contains growing voids, hence cutting down the area of the diffusion interface as a function of time. The law can be written as follows:

$$x = K \log (at + b)$$

where K, a and b are all constants.

The cubic law has been derived by Cabrera and Mott (16) for thin films and for cases where the oxide dissolves excess O_2. It has also been derived by Uhlig (17). The law is expressed as:

$$x^3 = K_c t$$

The validity of the law is questionable, i.e. data are sometimes found which appear to obey a cubic law, but often these same data can be shown to obey other laws as well.

Consider, then, for example, the cubic law. Cabrera and Mott (16) gave an explanation for this law which is only applicable to very thin oxide films where the transport occurs by p-type diffusion. Campbell and Thomas (18) pointed out that space charge effects could lead to cubic kinetics for thin films followed by a parabolic relationship for the thicker films. The observations of Dawson et al (19) are contrary to this and they suggest

the conversion from parabolic to cubic rates can be shown to be due to the change in the fraction of the total surface taking an active part in the oxidation.

Uhlig (20) has developed his theory, giving a logarithmic equation, based on the electron flow across the metal/oxide interface, which in turn is a function of space charge. The space charge is assumed to be composed of two parts: (1) a uniform charge density layer next to the metal, and (2) a diffuse charge density layer beyond the uniform layer. He has shown that under some circumstances the particular distribution of negative charge in the diffuse layer can lead to cubic oxidation rate. The basis for choosing the different distribution is not clear and confusion arises when Uhlig shows that the data which fit a cubic equation can also be shown to obey the two-stage logarithmic equation. For example, Draley et al (21) have shown that their results obey a cubic law whereas Uhlig (22) has replotted the data of these authors showing that the results fit his two-stage logarithmic equations.

The inverse logarithmic law is representative of a process in which the transport of normally immobile ions results from the existence of a strong electric field. The theoretical derivation of the law is attributed to Cabrera and Mott (16), although modification has been proposed by Dewald (23). The law is expressed by

$$\frac{1}{X} = \frac{1}{X_o} - K \log \left(a(t - t_o) + 1\right)$$

where X is the film thickness at time t, X_o is the film thickness at time t_o, (when steady state has been established). K and a are constants.

Quite often the oxidation of a metal may be broken down into a definite sequence of oxidation steps such as linear-parabolic-linear etc. The cause of shifting from one kind of behaviour to another may be due to changes occurring in the oxide layer. In the case where kinetics change from linear to parabolic, the law can be expressed as follows:-

$$X^2 + K_1X = K_2t$$

This means that the two processes are rate determining, the linear K_1 term in the initial stages and K_2 in the later stages of the process. This can also be written as:

$$\frac{t}{X} = \frac{1}{K}X + \frac{1}{K_1} \qquad \text{where}$$

$K = \frac{X^2}{t}$, is the parabolic rate constant, and K_1 is the linear rate constant. These may be evaluated by plotting t/X vs X.

For the sake of convenience, oxidation reactions may be classified as either low-temperature or high temperature processes. Nehru (24) has summarised these effects in the following table on the basis of the mutual inter-dependence of three main laws of oxidation.

Low Temperature	High Temperature
(Only slight ionic mobility)	(Ionic mobility)
1. Logarithmic growth (general case)	1. Partial logarithmic control (during formation of initially very thin film).
2. Linear growth (special case when the formation of a coherent oxide is impossible).	↓ Parabolic growth (diffusion)
	↓ Linear growth (if failure of Parabolic film occurs).
	2. Linear Law. (at very high temperatures the other two processes may occur too rapidly to be measured).

3. Evaluation of rate law parameters

Consider a polynomial equation

$$x^n = K_n t$$

Here n is obtained from the slope of the line showing x vs. t on a log-log paper and K_n is found from the slope of the line representing X^n vs. t on a linear plot. The graphic analysis of

such laws is considered in detail in chapters 5 and 6.

The plotting of a logarithmic equation is rather more complicated. If the logarithmic curve is known to pass through the origin, so that X = 0 when t = 0, then b = 1, and it is possible to determine the value of a and K by trial and error. If, however, b cannot be assumed to be unity, then the procedure adopted by Champion and Whyte (25) can be used. By differentiation of the equation we have

$$\frac{dx}{dt} = \frac{ak}{at + b}$$

$$\frac{dt}{dx} = \frac{t}{K} + \frac{b}{aK}$$

or

$$1/_{dx/_{dt}} = At + B$$

where

$$A = 1/K$$

$$B = b/aK$$

The reciprocal of the corrosion rate ($1/dx/dt$) is plotted against t, and from this linear plot the constants A and B are evaluated. Then

$$K = 1/A$$

$$a/b = A/B$$

Several pairs of values of X and t can now be read from the empirical corrosion/time curve, and a value of b can be calculated from each pair by the equation

$$\log b = XA - \log \left(\frac{A}{B}t + 1\right)$$

and from the mean value of b so determined, a can be calulated

from the equation

$$a = \frac{Ab}{B}$$

3. Effect of temperature on oxidation rates

The effect of temperature on the corrosion reaction is the same as for any chemical reaction and some rate parameters, such as the parabolic rate constant, are found to obey the familiar Arrhenius equation:

$$K_p = Ae^{-Q/RT}$$ where

K_p is the parabolic rate constant, A is a constant whose values depend on K and Q is the activation energy required for the chemical reaction. RT has the usual meaning. Activation energy for the oxidation process can be found by a plot of log k vs $1/T$ and the slope of this line is Q/R. There are, however, some notable exceptions which still need explanation, e.g. the action of halogens on copper and the reaction of iodine with silver are independent of temperature. A non-linear plot means that more than one process is involved and in the case of a distinct break in the curve, the process can be represented by the following equation:

$$K = A_1 e^{-Q1/RT} + A_2 e^{-Q_2/RT}$$

Gulbransen (26) has developed a modified form of the Arrhenius equation for the processes where the rate controlling step is the migration of cations only. He shows that A is no longer a constant but is slightly temperature dependent.

4. Kinetics of Zirconium Oxidation

Cubiccioti (27) has studied the oxidation of zirconium between 600 and 920°C at oxygen pressure of 0.1 to 202 mm Hg and observes the parabolic course of oxidation. Belle and Mallet (28), however, disagree with Cubiccioti (27) and show that the oxidation of zirconium between 575 - 950°C at 1 atm. of oxygen pressure, follows a cubic law. They reported the temperature dependence of the rate constant K_c(cm^3/sec) by the following expression:

$$K_c = 3.9 \times 10^6 \exp(-47{,}000/RT)$$

where 47,000 $\pm$ 1000 cal/mole is the activation energy for the reaction. Charlesby (29) also found indications for a cubic rate law in the electrolytic film formation in anodic oxidation.

Porte (30) found cubic behaviour from 400 - 900°C with oxygen pressure of 50 - 800 mm Hg. The solution of oxygen in zirconium together with the formation of ZrO_2 was suggested as an explanation for the cubic law. The effect of oxygen pressure on the kinetics was not appreciable, as would be expected for an n-type semi-conductor (31). The activation energy for the cubic rate was about 43,000 cal/mole.

Gulbransen and Andrew (32) found, in the temperature range of 500 to 700°C, an activation energy of about 29 K. cal/mole, and suggest cation diffusion as the rate controlling step. This is not in agreement with the diffusion in pure ZrO_2, but the authors claim that ZrO_2 out of the contact with metal behaves differently

and that such measurements do not give information of pertinence to oxidation.

Orthagen and Kofstad (33) studied the oxidation of zirconium and Zr-O alloys at 800°C. Pure zirconium followed the cubic law. The weight gain-time relationship became more steep as the concentration of oxygen in zirconium increased, but "saturated" at about 15% oxygen in the alloy. At short times at 800°C, parabolic kinetics were observed due to solution in the metal. At about 10% oxygen in the alloy the kinetics became linear and remained so with additional oxygen. The saturation effect is not explained but is tentatively ascribed to some change in the structure of the solid solution.

Smeltzer (34) suggested that the kinetics of zirconium oxidation could be rationalised on the basis of double mode of anion diffusion. The metal oxidizes primarily by O_2 diffusion through the oxide film to the metal, thus forming new layers at the metal-oxide interface. In the temperature range 300 - 600°C, the oxidation proceeds too rapidly to be explainable by the normal diffusion process. He postulates two parallel reactions of (1) lattice diffusion, and (2) a grain boundary diffusion, the latter predominating early in the oxidation process. The short circuiting paths need not be only grain boundaries, but could be dislocation pipes or other fast routes for ion migration. He has derived a theoretical rate law equation by assuming that the humber of short circuiting oxygen diffusion routes decrease exponentially with time.

In a recent contribution on the aqueous oxidation of zirconium between 50 - 90°C, Leach (35) has shown his experimental data to fit the following expression:

$$X^{2.6} = K_p t$$

The present investigations show that two different kinetic processes are taking place even in the early stages of oxidation and this is considered in detail in chapters 5 and 6.

5. The role of hydrogen in the Corrosion Reaction

Numerous investigators have reported the effect of corrosion product hydrogen on the corrosion rate of metals. The purpose of this section is to summarize the evidence for hydrogen induced damage and to discuss the various models explaining this phenomenon.

The early studies on the corrosion of zirconium, aluminium uranium and their alloys were mainly concerned with the practical aspect of the problem. Some important work in this field was done by the Westinghouse (36) Atomic Power Division and others - (37, 38, 39). These studies have revealed that the corrosion behaviour of zirconium, aluminium and uranium is to a great extent affected by the corrosion product hydrogen.

Uranium - 12% molybdenum specimens periodically withdrawn from the autoclave tests reveal that hydrogen concentration increases with time (36). 20% of the hydrogen released by the corrosion reaction is reported to be absorbed by the gamma phase

matrix of the alloy. It has been shown by Thomas and Kass (39) that zirconium exhibits "breakaway" when exposed to steam but does not when exposed to dry oxygen and this may mean that the hydrogen is associated with the "breakaway" phenomenon. Wanklyn and Hopkinson (40) have found that the cathodic polarization (evolution of hydrogen at the metal) of zirconium alloys in high temperature water can increase the corrosion rate.

Draley and Ruther (37) have observed the corrosion rate of the alloy Al 1100 is reduced by making it the anode in an electrolytic cell or by alloying with metals of low hydrogen overpotential. The corrosion of zirconium was found to be accelerated by making specimen the cathode of an electrolytic cell or by previous proton bombardment (36).

More recent work has shown that the corrosion rate of zirconium (41) and uranium (35) in some aqueous solutions increases with the increase in the hydrogen activity.

A fundamental approach to the hydrogen induced damage has been considered by Draley and Ruther (38). They suggested three alternative mechanisms by which hydrogen might alter the protective properties of the oxide film. They are as follows:

(1) Diffusion into the metal - Diffusion of hydrogen into the metal causes blistering by opening of the surface texture to allow more rapid attack on the metal which now has a greater surface area.

(2) Formation of gaseous hydrogen - Such gas can rupture

the barrier film as its pressure becomes sufficient to do so and this would result in increased corrosion.

(3) Formation of metal hydride - The hydride produced would be expected to reduce the adhesion of the barrier film and would probably result in recrystallization.

It is suggested that the disposal of hydrogen atoms is divided between these three competing processes; all can be expected to reduce the corrosion resistance.

During the corrosion in distilled water at elevated temperatures, zirconium produces a thin protective layer of the corrosion product. By determining the hydrogen content of the metal, Thomas (42) has shown that a significant fraction of the total hydrogen produced in the corrosion reaction is absorbed in the metal. Draley and Ruther have suggested for the case of uranium that the hydride formed could increase the corrosion rate by its reaction with water, forming the oxide and liberating hydrogen and the cycle can be repeated.

Blistering of the oxide by the corrosion product hydrogen has been observed in the case of aluminium (37). The hydride formation was observed, in the case of uranium by many workers (36, 43, 44), but Burkart (36) believes that the hydride phase has a higher corrosion rate than uranium and thus encourages preferential attack.

An alternative theory for the role of hydrogen in corrosion

reaction has been postulated by Leach (45) who suggested that the hydrogen effect on the oxide may be primarily of an electrical nature. The mechanism proposed by Leach is based on the dissolution of protons in the oxide which increases the electronic conductivity and this may in turn increase the ionic diffusion through the oxide. The increased electronic conductivity could accelerate the movement of cations as a result of the space charge created by the movement of excess electrons as proposed by Wagner (46) for the system Ag-Ag_2S-S. Here the increase in the conductivity associated with a non-stoichiometric silver excess of 2×10^{-3} gm.atom of Ag per mole of Ag_2S increased the diffusion co-efficient of the metal by a factor of 3×10^3.

One could also propose that the hydrogen is transported through the oxide in the form of atoms rather than ions. This is not impossible but is considered highly unlikely. First, the hydrogen atoms would be considerably larger than the ions, and this would make the migration through the oxide lattice much more difficult. Second, it appears unlikely that such a neutral atom could exist for a very long time in an environment such as oxide, with its very high local electric fields. Third, the driving force for the migration would be considerably lower than for the migration of protons. The potential gradient would not be influential and the only driving force for transfer would be the concentration gradient set by the removal of hydrogen atoms at the metal-oxide interface. This removal is not possible without hydrogen overvoltage to liberate gaseous hydrogen.

More recent work on zirconium (41) and uranium (35) show that the increase in corrosion rate with the cathodic polarization occurs without any appreciable change of the protective thickness. It is thought, on this basis, that a relationship exists between the hydrogen content of the oxide, its electronic conductivity and the corrosion rate.

CHAPTER 3

METHODS OF MEASUREMENTS

Numerous experimental techniques have been developed determining the oxidation rates of metals and alloys in various environmental conditions. The policy adopted in the present chapter, because of the advanced technicalities, is not to describe the equipment and experimental details of the methods available but to review the basic principles of some of the methods with their advantages and limitations. The methods discussed here are the gravimetric, manometric, electrometric, impedance and optical methods.

1. Gravimetric Method

The recent advancement in the gravimetric method owes its development to the general availability of accurate analytical balances in the laboratories. The method is commonly used because of its directness and general convenience and, in principle, a hot furnace and an accurate balance are the only requirements. The method can be used either continuously or intermittently and the weight gain or weight loss as a function of time can be obtained.

For intermittent weight gain measurements, the specimen is carefully heated in a furnace for a certain time, removed and weighed after cooling. The procedure can be repeated for different heating periods. Although it is very simple in practice, the method has certain drawbacks, (1) since the

thermal coefficient of the metal and oxide are generally different, the oxide may crack or even partially flake off on cooling and (2) the oxidation conditions are not the same as for a continuous experiment.

The weight-loss method is same as the weight gain method except that in this case the oxide is removed from the surface and the loss in weight is measured. Although it compensates for the first disadvantage of the weight-gain method, the technique has many objections: (1) The oxide removal by mechanical or chemical means is a difficult process. (2) Complete removal of the oxide without affecting the underlying metal is difficult.

The continuous gravimetric method can be used when the metal specimen is attached to a suitable balance and suspended in a long vertical tube. There are several types of balances available commercially. Gulbransen (47) has developed a very sensitive microbalance for gravimetric observation of thin films at different temperatures and various pressures, up to atmospheric pressure. The equipment designed by Mckewan and Fassell (48), however, can be used up to 40 atm. of oxygen pressure.

Although the continuous methods are more reliable than the intermittent methods, yet these are suitable only for gaseous/metal oxidation reaction rates. When the tests are carried out in aqueous environments, removal of the specimen from the reaction vessel is necessary before drying and weighing.

2. Manometric Method

The early work on the manometric method was reported by Hinshelwood (49) but owing to some disadvantages (see below) the method has not often been used. Recently, however, the modifications of Campbell and Thomas (50) have improved the method considerably.

In principle, the manometric method for the determination of oxidation rates is very simple and the basic requirements are a long heated tube, containing the specimen, connected to a manometer and a gas supply. The decrease in the oxygen pressure with the commencement of the oxidation reaction is recorded by the manometer. When the reacting gas consists of mixed gases, the method is disadvantageous because the metals are attacked by different gases at different rates. However, in general, the method is recommended only when pure gases are used provided a correction is made for accurate pressure measurement when the reaction tube and the manometer are not at the same temperature.

The manometric technique, developed by Campbell and Thomas (50) uses differential manometer containing oil of low vapour pressure (Apiezon oil B - vapour pressure at room temperature less than 10^{-7} mm Hg.) to measure the drop in pressure due to oxidation. The thickness measurements of the order of mono-molecular layer are reported. The method has the advantage of being less complicated and yet capable of giving very accurate measurements for the thin film region.

The manometric methods, however, cannot be used when a secondary reaction also occurs, e.g. decarburization of steel at high temperatures and the evolution of gases at elevated temperatures from metals which absorb gases at low temperatures.

3. Electrometric method

The electrometric method consists of determining the quantity of electricity needed for the cathodic reduction of the oxide either to the metallic state or to the lower state of oxidation. The oxide thickness is determined by making the specimen a cathode in a suitable electrolyte and recording the time taken to reduce the oxide by a small known current. The electrode potential during the reduction process remains substantially constant and when reduction is complete, the potential changes sharply to the hydrogen discharge potential and, therefore, the end point is taken as the point of inflection on the potential-time curve. The oxide thickness, X, in Angstrom units is given by the expression

$$X = \frac{ItM \times 10^5}{2dA \times 96000}$$

where I is current in milliamps, t is time in seconds, M is weight in grams of oxidation product giving one gram-atom of oxygen or equivalent on reduction, d is density of oxidation product and A is area in cm^2.

The method was first used by Evans and Bannister (51) in an open cell. Since then the method has undergone many

modifications and the most important amongst these is the closed cell version developed by Campbell and Thomas (52) in which they pre-boil the electrolyte and pass nitrogen before and during the experiment to eliminate the oxygen depolarization reaction. The method is very accurate and Winterbottom (53) has shown that the application of this technique has removed the previous discrepancies. However, the method has been further improved by Lambert and Trevoy (54) who employ the pre-electrolysed solution to remove dissolved oxygen and traces of plateable cations. The closed cell methods claim the detection of oxides of the order of monolayer.

In the cathodic reduction of oxides, the potential increase is often insufficiently abrupt and, therefore, Hauffe (55) considers these methods are of limited applicability in oxide thickness measurements. These methods can only be applied successfully if (1) the oxidation products are not soluble in water, and (2) the oxide is easily reducible.

4. Impedance Techniques

Impedance measurements have been used for many years for the determination of oxide thickness and for an assessment of the protective nature of the oxide. Young (56) interpreted impedance measurements on anodic films by considering the oxide to function as the dielectric of a parallel plate condenser of which the base metal and the solution form two

plates. Lorking (57) measured capacity and resistance of iron and aluminium electrodes using an a.c. bridge at 2000 c/s and has shown that when the oxide film is coherent the capacity across the oxide-covered surface is low and rises as the film thickness decreases. However, when the oxide has been rendered porous, the capacity values are high at low frequencies and vice versa. Therefore, for porous films, theoxide thickness and its capacity bear no direct relationship.

Amongst various investigators (58, 59) who have made the capacity measurements, Wanklyn et al. (60, 61) have included the weight gain of the specimens as well, e.g. they have shown that for a crack free film, $^{1}/_{cw}$ will be constant for all values of thickness but when film cracks, c will rise and, hence, $^{1}/_{cw}$ will decrease (where c is capacity and w is weight gain due to corrosion). They consider this as a useful means of comparing the protective thicknesses for various films.

Usually, measurements of capacity and resistance have been carried out on oxide films (anodic oxides) which are not likely to be affected by the measuring technique itself, i.e. a few volts of a.c. from the impedance measuring bridge. However, in the case of thin films and/or reactive metals, the application of a few volts of a.c. would probably alter the actual thickness. Leach (62) has made impedance measurements on uranium electrodes in which small a.c. signals were

used by employing a bridge developed by Denholm. Although the impedance measurements (improved methods) can furnish interesting information about the protective oxide layers, it is difficult to find an exact correlation between impedance and thickness measurements.

5. Optical Methods

Three types of optical methods for determining the oxide thickness on metals are considered. The first type depends on interference between light reflected from the two surfaces of the oxide and the second type depends on the fact that a beam of polarized light reflected at a metal surface suffers a change in its state of polarization. The third type depends on the fact that the intensity of light reflected from an optically absorbing oxide layer decreases continually with oxide growth.

5.a. Interference method

When monochromatic light falls on an oxide-covered metal, a part of it is reflected from the oxide/gas interface, a part is refracted by the oxide and reflected from the metal/oxide interface. Interference will produce an intensity minimum when

$$X = \frac{W}{4n}, \frac{3W}{4n}, \frac{5W}{4n}, \quad \ldots \quad (1)$$

where x and n are respectively the thickness and refractive index of the film and W is the wavelength of light. If, however, the two surfaces of reflection produce an additional phase change, c (in units of thickness) then we shall get

a minimum at

$$X = \frac{W}{4n} - c, \quad \frac{3W}{4n} - c, \quad \frac{5W}{4n} - c \quad \ldots \qquad (2)$$

The method adopted by Tammann (63) assumes that the colour produced by the film on the metal is determined solely by the wavelength which suffers maximum interference. The thickness of the film is then obtained by comparison with an air film that gives the same colour by transmitted light and then dividing it by refractive index of the film. The method is approximate because - as pointed out by Evans (64) - the following conditions may never be fulfilled: (1) that c is zero, (2) that the wavelength which suffers maximum interference is responsible for colour production, (3) that n does not vary with W.

However, once the thickness of the film corresponding to various colours have been measured by other methods, the colour of the film can be used to give its thickness with less error than the above method of comparison with the air film colours.

Consider equation (1) again where c = 0 and by rearranging we have

$$W = 4nx, \quad \frac{4}{3}nx, \quad \frac{4}{5}nx, \qquad \ldots \qquad (3)$$

Equation (3) gives the conditions for the destructive interference for a particular thickness as a function of wavelength and it is clear that there will be a number of interference bands which become closer and closer as the wavelength becomes

smaller and smaller because the ratio of the middle of the wavelength for the bands being $1:\frac{1}{3}:\frac{1}{5}:\frac{1}{7}$ . . . . Therefore, as the thickness increases, the bands will move towards the longer wavelength and will pass through the visible spectrum. When the film is very thin, the first interference band will be in the ultra-violet region and no colours will be produced. With increase in oxide thickness, the first band will move into the visible region, with the appearance of colours, but will finally reach the invisible infra-red region. Since the ratio of the wavelength in the visible region is approximately 1:2 and the fact that the ratio of the wavelength of the middle of the first and the second band is $1:\frac{1}{3}$, the second band will still be in the ultra-violet region when the first band has reached the infra-red region. Therefore, when the bands are narrow, the first order colours will be followed by no colours (silvery hiatus) but with increase in film thickness the second band will enter the visible region followed by the third band such that the second band is still in the visible region because the centres of the second and the third band are in ratio of $\frac{1}{3}:\frac{1}{5}$.

The application of the basic principle used by Tammann (63) can yield more accurate results, if spectroscopic study is made of the light reflected from the film-covered metal and the wavelength corresponding to the middle of the interference band is determined. Constable (65) has made such measurements on number of electrodes (assuming c = 0 in equation 2) and

Miley (66) has shown that his results, obtained by open-cell electrometric method, are in good agreement with the results obtained by Constable. Winterbotton (53), however, considers that Miley-Constable agreement is a curious coincidence because the "zero" error of the Miley's open-cell measurements and Constable's spectroscopic determination by assuming c = 0 are of the same order of magnitude and, furthermore, he claims that the discrepancies between the Constable-type interference measurements and more accurate closed-cell electrometric results can be reconciled, if the phase change is taken into account.

The method, however, has the following limitations. (1) With transparent films on highly reflecting surface, bands of zero width will occur, i.e. there would be no interference colours. This was shown by Price and Thomas (67) for sulphide films on polished silver surface. (2) Accurate estimation of the film before the interference colours appear is not possible. (3) The non-uniformity of the surface will affect the interference band. (4) A predetermined thickness-colour tabulation is necessary.

5.b. Polarized light method

If polarized light is reflected at a metal surface, it suffers a change in its state of polarization which depends on its angle of incidence, the optical properties of the metal, the film and the surrounding medium. The film thickness can be obtained by comparing the determined values of the optical

constants of the film-free metal and the film-covered metal. The optical constants can be obtained experimentally by determining the changes in amplitude and phase of the perpendicular and parallel (to the plane of incidence) components of the reflected light.

The anodic films on iron were measured by Tronstad (68) using approximate expressions to calculate the data obtained by the optical system developed by him. Winterbottom has, however, recapacitated the classical theory of metal and film optics, the mathematical, graphical and equipmental details can be seen from his original papers (69). He has calculated the film thickness from measurements obtained by his apparatus, i.e. from the difference in the phase retardation, P, and the relative amplitude reduction, A, of the components parallel and perpendicular to the plane of incidence. The values of P and A, thus, obtained are used to determine the optical constants of the film-free metal using the strict expressions obtained from the optical theory. The P and A values of the film-free and film-covered metal are then plotted on a polar diagram (v*ctorial representation) with A as the radial and P as the angular co-ordinate. The optical constants of the film and its thickness are then determined from a satisfactory fit for theoretical curves plotted for the determined optical constants of the film-free metal and the various assumed optical constants of the film.

Although the method can yield very accurate results,

the conditions for satisfactory observations can be very difficult, e.g. (1) the film-free surface should be macroscopically uniform, (2) the surface should be completely film-free or means of producing film-free surfaces should be available , (3) the growth process should be such that it produces uniform layers! Once these conditions are fulfilled, the actual experimental observations can be simply and quickly done. The evaluation and interpretations of these results, however, require laborious computations.

5.c. Intensity measurements

It is clear that the methods considered so far (except 5.b.) are not convenient for the continuous measurement of oxidation rate during the course of aqueous corrosion reaction. A method was, therefore, sought which could be used "in situ" because it is believed that disturbance of the actual environmental conditions would give information which is less likely to be the true representative of the process under examination. The principle of the method, fulfilling these requirements, used in the present work is given below:

If light is reflected from an optically absorbing film, the intensity of light decreases with increase in thickness according to the equation:

$$I = I_o e^{-2\theta X}$$

where I_o and I are respectively the intensity of reflected light from the film-free and film-covered surface, X is film thickness and θ is absorption coefficient of the film. The

decrease in light intensity reflected from the metal surface with oxide growth is measured and a comparison with the intensity of light obtained from film-free surface, gives the relative oxide thickness. The method assumes, however, that the absorption coefficient does not change with increase in thickness. This is considered at some length in the last chapter. It is not opportune here to consider the theory of film optics but the complicated and complex mathematical equations relating the reflection of light from an absorbing medium with its optical constants can be seen from standard references (69, 70, 71).

Although the method using polarized light is more accurate than the present method, yet its cumbersome requirements make it less desirable in practice. The present method has several advantages: (1) It can give continuous rate measurements. (2) It has the advantage over the interference methods in that the oxide thickness can be estimated at very early stages, long before the first minimum in the interference pattern is reached. (3) The kinetics of the growth processes can be satisfactorily and easily elucidated because the conditions of experimentation and interpretation of the data are very simple. The method, however, cannot give absolute thickness of the oxide without a knowledge of the optical properties of the system but this may not be a serious disadvantage because the absolute thickness is less important in kinetics study. Furthermore, if the optical constants

change during the course of oxidation, the method would become invalid.

CHAPTER 4

EXPERIMENTAL TECHNIQUE

While attempting to relate the electrical properties of the oxide formed to the corrosion rate of the metal, Leach (45) suggested that the incorporation into the oxide lattice of ionic hydrogen might influence the diffusion of other ionic species without causing a change in structure. Accordingly, Nehru (15) carried out investigations in this direction at low temperatures. He did not extend his work to higher temperatures because of the difficulties associated with the construction of a suitable equipment and the experimentation at elevated temperatures.

The present investigation has been carried out to examine in detail the effect on the oxide film, and, hence, on the corrosion rate of the metal, of corrosion product hydrogen and other influencing variables such as pressure, temperature and solution pH. Therefore, an autoclave is designed which permits corrosion studies at high temperature, pressure, potential and pH, and the corrosion rates are measured by an optical technique without disturbing the corrosion process.

The results obtained in the autoclave were compared with the results obtained in a glass cell so that the present data could be related to data previously obtained. Polarization experiments on a platinum electrode were made for comparison of hydrogen overvoltage behaviour. Therefore, a glass cell is discussed briefly before giving a detailed description of the autoclave and the optical technique.

I. GLASS CELL

The purpose of using a glass cell was to set up a standard experiment for comparison with the autoclave. This was achieved by studying the polarization behaviour of a platinum electrode (inert metal). The glass cell is shown in Fig.(4). A hydrogen electrode was used as the reference electrode with two separate platinum wires as anode and cathode. Cathodic polarization was achieved using a potentiostat (A.E.R.E. 1465A) and was measured by a valve voltmeter (E.I.L. pH meter 23-A). A sensitive galvanometer was employed for recording the current. The electrical circuit of the experiment is shown in Fig.(5). The cell was flushed with hydrogen gas for an hour before starting the polarization experiments. A constant potential was applied and the corresponding current was noted after one minute. The potential was then decreased in steps of 50 mv and the above procedure was repeated.

II. OPTICAL TECHNIQUE AND AUTOCLAVE

The methods generally used for the estimation of corrosion rates have already been considered at some length in the previous chapter. The relative merits and demerits of the technique chosen are given in Chapter 3 (5.c.) and some points are further elaborated in Discussion.

Light from a strong source is focussed on a mirror placed at nearly 45 degrees to the incident light and is reflected perpendicularly. This light passes through a lens placed at its focal

length from the mirror and is rendered parallel. The parallel light falls on the flat specimen placed immediately behind the lens in the liquid and is reflected back through the lens and on to a photocell. During the corrosion reaction, the decrease in the intensity of the reflected light due to absorption in the film is measured.

The thickness of the oxide film is given by

$$I = I_o e^{-2\Theta X}$$

where I_o is the intensity of light reflected from the initial surface and I is the intensity reflected at thickness X and Θ is the absorption coefficient of the oxide. If X is a function of time t, then

$$I = I_o e^{-2\Theta f(t)}$$

or

$$\log I_o - \log I = 2\Theta f(t)$$

A plot of ($\log I_o - \log I$) versus t gives relative film thickness as a function of time.

The technique is discussed below under two broad headings.

(A) Equipment

(B) The Actual Operation

(A) Equipment

The description of the equipment is divided into the following sub-sections:

(1) the optical system

(2) the autoclave

(3) the specimen preparation

(4) the heating unit, and

(5) the polarization requirements

These are discussed below with other necessary details.

(1) Optics

The optical arrangement is shown diagrammatically in Fig. (6). Light from 250 watts Atlas Iodine Quartz lamp is focussed by the condensing lens on the half-silvered mirror M mounted inside the main tube A. The reflected light falls on Lens L, which is placed at its focal length from mirror M. The transmitted light is rendered parallel and falls on the clean metal placed near the lens. The reflected light from the specimen is measured by photocell P_1. Any photo-currents produced by the light reflected from the surfaces other than that of the specimen are cancelled out by the reference photocell P_2 which is connected in opposition to P_1 and also acts as a standard for light intensity. Power to the light source comes through a voltage stabilizer (Advance CU 150 A) for constant intensity of light.

The measuring circuit is shown in Fig. (7). The potentiometer R_2 is used to adjust the recorder to coincide with the amount of light reflected from a heavily corroded (standard) specimen. The potentiometer R_1 is used to give a full scale (0 - 1 mv) deflection on the recorder due to light reflected from the initially polished specimen.

(2) Autoclave

The autoclave (test cell) is made of a $\frac{1}{4}$" thick 18/8

stainless steel 4" diameter cylinder and is 6.5" long. It is shown in Fig.(8). The bottom of the autoclave is a ½" thick "Armour plate" (Pilkington Bros.) toughened glass disc. The glass plate was selected after careful consideration of its physical and chemical properties. It is extremely strong (allowable working stress 6,500 lb/sq. in.) and under the present conditions of operation is chemically inert to most electrolytes. The various electrolytes used include potassium sulphate, sodium carbonate, a mixture of sodium carbonate and bicarbonate and potassium hydroxide, of all these only N/10 KOH at high temperature (150°C) shows some attack after prolonged exposure.

The top plate of the cell is 3/8" thick stainless steel. It has arrangements for pressure tight insulated electrical leads, gas inlet, gas outlet, thermocouple pocket and a special unit for introducing the specimen. The gas inlet, gas outlet, and the thermocouple pocket are all 3/8" diameter stainless steel tubes and are hard soldered into the top plate. The thermocouple pocket is closed at the bottom end and its length is adjusted such that it is very near to the specimen. This minimises the effect, if any, of the temperature difference due to thermal gradients.

The gas inlet is fitted with a stainless steel valve to help control the flow of gas but was found unnecessary because the gas cylinder gauge and the relief valve used were sufficient to regulate the flow rate and the pressure required. The inside of the gas inlet is fitted with a stainless bubbler.

The gas outlet is about 2½ feet long and is inclined at about

60 degrees to the top plate so that any water vapour which condenses inside the tube falls back into the liquid. The outlet was also cooled externally by water flowing through ¼ helical lead tubing. The natural cooling was sufficient when working near 100°C but at high temperatures water cooling was necessary for condensation of vapours. The gas outlet is also fitted with a pressure gauge and a relief valve (I.V. 187/9). The relief valve is provided with five different springs for working in various pressure ranges. The pressure inside the autoclave is kept constant to any required value by using the right spring and by proper adjustments. Any increase of pressure in the system caused by gaseous evolutions on the electrodes by electrochemical reaction and/or by heating is blown off by the valve. The gas stream, on leaving the valve, is passed through water for a flow rate assessment.

A special arrangement is provided to take the specimen in and out of the autoclave without dismantling the whole unit. This caused great difficulty and various partly successful designs were made but they will not be discussed here. The final design is shown in Fig. (9). A stainless steel plate sits on the top plate of the autoclave and has arrangements for taking a P.T.F.E. gasket and a pressure seal. A "follower" is used to keep the seal seat horizontal and is then pressed down by screwing the central bolt. The arrangement for introducing other electrodes (permanent) is the same in principle but is much smaller in dimensions as shown in Fig. (10). Ferranti (TD/C-397) pressure seals are used for

attaching all the electrodes (and the specimen) inside the autoclave with the stainless steel connectors. The pressure seals are made of Nilok and magnesia and, under the present conditions of operation, are extremely satisfactory.

The top and bottom plates are joined together through the main cylinder by six bolts (outside the cylinder) using P.T.F.E. gaskets wherever necessary.

(3) Specimen Preparation

The specimen preparation will be discussed in two parts:

a. the actual making of the specimen, and

b. polishing of the specimen.

a. The specimens were made from an 0.012 inch thick sheet of zirconium supplied by Imperial Metal Industries with the following composition:

	(ppm)
Al	20 - 30
Cu	15 - 20
Hf	65 - 100
Fe	400 - 600
O	1000 - 1100
Sn	100
Ti	30 - 45
N	15 - 45
H	10 - 35
Nb	75

No other metal is likely to be present more than 50 - 75 ppm. Specimens were made in different designs but all but one proved to be unsatisfactory. The various stages in making the satisfactory pattern of specimen are shown in Fig. (11). Initially the sheet is cut into a $\frac{3}{4}$" diameter central piece with $\frac{1}{8}$" wide and $\frac{3}{4}$" long tails. These tails are bent backwards and are connected to a stainless steel wire. The back of the specimen and the connecting wire are insulated by using high temperature Araldite (Ciba AY-105, Ht-972) which is cured at 80°C for 3-4 hours. Since the Araldite used becomes a fairly thin liquid at the curing temperature, glass tubing of suitable sizes were used as moulds which were gently broken after the Araldite had set hard.

b. Two different polishing techniques were used: (1) an electro process, and (2) chemical polishing.

b.1. The electrolytic polishing of zirconium has been discussed by Jaquet (72) in detail. The method used in the present work is the one recommended by Tegart (73). The specimen is made the anode and is rotated by using the usual mercury contact technique. The chemical solution was externally cooled by ice and the temperature of the bath was constantly watched because the reaction is extremely exothermic and explosive above 50°C. The composition of the solution and the conditions of operation are as follows:

50 - 100 c.c.	$HClO_4$ (Sp. gr. 1.6)
1000 c.c.	glacial acetic acid
Cathode	S. Steel
Voltage	40 - 50 volts
C.D.	45 A/dm^2
Time	45 sec.
Temp.	30°C

The polished specimen is rinsed in 2 - 4 ml. of glacial acetic acid in 50 ml. of water.

b.2. The chemical polishing process was finally used and the composition of the solution is as follows: (in parts)

$$IHF + 4HNO_3 + 5H_2O$$

It was observed that the specimen polished in this way was much brighter than the specimen polished by the electrochemical technique. Therefore, the electrochemical method was discarded because of (1) difficulty in operation, (2) dangerously explosive chemicals, and (3) dull finish. The method finally used was susceptible to fluoride contamination and the specimen was given a long thorough washing before being put into the autoclave.

(4) Heating Unit

The autoclave is heated externally by using a high wattage armoured heater (Gallenkamp H.E.-220). The heating coil is wound outside the main cylinder and the heat losses (by radiation, convection etc.) are minimised by covering the whole autoclave with asbestos lagging. The temperature is kept constant using a temperature controller (Kelvin and Hughes). Reproducibility

of temperature to $\pm$ 1°C is obtained easily. The electrolyte temperature is measured by using an iron constantan thermocouple placed in the pocket fitted in the top plate of the autoclave.

(5) Polarization Requirements

Cathodic polarization is achieved using a potentiostat (A.E.R.E. - 1465A) and is measured by a vacuum tube voltmeter (E.I.L. pH meter type 23A) with reference to a hydrogen electrode. The potentiostatic technique was used since it permitted a quantitative estimation of the effect on the corrosion rate of corrosion product hydrogen. The choice of the electrolyte was made according to the pH range desired. Some of the electrolytes used are listed below showing concentration vs. pH.

0.1N K_2SO_4	pH 5.4
0.2N Na_2CO_3 + 0.2N $NaHCO_3$	pH 9.7
0.1N Na_2CO_3	pH 11.6
0.1N NaOH	pH 13

All the solutions were made using Analar reagents and distilled water. The hydrogen electrode was made (platinizing a platinum wire) by electrodeposition of platinum using 2% solution of chloroplatinic acid in normal hydrochloric acid. The process was carried out for 2 minutes at 0.1 amp/sq. cm. of the platinum cathode surface and the electrode thoroughly washed with distilled water before use.

Under cathodic polarization, hydrogen gas is evolved at the surface of the specimen. Since the surface area was large, the gas undergoing discharge at the specimen, adhered to the surface. It

was noticed under those conditions that the gas bubbles interfered with the intensity of the reflected light. Therefore, the whole unit, i.e. optical box and the autoclave, was fitted with arrangements such that it could be tilted to any required angle. It was found that the time taken by the bubbles to leave the surface of the specimen is minimised by inclination, thereby reducing the interference with reflected light intensity.

The equipment described so far enables one to study the effect on the corrosion kinetics of the following variables: temperature, pressure, polarization, alloy composition and pH of the electrolyte.

(C) Actual Operation

The procedure adopted during both low and high temperature measurements is discussed below:

(1) The autoclave is filled ($\frac{3}{4}$ volume) with the required electrolyte.

(2) All extraneous light is backed off with the potentiometer R_2. An adjustment is made with this potentiometer to give 0.1 mv deflection on the 0-1 mv scale of the recorder by maximum reflection from the surface of a heavily corroded specimen.

(3) When working at high temperatures, the system is heated to about 70 - 80°C before putting the specimen in the autoclave. This helps in achieving the final temperature in a relatively short time after the introduction of the specimen into the system.

(4) The specimen is polished using the fluoride etch and is

thoroughly washed with distilled water before the experiment.

(5) The specimen is introduced to the test cell which is then flushed with hydrogen gas for about 10 minutes. The relief valve is adjusted according to the aqueous vapour pressure at the working temperature.

(6) The reflected light falls on the photocell P_1 and adjustment is made using potentiometer R_1 to give full scale deflection on the 0-1 mv scale of the recorder.

(7) The system is quickly heated (5 - 10 minutes) to the required temperature and is kept constant by the temperature controller.

(8) The potential on the specimen is adjusted to the desired value with the potentiostat and the decrease in the reflected intensity with the growth of the oxide film is recorded.

CHAPTER 5

RESULTS

This chapter is divided into two main parts comprising respectively the results of the polarization and oxidation experiments. The purpose of the polarization experiments (cf. previous chapter) is: (1) to establish the reproducibility of the reversible electrochemical reactions under the conditions of operation; and (2) to provide a basis for comparison of the results obtained using the autoclave with the experiments performed in a glass cell.

A. Polarization Experiments

The polarization behaviour of a platinum electrode was studied using a hydrogen electrode as the reference electrode. Two types of polarization experiments were performed: (a) the cathodic polarization in which only cathodic reaction takes place (i.e. unidirectional current) and (b) the polarization in which the current changes from anodic to cathodic.

The results are as follows:

1. The potential-current diagrams of a platinum electrode under cathodic polarization in a glass cell and the autoclave are shown in Fig. (12) and Fig. (13) respectively.

2. The polarization cycle, in a glass cell and the autoclave, where reversal of current occurs are shown in Fig. (14) and Fig. (15) respectively.

3. The results of polarization cycle in the autoclave at higher pressures are shown in Figs. (16, 17, 18).

The following observations are of interest:

1. The electrochemical reactions are reproducible under the present conditions.

2. The results of experiments performed in a glass cell and the autoclave are identical.

3. Within the range of pressure studied, no effect of hydrogen pressure is discernible on the kinetics of the cathodic reaction.

4. The anodic reaction shows a region of current limited kinetics, the value of the limiting current varying with hydrogen pressure but it is not possible at this stage to give a precise relationship of limiting current and hydrogen pressure.

B. Corrosion Behaviour

The results in this section were derived from absorption curves using "white" light. The relative advantages of this technique over the interference method have already been discussed (cf. Chapter 3 and Chapter 6) together with the implications of assuming that the absorption coefficient of the oxide is not significantly influenced by its thickness.

Data Calculations

The relative oxide thickness vs. time plots obtained by the procedure described in the previous chapter are further analysed to find the exact laws controlling the oxidation reaction.

Fig. (21) shows a typical measured thickness vs. time trace and Fig. (22) shows this original data on a log-log paper. The transition point on Fig. (22) represents the thickness and time at which the first process changes to a different process, in this case into a slower process. The slope of these lines gives the value of n, the characteristic of a particular rate law, for the following equation:

$$X^n = Kt$$

The transition point co-ordinates of Fig. (22) are noted and the original data of Fig. (21) are replotted on a log-log paper using the equation

$$(X - X_t)^n = K(t - t_t)$$

where X_t and t_t are the thickness and time co-ordinates respectively at the transition point. The new line, thus obtained is shown in Fig. (23). The slope of this new line is also measured.

An explanation and the possible effect of this procedure on understanding the oxidation behaviour and the interpretation of the kinetics data are discussed in detail in the last chapter. It is important to note here that, henceforth, the pre-transition reaction and the post-transition reaction of Fig. (22) will be described as the First and Second reaction respectively and the reaction of the type shown on Fig. (23) will be mentioned as the True reaction. Similarly, n_1, n_2 and n are representatives of the First, Second and the True rate laws respectively.

The following table summarizes the various values of n_1,

n_2 and n as a function of temperature and potential.

Potential E_H - mV	Temp. °C	First Law n_1	Second Law n_2	True Law n
300	90	1.0	1.71	1.65
"	110	1.0	2.34	1.78
"	120	1.31	3.15	1.95
"	130	1.23	2.95	1.80
"	145	1.30	2.98	1.94
600	90	1.19	2.30	1.98
"	110	1.23	2.95	2.11
"	120	1.23	2.96	1.75
"	130	1.52	2.96	1.73
"	145	1.65	3.05	1.83
900	90	1.22	2.54	1.64
"	110	1.29	3.36	2.00
"	120	1.32	2.96	1.86
"	130	1.55	3.16	1.97
"	145	1.43	2.96	1.92

Fig. (24) represents n_1 and n_2 an a function of temperature and potential and the graphic mean values, thus, found are 1.26 and 3.0 respectively. Similarly, the graphic mean value for n as 1.9 is obtained from Fig. (25). (see last Chapter). The First process,

therefore, can be represented by

$$X^{1.26} = K_1 t$$

and the True second process by

$$X^{1.9} = Kt$$

Therefore, the values $n = 1.9$ and $n_1 = 1.26$ are used in all the data evaluations, e.g., the calculations of individual rate constants and the activation energies for both the reactions. The rate constant, K_1, for the First process is found from the slope of a line representing $X^{1.26}$vst. (obtained from the first part of a graph of the type shown by Fig. (22)) and a typical trace for the First rate constant is shown in Fig. (26). Similarly, the slope of the line relating $X^{1.9}$vst (found from traces like Fig (23)) gives the value of the True second rate constant, K, and a typical graph for the True second process is shown by Fig. (27).

The effect of environment on the corrosion kinetics of zirconium have been investigated as a function of the pressure of the system, cathodic polarization of the specimen, temperature and pH of the solution. The activation energies for the First and True second processes have been calculated as a function of cathodic potential. A relationship between the transition point thickness, X_t, and the First rate constant, K_1, has been shown. The results of all these experiments are given below.

1. Effect of Pressure

The effect of pressure on the corrosion kinetics of zirconium was investigated by changing the pressure of the system under fixed

conditions of observation. Fig. (28) shows the results of the experiments performed under the following conditions

Solution pH	=	9.7
Solution Temperature	=	90°C
Cathodic Potential, E_H	=	- 300 mV
Pressure (P.S.I.)	=	(i) 14.7 (ii) 30 (iii) 60

Fig. (28) also shows the results of the experiments performed under similar conditions at 110°C. The following observations are of interest:

(1) Within the range studied, pressure appears to have no effect on the corrosion kinetics of zirconium.

(2) The oxidation reaction is following two different processes and that the first reaction is faster than the second reaction.

The pressure range investigated is the type of pressure encountered during the experiments performed at high temperatures (i.e. vapour pressure of the electrolyte). Although, in general, the effect of pressure on the oxidation reaction in condensed systems will not be to alter the thermodynamics, it might alter the kinetics. These results show that pressure has no effect on the corrosion kinetics of zirconium within the range studied.

2. Effect of Cathodic Polarization

A constant potential was applied using a potentiostat and was measured by a voltmeter with reference to the hydrogen electrode (cf. previous Chapter). Fig. (29) shows the results of the

experiments performed under the following conditions:

Solution pH = 9.7

Solution Temperature = 110°C

Potential, E_H = (i) - 300 mV
(ii) - 600 mV
(iii) - 900 mV
(iv) - 1200 mV

Similar experiments were also performed at higher temperatures and their results are considered in the next section. The following observations are of interest:

(1) The corrosion rate increases at more negative potentials, i.e. with increasing hydrogen activity.

(2) The corrosion reaction is following two different kinetics and that the protective kinetics, True rate law, appear to control the corrosion process after the First reaction.

(3) The value of the rate constant, K, at a given temperature, increases at more negative potentials, Fig. (30) shows a plot of rate constants and potentials at various temperatures and it may be concluded that the rate constant is directly proportional to potential on the hydrogen ~~plate~~ scale.

(4) Fig. (31) shows the variations of the First rate constant, K_1, as a function of potential at different temperatures. A comparison of Fig. (30) and Fig. (31) will show that K_1 behaves differently from K and that no simple relationship between K_1 and E_H is, thus, possible. (also see activation energies)

The various values of K_1 and K as a function of temperature and potential are given in the following table:

Temperature °C	Potential E_H(-mV)	K_1 ($X^{1.26} = K_1 t$)	K ($X^{1.9} = Kt$)
90	300	8.64	7.15
110	"	12.90	4.46
120	"	10.40	5.36
130	"	15.60	7.00
145	"	20.70	11.10
90	600	7.75	4.45
110	"	10.60	7.40
120	"	17.90	10.10
130	"	24.50	9.55
145	"	32.50	21.20
90	900	8.95	6.45
110	"	24.00	11.00
120	"	27.90	13.70
130	"	37.50	16.40
145	"	46.20	21.70

3. Effect of Temperature

The autoclave was externally heated using a high wattage heating coil and the temperature was kept constant by a temperature controller. The solution temperature was measured by a thermo-couple placed in a pocket near the surface of the specimen

(cf. previous Chapter). Fig. (32) shows the results of the experiments performed under the following conditions:

Solution pH = 9.7

Potential E_H = - 300 mV

Solution Temperature = (i) 90°C
(ii) 110°C
(iii) 120°C
(iv) 130°C
(v) 145°C

Similar experiments were also performed at other potentials, e.g. - 600 mV and - 900 mV. The following observations may be noted:

(1) The corrosion rate increases with increase in temperature.

(2) The rate constants K and K_1, at a given potential, increase with increase in temperature. This can be seen from Fig. (30) and Fig. (31) respectively.

(3) The transition point thickness, X_t, appears to be linearly related to the First rate constant K_1 as shown in Fig. (33) and, hence, because of the interdependence of the rate constant K_1 and the reaction temperature, it may be deduced that the transition point thickness bears some relationship with temperature, i.e. X_t increases with increase in temperature. The various values of K_1 and X_t as a function of potential and temperature are given in the following table:

Temperature °C	Potential E_H(-mV)	Thickness Co-ordinate at transition point X_t	K_1 ($X^{1.26} = K_1 t$)
90	300	0.20	8.64
110	"	0.36	12.90
120	"	0.60	10.40
130	"	0.85	15.60
145	""	1.00	20.70
90	600	0.40	7.75
110	"	0.85	10.60
120	"	0.90	17.90
130	"	1.10	24.50
145	"	1.20	32.50
90	900	0.60	8.95
110	"	0.90	24.00
120	"	1.00	27.90
130	"	1.00	37.50
145	"	1.10	46.20

3(a). Activation Energy

The activation energy for a particular oxidation reaction is calculated from a graph of log K vs. $\frac{1}{T}$ (where K is the rate constant and T is the absolute reaction temperature) and the slope of such a plot is equal to $Q/2.3R$ where Q is the activation energy for the reaction and R is the gas constant. It is clear from Fig. (22)

that two different processes are taking place and, therefore, the activation energy for each process is calculated separately. Fig. (34) and Fig. (35) show the temperature dependence of First reaction and True second reaction respectively as a function of potential. The various values of activation energies calculated from the slope of these lines are given in the following table.

Potential E_H(-mV)	Activation Energies K.Cal/mole	
	First Process $X^{1.26} = K_1 t$	True Process $X^{1.9} = Kt$
300	4.7	9.05
600	8.17	8.35
900	5.84	6.55

It may be noted that, whereas the activation energies for the True second process decrease as the potentials become more negative, these values for the First Reaction appear to have no direct relationship with potential. The irregularities of temperature dependence as a function of potential for the First Reaction are clear from Fig. (34) and this is discussed in the last chapter.

4. Effect of solution pH

Various electrolytes of different pH were used but since the corrosion rates were very slow in the acidic solutions, most of the experiments were conducted under alkaline conditions. Strong

alkaline solutions were not used (although higher corrosion rates were obtained) because of the irreproducibility of the results and the chemical attack on the autoclave, especially the glass window. Fig. (36) shows the results of the experiments performed under the following conditions:

Solution Temperature = 110°C

Solution pH = 5.4

Potential E_H = (i) - 600 mV
(ii) - 300 mV

These results are compared with the previous results obtained in solution of pH 9.7. The following conclusions may be drawn from these results:

(1) The corrosion rates are much slower in acidic solutions than in alkaline solutions.

(2) The effect of potential is the same as that under alkaline conditions, i.e. the rate increases with decrease in potential.

(3) The corrosion reaction is following two different processes (as in alkaline solutions) and that the first process is faster than second process.

CHAPTER 6

DISCUSSION

1. Polarization Experiments

In the previous chapter it was stated that the polarization experiments were performed to establish the reproducibility of the electrode reactions under the present conditions of operation and to provide a basis for comparison of the results obtained using a glass cell and the autoclave. The results of the experiments conducted in a glass cell are shown in Figs. (12-14) and Figs. (15-18) show the results, under otherwise similar conditions, using the autoclave. A study of these results will show that both the systems provide identical and reproducible graphs.

Overpotential measurements are important in investigating various electrochemical processes as they permit studies of the reaction mechanism, the kinetics of corrosion phenomenon and metal deposition. In interpreting the detailed properties of these curves, the discussion is divided into two parts: (a) the reversible systems and (b) the irreversible systems.

(a) Reversible System

The meaning of equilibrium potential E_o, the exchange current i_o, the anodic current i_a and the cathodic current i_c have been given in the derivation of the Tafel equation (cf. App. II)

$$\eta = a + b \log i$$

Theoretically, the i-η graph on a linear paper would appear as

Fig. (2) and the point of intersection of these lines gives the value of i_o. If, therefore, η is more positive than E_o, then anodic reaction will take place but if η is more negative than E_o, then reduction reaction will occur. Since the reaction is reversible and the reaction rates are equal, the symmetry of the curve in both oxidation and reduction region is, therefore, expected. However, the measured i-η plot on a log-linear paper would look like Fig. (3). The extrapolation of the straight line portion of the oxidation and reduction curves produces an intersection at i_o, the exchange current and the potential associated with it is E_o, the equilibrium potential. This procedure, therefore, is the graphic method of finding E_o and i_o. The exchange current can also be calculated from a knowledge of the Tafel constants (a and b) and the relationship can be found from Tafel equation when Lt $\eta = 0$, then $i = i_o$, and hence

$$i_o = - a/b \qquad \eta \rightarrow E_o$$

The polarization of a platinum electrode is a reversible system which is apparent from the polarization results shown in Figs. (12-18). This is discussed by considering the following equilibrium

$$H_2 \rightleftharpoons 2H^+ + 2e \qquad (1)$$

Stern (74) has studied in detail the hydrogen evolution reaction and has shown the mechanism of evolution is dependent on the electrode current and pH of the solution. Two cathodic reactions have been proposed for a given pH as a function of current density.

(1) at low current density

$$2H^+ \text{ (from hydronium ion)} + 2\bar{e} \longrightarrow H_2 \qquad (2)$$

(2) at high current density

$$2H_2O + 2\bar{e} \longrightarrow H_2 + 2\bar{O}H \qquad (3)$$

Reaction (2) and (3), however, are only possible in the absence of oxygen. Lorch (75) has shown the effect of O_2 on the H_2 evolution reaction and the cathodic reaction in the presence of O_2 are said to be as:

$$4H^+ + O_2 + 4\bar{e} \longrightarrow 2H_2O \qquad (4)$$

$$2H_2O + O_2 + 4\bar{e} \longrightarrow 4\bar{O}H \qquad (5)$$

Reactions (4) and (5) are called the cathodic oxygen depolarization reactions.

On the anodic side, the O_2 evolution is not possible in the potential range which is very near to the equilibrium potential (Pourbaix diagrams). However, the following anodic reaction is possible in this region.

$$\bar{O}H + \tfrac{1}{2}H_2 \longrightarrow H_2O + \bar{e} \qquad (6)$$

By analogy with the cathodic oxygen depolarization reactions (4 and 5), this could be designated the anodic hydrogen depolarization reaction. It may be pointed out that in equation (6) the reactants involve a neutral species (H_2 gas) and, therefore, at high currents, the rate determining factor may be the diffusion of H_2 to the anode. When the anodic reaction will be faster than the diffusion rate, the potential will increase rapidly at a limiting current value and in conformity with the Pourbaix diagram the

process will ultimately lead to the oxygen evolution reaction.

(b) Irreversible System

In the reversible system only one reaction, of the type already considered, takes place but, when the metal itself is undergoing electrochemical reaction, a net reaction will take place. Therefore, two simultaneous processes will occur at the metal surface and consequently the overall process will be an irreversible reaction. Theoretically, the processes will appear as in Fig. (37) with each reaction having different equilibrium potential and its exchange current and it is clear that their relationship with corrosion potential and corrosion current cannot be simple. The measured current will be additive of all partial current densities. This important principle of additive combination of all partial processes at an electrode surface to obtain the total current-potential curve was first formulated by Wagner and Traud (76).

In accordance with Tafel's equation, Pourbaix School has made use of the reaction current as a quantitative measure of the rate of corrosion and has employed potentiostatic methods to determine the corrosion rates.

Butler and Armstrong (77) have shown that the overpotential of a reversible electrode is a linear function of the applied current for values of η slightly removed from the reversible potential. It may be pointed out that this is a property of the i-η equations which can be shown as follows:

Consider the expansion of a series

$$e^X = 1 + X + \frac{X^2}{2!} + \ldots\ldots$$

when X is small, the terms with powers of X greater than 1 can be neglected and, therefore, it can be approximated as:

$$e^X = 1 + X$$

Consider, now, equation (9) derived in App. II and by expanding and simplifying as above, we can write

$$i = i_o X n F/RT$$

and, hence, the linearity of i-η_a trace is obvious.

2. Experimental Technique

In the third chapter (5.c.) the relative advantages of the optical method used in this work are described and it was assumed that the absorption coefficient of the film did not vary with thickness. It is considered relevant to check this assumption by careful analysis of the available information. Charlesby (78) has calculated the refractive index of zirconium films as 2.2 and he has shown that the refractive index does not change with thickness. This value, however, is different from the earlier value of 3.45 reported by Gunterschulze and Betz (79). Charlesby (78) has shown that these authors (79) used the approximate equations, neglecting the effect of glancing angle. The mathematical mean value of the glancing angle as reported by Charlesby (78) is 0.67 and, therefore, the corrected value, accordingly, of Guntherschulze and Betz refractive index should be 3.45 x 0.67 = 2.31.

The previous experiments (24), conducted under the conditions

similar to the present arrangement, have indicated that the oxide thickness, obtained from the interference pattern measurements is equal to the thickness obtained from the reflectivity method, provided it is assumed that the ratio of the refractive index to the absorption coefficient remains constant. Since the refractive index is found to be constant, it would, therefore, appear that the absorption coefficient is also constant.

The second point which needs to be expounded is the effect of reduction in the intensity of light due to destructive interference. When the film is thin, no interference colours will be produced but as the film will grow, periodic maxima and minima would occur. This complex behaviour of reflected light would result in near periodic irregularities of the reflected trace. Since it is not likely that the process would change periodically, this effect, when it occurs, must be taken into consideration. With absorbing film, the amplitude of oscillation, associated with periodic interference, is a decaying function (69) and, hence, at higher thickness it will achieve a "constant" value. Therefore, when the reflected trace shows irregularities coupled with the appearance of interference colours, the present method will not be applicable and some modification would be necessary.

Fortunately, however, it was found that (1) no interference colours were visible to naked eye (spectroscopic investigation of the oxide film was not possible because of the nature of the specimen) and (2) "smooth" reflection trace was obtained indicating

that the decrease in the intensity of reflected light was mainly caused by the absorption in the film. It would appear, therefore, that under the present conditions of operation, this method is satisfactory.

3. Interpretation of kinetics data

The kinetics data in the previous Chapter were calculated from the log-log plots where the transition point co-ordinates (X_t, t_t) of Fig. (22) were introduced. The further data were calculated including these co-ordinates but no details were given there. The following section gives an explanation for this analysis and shows the effects of the transition point co-ordinates on subsequent interpretations and understanding of the corrosion behaviour.

The rate law for any reaction can be determined from the following general equation:

$$(X - a)^n = K(t - b)$$

where X and t are thickness and time respectively, K, a and b are constants and the value of n is the characteristic of a particular law, e.g., for linear law n = 1 and for Parabolic law n = 2, etc. The slope of the line when only one process occurs, obtained from the thickness, (X) vs. time (t) plot on a log-log paper gives the value of n. Such a plot, however, assumes that over the range of values of X and t of interest the values of a and b are negligible by comparison.

Consider now the case of two processes occurring at different

stages of a reaction such that the first process is accurately represented by

$$X^{n_1} = K_1 t \quad \text{up to } X_1\ t_1$$

and second by

$$(X - X_1)^{n_2} = K_2 (t - t_1)$$

An X vs. t plot when $n_2 = n_1 = 1$ of these processes would appear as in Fig. (19). However, a plot of log X vs. log t would look as in Fig. (20). The transition period represents the region where

$$X \text{ is not} \gg X_1 \qquad \text{and}$$

$$t \text{ is not} \gg t_1$$

and thus the reaction must be described by the equation:

$$(X - X_1)^{n_2} = K_2(t - t_1)$$

and not by

$$X^{n_2} = K_2 t$$

Fig. (20) examined in isolation could give rise to the impression that the process involved a linear (non-protective) regime followed by a protective regime which was again followed by a linear regime whereas this was generated from two linear processes (Fig. 19).

When such an analysis is applied to more complex systems, e.g. where n is greater than one or where n is different in the two regimes the complications are very much greater. Consider, for example, Fig. (21), already analysed in the previous chapter, which shows a present measured thickness vs. time trace and

Fig. (22) shows the same data on a log-log paper. This clearly indicates that the reaction is following two different kinetics. The value of n_1 for the first part (faster process) and n_2 for the second part (slower process) are apparently 1.29 and 3.36 respectively.

From Fig.(22) approximate values of X_1 & t_1 can be derived and Fig. (23) shows the trace where the transition point co-ordinates X_1 & t_1 have been subtracted from the remaining trace as shown in the previous chapter (data calculation). The slope of this line gives the value of n as two which is exponent of X for the parabolic equation, as contrasted to n = 3.36 obtainable from the first (incorrect) plot. For n = 2 there is some model for the process, but n = 3.36 has no known mechanistic significance.

The main points of interest (using the terminology of the previous chapter) of interest are:

(1) Two different processes are taking place and that the first process is faster than the second process.

(2) The process after the transition point follows parabolic kinetics instead of what could have been, otherwise, interpreted as a cubic kinetics.

The trace in Fig. (21) represents the cumulative oxide growth. The pre-transition reaction is faster than the post-transition reaction. It is necessary to find the values of X and t at which this change in kinetics takes place and then to subtract these transition point co-ordinates from the remaining trace to find the

true behaviour of oxidation after the initial reaction.

The determination of the true value of X and t at which the transition occurs is not very easy with real cases as contrasted to that shown by Fig. (19). In a real situation it is unlikely that the change would occur simultaneously for the whole specimen. This would lead to a blurring out of the transition, which cannot now be defined as the value of X and t at which the log-log curve first departs from the initial regime.

Nevertheless, this difficulty does not invalidate the argument and value of n derived from log-log plots must be suspect unless precautions are taken to include the effect of the transition thickness and time.

The models for the various mechanisms associated with a cubic law are ill defined at present and that the most important practically and theoretically best established of all oxidation mechanisms is Wagner's interpretation of parabolic oxidation. The second process of Fig. (22) which could have been reported as a cubic law appears to be a parabolic process and, therefore, can now be explained by Wagner's theory of oxidation.

The values of the rate constant and activation energy of an oxidation reaction can only be meaningful if it is known that these variables (temp. potential, etc.) are not changing the value of n for this reaction. Consider Fig. (24) which shows n_1 and n_2 as a function of temperature and potential. It is clear that the values of n_2 for the incorrect process after transition show wide

scatter and it is difficult to ascribe any graphic mean value to the process. (A line at $n_2 = 3$ has been drawn to show the degree of scatter). However, Fig. (25) shows the values of n after transition derived by the improved procedure as a function of temperature and potential and a comparison of Fig. (24) and Fig. (25) will show that the scatter is much less where the transition point co-ordinates have been considered. The reduced scatter suggests that a more realistic mean value for n can now be given to this process and, therefore, a more reliable information about the effect of oxidation variables on the subsequent reaction can, thus, be obtained.

Cox (80) has previously considered this problem and provided a qualitative analysis of oxidation data for the system in which a protective process is changing to a linear process. He has described a situation where the transition point co-ordinates have no effect because the linear process is represented by a line which may be extrapolated back and pass through the points $X = 0 \quad t = 0$. In practice, however, the fulfilment of this condition appears to be unlikely and it may be pointed out that this, for obvious reasons, is the only situation in which a linear process will appear as a linear line immediately after the transition point. For cases when the transition is occurring at other points not linearly related to the origin, the linear process would not look linear and Cox (80) suggests that the linearity will reappear after of time long compared with the time to transition. This will

undoubtedly be true but the analysis of Figs. (19 ε 20) show that this time might be so long that it could be interpreted as a regime of kinetics different from those immediately before and after.

For systems where the process after transition is not linear, the complications will be very much greater. However, the present method of analysis can be applied whatever the nature of the transition and irrespective of the relationship of the transition point and the origin.

4. The Meaning of the Transition Point

In the previous pages the transition point (X_t, t_t) has been regarded as the point at which the second (slower) process starts. Strictly speaking, this is not true. Consider, for example, the following equation:

$$X = K't^m \quad \text{——} \qquad (1)$$

where $m = \frac{1}{n}$ and, then, $m_1 = \frac{1}{n_1}$ etc. For a protective process, therefore, m must be less than one but greater than zero and for faster to slower reactions, m must vary as $1 \gg m_1 \gg m \gg 0$. Differentiating eq. (1) w.r.t. t

$$\frac{dx}{dt} = K'mt^{m-1}$$

Since m - 1 is negative, the rate can be written as

$$\frac{dx}{dt} = \frac{K'm}{t^{1-m}} \qquad (2)$$

The value of $\frac{dx}{dt}$ decreases continually as t increases, and

$$\underset{t \to \infty}{\text{Lt}} \frac{dX}{dt} = \underset{t \to \infty}{\text{Lt}} \frac{K'm}{t^{1-m}} = 0 \qquad \text{also} \quad \frac{dX}{dt}$$

approaches infinity as t decreases towards the value t = 0. If indeed this is so, then the second process cannot be the rate determining process at the point at which it starts because of its infinite rate. Hence, the slower process does not start at the transition point but somewhere between X = 0, t = 0 and $X = X_t$; $t = t_t$. The second process starts with an infinite rate, rapidly slowing down as the thickness increases, at the transition point the rates of the faster and slower processes become equal and beyond this point the second process ultimately takes control of the oxidation reaction. The situation, therefore, involves finding the point at which the second process originates and to show its relationship to the transition point so that the data calculated in the present analysis may be regarded as meaningful. The various possibilities of finding this point are discussed below.

Considering eq. (2) again, a graph of dX/dt vs. t for the various processes can be obtained. The point of intersection of these curves will give the point at which the rates of the two processes are equal but will give no information about the point at which the second process originates and, hence, is not useful for the present purpose.

Consider, now, the equation of type

$$X^n = Kt \qquad \text{where } n \gg n_1 \gg 1$$

differentiating w.r.t. t

$$\frac{dX}{dt} = \frac{K}{nX^{n-1}} \qquad (3)$$

It is clear that a plot of $\frac{dx}{dt}$ vs X obtained from eq. (3) will intersect at a different point from $\frac{dx}{dt}$ vs. t plot obtained from eq. (2) because the factor common to the two processes is t not x.

On the basis of this argument, a mathematical and a graphical method was developed and it was found that the True second process originates from a point close to the transition point, but because both these methods were lengthy and laborious, it was decided not to include their details. However, to confirm these results, a programme was written so that it could be analysed by a KDF9 Computer. The results obtained from computer have been (81) interpreted as suggesting that the origin of the True second process and the transition point are very close. The computer programme and the results obtained are inserted in the back folder.

It may be pointed out that any small decrease in the transition point thickness X_t will only increase the value of the first few points in Fig. (23), e.g., the points which were originally below the line will now lie on the line itself but will have no detectable effect on the higher values of thickness. Therefore, the transition point obtained from Fig. (22) can be taken as a near enough approximation to the thickness at which the True second process originates and the subsequent calculations made on this approximation may be regarded as satisfactory.

5. Corrosion Behaviour

While it is difficult to provide a comprehensive explanation

for the corrosion of zirconium from the results of the present research, it is possible, however, to make two general deductions concerning the experimental approach most likely to contribute to an understanding of the mechanism involved.

It seems necessary that, in order to investigate successfully the effect of hydrogen on the kinetics of corrosion, the rate measurements be conducted (1) under potentiostatic control, and (2) the application of a continuous rate measuring technique without disturbing the actual corrosion process.

The effect of cathodic potential on the corrosion rate has been shown and an explanation is given to account for the enhanced corrosion rate due to hydrogen. Most of the experiments were conducted in alkaline conditions because the corrosion rates were very slow in the acidic solutions.

The analysis in the previous chapter has confirmed that the corrosion process can be represented by two different rate laws, namely

$$X^{1.29} = K_1 t \quad \text{and} \quad X^{1.9} = Kt$$

Since the First process is closer to a linear rate law, Wagner's model of oxidation is not applicable in this region. Therefore, factors which are likely to increase the conductivity of the oxide and consequently increase the corrosion rate and decrease the activation energy, appear to have no effect on the pre-transition regime. A comparative study of the variation of activation energy as a function of potential will show, Figs.(34

and 35), that whereas the True second process undergoes decrease in activation energy with increase in negative potential, the corresponding changes for the First process are irregular.

The linear relationship between the transition point thickness X_t and First rate constant K_1 is shown in Fig. (33). Since the rate constant is related to temperature, it would appear that X_t and the reaction temperature also bear some relationship.

It is not possible to consider the First process in detail here; nevertheless, it is noteworthy that the transition of kinetic process in such early stages has not been reported by the previous investigators, probably because of their experimental limitations. However, the importance of the application of a rate measuring technique capable of detecting the changes in kinetics in very early stages of oxidation is obvious because the transition point co-ordinates determine the subsequent character of the oxidation process. The effect of various environmental variables on the True second process are considered in detail in the following pages.

5.a. Effect of Cathodic Polarization

The results in Fig.(29) show the effect of cathodic polarization on the corrosion rate of zirconium. It is clear that in all cases decreasing the electrode potential increases the corrosion rate and that the protective kinetics control the reaction. Wanklyn and Hopkinson (40) also showed increases caused by cathodic polarization in the corrosion rate of zirconium in high temperature

water (350°C). They rejected, on two counts, the cathodic reduction of the oxide as possible explanation (1) as thermodynamically unlikely, and (2) as controverted by the enhanced film growth. Draley and Ruther (38) have discussed the effect of hydrogen on the corrosion of uranium and offer three alternative suggestions to explain the increase in corrosion rate (see chapter 2). Leach (45) suggested, from conductivity measurements on U/UO_2 electrodes, that a further possible effect of hydrogen is to increase the rate of ionic diffusion within the oxide without causing a change in mechanism. This hypothesis suggested for the role of hydrogen is supported by the observations of some other workers, it remains to be shown by which method the hydrogen can increase the corrosion rate of zirconium. Two factors are relevant: (1) the state of hydrogen within the oxide and (2) its position in the lattice.

A relationship between the electronic conductivity and the ionic diffusion coefficients of semi-conducting compounds has been demonstrated. An increase in conductivity will generally result in enhanced diffusion rates. Wagner (46) has shown that the diffusion coefficient of silver in the system $Ag-Ag_2S-S$ is increased by a factor of 3×10^3 due to increase in conductivity associated with a non-stoichiometric silver excess of 2×10^{-3} gm-atom of Ag per gm-mole of Ag_2S. An excess of silver in Ag_2S corresponds to a prevalence of excess electrons (i.e. n-type conduction), and the increase in diffusion rate is attributed to a space charge, created by these electrons, which tend to

accelerate the Ag ions.

It is clear from the present results that hydrogen increases the rate of ionic diffusion within the oxide. It can be argued, therefore, that as the conductivity is likely only to be affected by the presence of charge-carrying species, it is a reasonable assumption that the increase in the corrosion rate of zirconium is caused by the incorporation into the oxide lattice of hydrogen in the ionic state. The direct relationship between the corrosion rate of the metal and the hydrogen activity (or potential) at the oxide/electrolyte interface (Fig. 30) is probably relevant to this argument, although it is not possible at the present stage to enlarge on this observation.

Considering from the stand-point that hydrogen is ionized within the oxide film, there are several possible lattice sites in which it can be incorporated. Leach (45) has proposed the following:

(1) Sites which are normally occupied by the metal ions

(2) Interstitial sites other than those normally occupied by the metal ions

(3) Sites associated with oxygen ions.

It is interesting that, from this theory, the increase in the conductivity and consequent increase in the corrosion rate, shown in the results, can only be caused by the incorporation of protons in the lattice - if the oxide itself is an n-type semi-conductor. Consider, then, the n-type semi-conducting oxide

ZrO_{2-x} formed during the corrosion of zirconium (82 ε 83) in terms of the following equation:

$$ZrO_{2-x} = Zr^{4+} + (2-x)O^{2-} + 2x\bar{e}$$

where $2x\bar{e}$ is the number of excess electrons required to maintain the charge balance. It is clear that, in order to maintain the charge balance, the addition of an H^+ ion to the right hand side of the equation will require the inclusion of an extra excess electron. The resulting increase in electronic conductivity will tend to reduce the potential gradient opposing the diffusion of negative ions towards the metal and, hence, will encourage further oxide growth. Another example of the enhanced oxidation rates caused by externally induced electronic conductivity is apparent in the work of Jacobs (84). He has shown that anodic films (Ta_2O_5) on tantalum will continue to grow beyond the thickness defined by a given formation-voltage when the electron conductivity of the oxides is increased by ultra-violet irradiation.

5.b. Effect of Pressure and Temperature

Fig. (28) shows the results of the experiments conducted under different pressures. It appears that the pressure range investigated has no effect on the corrosion kinetics of zirconium. It is relevant to mention here that high pressures are encountered when working in autoclaves above the boiling point of the electrolyte (i.e. vapour pressure). Thus it is concluded from these results that the corrosion reaction is not affected by the

pressure involved and, therefore, no future reference will be made to the pressure of the system when discussing the effect of high temperatures on the corrosion rates.

Figs. (32, 35) show the effect of temperature on the corrosion rate of zirconium. The following points are considered relevant to the discussion:

(1) The decrease in activation energy with increased cathodic polarization.

(2) The comparison of the low activation energies for the aqueous corrosion of zirconium calculated here, with the values reported, by other workers, for the self diffusion in these oxides.

A decrease in experimental activation energy from 9.05 K.cal/mole to 6.55 K.cal/mole is shown in the potential range - 300 mv E_H to - 900 mv E_H.

Oxide growth on zirconium in air or oxygen at high temperatures occurs by the inward diffusion of oxygen involving an activation energy of 30 - 40 K.cal/mole (85) very near the value of the activation energy for the self diffusion of oxygen in zirconia and undoubtedly much lower than the value for self-diffusion of the metal. It is known, however, that aqueous conditions can cause a significant change in the mechanism of the oxide growth, and this applies over a wide range of temperature to several metals (86, 87, 88) including zirconium (89) and some alloys (90). It is relevant to mention here that some of the zirconium alloys behave in a

similar manner, e.g. in the case of Zircaloy-2, an estimation from the data of Thomas and Forscher (90) gave a value of 10 K.cal/mole for high temperature aqueous corrosion, which is in close agreement with the values reported by other workers (41). However, these values differ significantly from 28.6 K.cal/mole quoted (32) for the oxidation of the alloy in oxygen at high temperatures.

Few explanations for the lowering of the activation energy due to presence of water are generally available in literature. One offered for the corrosion of magnesium (87) involves the assumption that hydrogen ions will convert the O^{2-} ion in the lattice to $\overline{OH}$ ions, necessitating the introduction of vacancies at the cation sites to maintain electrical neutrality. It is believed that the consequent distortion of the lattice reduces the activation energy for the diffusion of Mg^{2+}, but an explanation on these terms is unlikely for a system in which oxygen is the main diffusing species. Alternate arguments which arise, e.g., either the diffusion of both anions and cations in aqueous conditions or a lower energy barrier in opposition to hydroxyl ions diffusion than that opposing oxygen ion diffusion are so far unable to account for the lower activation energies. Decreases in activation energy due to diffusion via low-resistance short-circuit paths such as grain boundaries rather than entirely through the bulk by lattice vacancies are probably too small to account for the very low values obtained (34).

Values of activation energy calculated under the present experimental conditions are difficult to reconcile with the rate-controlling step during corrosion being oxygen diffusion either via low resistance paths or through lattice vacancies. Nor do other simple explanations appear applicable. Similar observations (i.e. decrease in activation energy with cathodic potential) reported, for the corrosion of uranium, by Leach and Nehru (86) have suggested that the activation energies for corrosion approximated closely to established values of activation energy for electronic semi-conduction in uranium oxides.

It is difficult at the present stage of research to visualize a specific relationship between the ionic and electronic conductivities in corrosion-product oxides formed on metals such as uranium and zirconium. What does appear clear, however, is that those factors which alter the electronic conductivity appear to exert an influence on the rate and energetics of ionic diffusion.

5.c. Effect of solution pH

Since the corrosion rates were very slow in the acidic solutions, most of the experiments were conducted under alkaline conditions. Fig. (36) shows the results of corrosion rates in acidic and alkaline solutions. The increase in corrosion rate in alkaline solutions may be explained by treating the oxide as a solvent for hydrogen and hydroxyl ions and in alkaline solutions there will be greater tendency for the oxide to contain hydroxyl ions arising from an attempt to achieve a balance between the $\overline{OH}$

activity in both the aqueous and oxide solvent. These hydroxyl ions can also be produced in the film by the combination of a hydrogen ion and a lattice oxygen ion, and this is probably the most favoured state for a proton in the lattice. Thus alkaline solutions should encourage the absorption of hydrogen into the oxide, which in turn leads to enhanced electronic conductivity. A recent study (91) of anodic films on zirconium has also shown that oxides formed in alkaline solutions are better electronic conductors than their counterparts formed in more acidic solutions.

SUMMARY

1. The pressure in the range investigated appears to have no effect on the corrosion kinetics of zirconium.
2. Cathodic polarization of zirconium increases the corrosion rate of the metal and it is found that the corrosion rate is directly proportional to the potential.
3. It is established from the results that the activation energy for the aqueous corrosion of zirconium is generally lower than the activation energies for either atmospheric oxidation or for the self-diffusion of oxygen in zirconia.
4. It has been shown that factors such as potential, temperature and pH of the environment which have a significant effect on the corrosion behaviour also tend to influence the activation energy. These results are in agreement with the earlier investigations (41).
5. It is not clear at the present stage what mechanism permits corrosion to proceed with the low activation energies observed but the results support the proposal by Leach (45) that the electronic conductivity is an important parameter in corrosion kinetics.
6. The oxidation of zirconium follows two different kinetic processes which can be represented as:

   (i) First Process $X^{1.26} = K_1 t$

   (ii) True second Process $X^{1.9} = Kt$

7. For systems where more than one process occurs, the kinetic data can only be successfully interpreted if the effect of the transition point co-ordinates is included in characterizing the rate law after the transition point.

APPENDIX I

The Construction of the Pourbaix Diagram

In the first chapter the Pourbaix diagrams were qualitatively considered. However, the quantitative treatment illustrating the construction of the diagram for Cu-H_2O system is given here. The horizontal line in Fig. (38) represents the critical condition for the corrosion reaction.

$$Cu \rightleftharpoons Cu^{++} + 2e \qquad (1)$$

The regions corrosion, immunity and passivity have already been defined (cf. first chapter). To understand the graphical representation, it is helpful to write reaction (1) as

$$Cu^{++} - Cu + 2\bar{e} = 0 \qquad (2)$$

where the signs are chosen so that the number of electrons is a positive quantity. Consider a more general reaction (written in reverse direction) of the type

$$Cu(OH)_2 + 2H^+ + 2\bar{e} = Cu + 2H_2O \qquad (3)$$

This can also be written as

$$Cu(OH)_2 - Cu - 2H_2O + 2H^+ + 2\bar{e} = 0 \qquad (4)$$

Equation (4) is an example of the corrosion reaction, which Pourbaix writes in the generalized form,

$$kA + bB + cH_2O + mH^+ + n\bar{e} = 0 \qquad (5)$$

where k, b, c, m and n represent coefficient of the five quantities in equation (4) and for this reaction have the value 1, -1, -2, +2 and +2 respectively.

The chemical equilibrium involves a characteristic energy, the free energy F (2) and the reported values of free energy are referred to pure elements and certain standard conditions, e.g. the free energy of $Cu(OH)_2$ is - 85000 cal/mole, i.e. its free energy is 85000 cals. lower than the free energy of pure copper, oxygen and hydrogen from which it is made. From considerations of the free energy value obtainable from standard books, one can predict that a given reaction will take place if a decrease in free energy accompanies the reaction. However, two other factors are important in this connection: (1) the concentration of the species in the reaction and (2) the electrode potential E. The concentration factor is given by

$$RT \ln \frac{(a_{Cu})\ (aH_2O)^2}{(a_{Cu(OH)_2})(a_{H^+})^2}$$

where R is the gas constant, T is the absolute temperature and a_A is called the activity of substance A (for dilute solutions, activity can be replaced by concentration). The electrical energy can be given as nfE, where E is the electrode potential, f is the charge carried by one mole of electrons and n is the number of electrons taking part in the reaction. Thus the reaction of equation (3) is at equilibrium when the sum of three terms is zero:

$$\Delta F + RT \ln \frac{(a_{Cu})(a_{H_2O})^2}{(a_{Cu(OH)_2})(a_{H^+})^2} + nfE = 0 \qquad (6)$$

where $\Delta F = F_{Cu} + 2F_{H_2O} - F_{Cu(OH)_2} - 2F_{H^+}$

By rearrangeing equation (6) as

$$- \Delta F + RT\ln(a_{Cu(OH)_2})(a_{Cu})^{-1}(a_{H_2O})^{-2}(a_{H^+})^2 - nfE = 0 \quad (7)$$

By writing the free energy term and the logarithmic term in the generalized form, we obtain,

$$\log a_A^k a_B^b a_{H_2O}^c a_{H^+}^m + \frac{-\Delta F}{2.303RT} = \frac{f}{2.303RT} nE \quad (8)$$

when a change is made to logarithms to the base 10, the term involving the ion concentration is simplified using the definition

$$pH = - \log(H^+) \text{ (approx)} = \log a_{H^+} \quad (9)$$

When the logarithmic term in equation (8) is expanded and the definition of equation (9) is substituted, the result is

$$k\log a_A + b\log a_B + C = mpH + \frac{nE}{0.0591} \quad (10)$$

where

$$C = \frac{1}{1363} (kF_A + bF_B + cF_{H_2O}) \quad (11)$$

Equation (10) can be used to determine the domain of thermodynamic stability of aqueous solutions. One limit of stability is fixed by the hydrogen reduction reaction written as

$$2H^+ + 2\bar{e} - H_2 = 0 \quad (12)$$

Equation (10) becomes very simple for this reaction since most of the terms are zero, i.e.,

$$0 = 2pH + \frac{2E}{0.0591} \quad \text{or}$$

$$E = - 0.0591 \text{ pH} \quad (13)$$

This equation is plotted as the lower sloping line, a, in Fig. (38) and represents the electrode potential at which an aqueous solution of given pH is in equilibrium with H_2 gas. With increase in potential, i.e. below this line, water is unstable and tends to decompose with the reduction of H^+ to gaseous hydrogen.

The other limit of the domain of aqueous stability is determined by the oxidation reaction

$$- H_2O + O_2 + 4H^+ + 4\bar{e} = 0 \qquad (14)$$

for this reaction, C from equation (11) is

$$C = \frac{1}{1363} (-2) (-56690) = + 8.32$$

so that equation (10) becomes

$$+ 8.32 = 4 \text{ pH} + \frac{4E}{0.0591}$$

or

$$E = 1.23 - 0.0591 \text{ pH} \qquad (15)$$

This equation is plotted as the upper sloping line, b, and represents the limit above which water tends to decompose with liberation of oxygen gas. Thus the area between the two sloping lines (a and b) is the domain of thermodynamic stability of water.

Consider reaction (2), for which equation (10) becomes

$$\log a_{Cu^{++}} - 0 + C = 0 \text{ pH} + \frac{2E}{0.0591} \qquad (16)$$

and from equation (11)

$$C = \frac{1}{1363} (F_{Cu^{++}} - F_{Cu})$$

$$= \frac{1}{1363} (15530-0) = 11.4$$

Substituting this value in equation (16),

$$E = 0.337 + 0.0296 \log a_{Cu^{++}} \qquad (17)$$

By definition $\log a_{Cu^{++}}$ is approximately $\log (10^{-6}) = -6$, since in dilute solutions the activity is same as concentration. Equation (17) then, becomes

$$E = 0.159 \text{ volt} \qquad (18)$$

This equation is plotted in Fig. (38) as the horizontal line labelled as Cu^{++}/Cu and, therefore, below this line lies the region of immunity and above this line the corrosion region.

Similarly, the vertical lines separate the region of corrosion and passivity and $Cu(OH)_2$ in this case can confer passivity on the metal. Writing this reaction as

$$Cu(OH)_2 - Cu^{++} - 2H_2O + 2H^+ = 0 \qquad (19)$$

substitution in equation (10) gives

$$0 - \log a_{Cu^{++}} + C = 2pH + 0 \qquad (20)$$

with

$$C = \frac{1}{1363} (- 85000 - 15530 - 2 \times - 56690) = 9.21$$

With 10^{-6} molar concentration of cupric ion, equation (20) reduces to pH = 7.6. This line is plotted vertically and is labelled as $Cu^{++}/Cu(OH)_2$. In addition to this reaction, it is necessary to consider the reaction of cuprous oxide formation as

$$- Cu_2O + 2Cu^{++} + H_2O - 2H^+ + 2\bar{e} = 0 \qquad (21)$$

so that equation (10) becomes

$$0 + 2\log a_{Cu^{++}} + C = -2pH + \frac{2E}{0.0591} \qquad (22)$$

with C = 6.86 and 10^{-6} (Cu^{++}) molar concentration, equation (22) becomes

$$E = -0.152 + 0.0591\ pH \qquad (23)$$

This equation is plotted as the sloping line labelled as Cu^{++}/Cu_2O. The other lines on the right of the diagram are similarly constructed by considering the additional reactions. These reactions are

(a) $2Cu + H_2O = Cu_2O + 2H^+ + 2\bar{e}$

with

$$E = 0.471 - 0.0591\ pH$$

for the line Cu_2O/Cu

(b) $Cu(OH)_2 = HCu\bar{O}_2 + H^+$

leading to the equa ion

$$pH = 11.52$$

for the line $Cu(OH)_2/HCu\bar{O}_2$

(c) $Cu_2O + 3H_2O = 2HCu\bar{O}_2 + 4H^+ + 2\bar{e}$

leading to equation

$$E = 1.428 - 0.1182\ pH$$

for the line $Cu_2O/HCu\bar{O}_2$,

(d) $Cu_2O + 3H_2O = 2Cu\bar{\bar{O}}_2 + 6H^+ + 2\bar{e}$

leading to equation

$$E = 2.205 - 0.1773\ pH$$

for the line $Cu_2O/Cu\bar{\bar{O}}_2$

This completes the derivation of the Pourbaix diagram for the Cu - H_2O system.

APPENDIX II

The Tafel Equation

The general usefulness of the various aspects of Tafel equation have already been discussed in the previous chapter and it is considered relevant here to give a detailed mathematical derivation of the equation explaining the associated phenomenon.

Let us consider a general oxidation-reduction reaction at the surface of an electrode as

$$\text{Reduced species} \rightleftharpoons \text{oxidised species} + ne \qquad (1)$$

The rate of the electron exchange reaction at the surface of the electrode may be expressed as molecules reacting per unit time per unit area. If we suppose that the process is of the first order, the reaction rates (forward and backward) will be proportional to the concentration of the reactants. Therefore,

$$\text{rate of oxidation} = K_1 (\text{Red})_e$$

$$\text{rate of reduction} = K_2 (\text{Ox})_e$$

where K_1 and K_2 are the rate constants for the oxidation and the reduction reaction respectively and $(\text{Red})_e$ and $(\text{Ox})_e$ are the concentrations of reductant and oxidant respectively at the surface of the electrode.

Let the currents associated with the oxidation reaction be i_a (anodic current) and with the reduction reaction be i_c (cathodic current). The reaction representing equation (1) has

a finite probability for the forward and the backward reactions becoming equal and when this occurs, the system is said to be in Equilibrium State. Therefore, at this point

$$i_a = i_c \quad \text{(in magnitude)}$$

or

$$i_a - i_c = 0$$

and, hence, at equilibrium, no net current will flow although each individual process has a finite rate. This finite rate is called the exchange current, i_o.

When oxidation rate = reduction rate,

$$i_a = i_c = i_o$$

Disturbance of equilibrium will either increase the anodic or the cathodic current and in practice, therefore, the measured values are the resultant of both these currents, e.g. the measured current for an anodic process

$$= i_a - i_c$$

and for the cathodic process

$$= i_c - i_a$$

The quantities defined above will be used in the actual derivation of the Tafel equation. Let an electrode M of unit area be in a reversible equilibrium with its cation M^{x+} in solution. This situation means that the rate of ionization of M and the rate of discharge of M^{x+} ions is equal and, therefore, no net current is flowing. According to the fundamental laws of thermodynamics only those M atoms will ionize which have

achieved a certain minimum energy and the further rate of the reaction will depend on the magnitude of this value. The same is true for the discharge reaction, although the value of the minimum energy may be different. This energy is called the free energy of activation, say, ΔG_1^* and ΔG_2^* for the oxidation and the reduction reaction respectively. The difference of these two energies is called the free energy of reaction, ΔG, (Pourbaix calls this energy as Free Enthalpy) and has been related to the reversible electrode potential, E_o, by the relation.

$$\Delta G = XE_oF \qquad (2)$$

where F is Faraday and X is the number of electrons taking part in the reaction. Consideration of the Maxwell's distribution law, which governs the distribution of energy among the reacting particles, will, therefore, give the rates of the reactions as:

$$\text{oxidation rate} = y_1 = K_1 \exp\left(\Delta G_1^*/RT\right) \qquad (3)$$

and

$$\text{reduction rate} = y_2 = K_2 \exp\left(\Delta G_2^*/RT\right) \qquad (4)$$

where K_1 and K_2 are the rate constants for the oxidation and reduction reaction respectively. At equilibrium where $y_1 = y_2$ and $i_a = i_c = i_o$ and the fact the rates are proportional to the current densities, the following equation may be written

$$y_1 = y_2 = i_o \qquad (5)$$

This analysis only applies to the reversible systems but the situation will change if the equilibrium is disturbed, e.g. to the right in equation (1) which will result in net oxidation

reaction. Because of the irreversibility of the process, the equilibrium value will change by amount η_t, called the overpotential. The overpotential is said to have two effects:

(1) a part of it makes the ionization of M more rapid by decreasing the activation energy for the oxidation from ΔG_1^* to $\Delta G_1^* - fxn_tF$, and (2) the remainder reduces the rate of discharge of M^{X+} by increasing the activation energy for the reduction process from ΔG_2^* to $\Delta G_2^* + (1 - f)Xn_tF$, where f is the fraction of the overpotential assisting the oxidation reaction.

The rates under irreversible conditions can, therefore, be written as: (using equations (3) and (4))

$$\text{oxidation rate} = y_3 = K_1 \exp\left(-\frac{\Delta G_1^* - fXn_tF}{RT}\right)$$

$$= y_1 \exp\left(\frac{fXn_tF}{RT}\right) \qquad (6)$$

$$\text{reduction rate} = y_4 = K_2 \exp\left(-\frac{\Delta G_2^* + (1 - f)Xn_tF}{RT}\right)$$

$$= y_2 \exp\left(-\frac{(1 - f)Xn_tF}{RT}\right) \qquad (7)$$

For an overall oxidation reaction; $y_3 > y_4$ and remembering that the rates are proportional to the current densities, we obtain using equations 5, 6, and 7 the following equation

$$i_a = i_3 - i_4 = i_o \exp\left(\frac{fXn_tF}{RT}\right) - i_o \exp\left(-\frac{(1 - f)Xn_tF}{RT}\right) \qquad (8)$$

The equation (8) is also applicable to the cathodic reaction provided the associated potential is more negative than the

equilibrium potential and, hence, the equation can be written in the general form to describe both the processes as:

$$i = i_o \exp\left(\frac{fXn\eta F}{RT}\right) - i_o \exp\left(-\frac{(1-f)Xn\eta F}{RT}\right) \qquad (9)$$

where i is i_a or i_c depending upon whether η is positive or negative with respect to the equilibrium potential. Equation (9) is a general equation of electrode kinetics and belongs to the family of equations commonly known as i - η equations.

Consider a special case of equation (9) at high irreversibility (η > 0.05 volt), i.e. the situation in which the factor contributing the opposite reaction is very small and, therefore, in this case the second term on the right hand side of equation (9) can be ignored and the new equation, thus obtained is:

$$i = i_o \exp\left(\frac{fXn\eta F}{RT}\right) \qquad (10)$$

This equation can be written for oxidation and reduction processes as follows:

$$\eta = -\left(2.303RT/_{fXF}\right) \log i_o + \left(2.303RT/_{fXF}\right) \log i_a \qquad (11)$$

and

$$\eta = +\left(2.303RT/_{fXF}\right) \log i_o + \left(2.303RT/_{fXF}\right) \log i_c \qquad (12)$$

Writing a for $\pm\left(2.303RT/_{fXF}\right) \log i_o$, b for $\left(2.303RT/_{fXF}\right)$ and i for i_a or i_c, equation (11) and (12) can be written in the general form as

$$\eta = a + b \log i \qquad (13)$$

Equation (13) is known as the Tafel equation.

ACKNOWLEDGEMENTS

The author is extremely indebted to his supervisor, Professor J. S. L. Leach, for his constant encouragement, kindness and advice. The discussion with other members of the Corrosion Group, especially Dr. A. Y. Nehru, are sincerely appreciated. He would also like to thank Dr. P. A. Brook for writing the computer programme and interpreting the results, and expresses his gratitute to Miss J. Parry who, at short notice, undertook the typing of this thesis.

The financial support for this work by the U.K.A.E.A., a scholarship from Colombo Plan seconded by the Pakistan Atomic Energy Commission and the provision of laboratory facilities by Professor J. G. Ball are gratefully acknowledged.

REFERENCES

1. P. Van Rysselberghe

   (a) Introduction to "Atlas of Electrochemical Equilibria in Aqueous Solutions" by M. Pourbaix. Pergamon-London (1966).

   (b) First chapter. "Modern Aspects of Electrochemistry" vol. 4. Butterworths - London (1954)

2. M. Pourbaix, "Atlas of Electrochemical Equilibria in Aqueous Solutions". Pergamon-London (1966)

3. U. R. Evans, "The Corrosion and Oxidation of Metals". Arnold-London (1960)

4. R. M. Garrels. P. 89 Ref. No. 2.

5. D. C. Grahame, Chem. Rev., 41, 441, (1947).

6. J. Tafel, Z. Physik. Chem. 50, 641, (1905)
   Reported by Ref. No. 9.

7. T. Erdey-Gruz and M. Volmer, Z. Physik. Chem. 150A, 203, (1930). Reported by Ref. No. 9.

8. J. Horiuti and M. Ikusima, Proc. Imp. Acad. (Tokyo) 15, 39, (1939).

9. F. P. Bowden and J. N. Agar, Ann. Rept. Progr. Chem. 35, 90, (1938).

10. J. N. Agar and F. P. Bowden, Proc. Roy. Soc. 169A, 206, (1938-39).

11. E. C. Potter, 'Electrochemistry'
    Clever-Hume, London (1961)

12. E. R. G. Eckert, "Heat and Mass Transfer", 2nd Edition. McGraw-Hill, New York (1959).

13. J. O'M. Bockris, "Modern Aspects of Electrochemistry" Butterworths-London (1954)

14. W. B. Pilling and R. E. Bedworth, J.I.M., 29, 529, (1923)

15. U. R. Evans, "The Corrosion and Oxidation of Metals". Arnold-London (1960)

16. N. Cabrera and N. F. Mott, Repts. Progr. Phys. 12, 163, (1948-49)

17. H. H. Uhlig, J. Pickett and J. Macnairn, Acta Met., 7, 111, (1959).

18. W. E. Campbell and U. B. Thomas, Trans. E.C.S. 91, 623, (1947)

19. J. K. Dawson, G. Long, W. E. Seddon and J. F. White, Report GCM/U.K./B-21 U.K.A.E.A. (1967).

20. H. H. Uhlig, Acta Met., 4, 541, (1956).

21. D. H. Bradhurst, J. E. Draley, and C. J. Van Drunsen, J.E.C.S. 112, 1171, (1965).

22. H. H. Uhlig, J.E.C.S. 113, 1345, (1966).

23. J. F. Dewald J.E.C.S. 102, 1, (1955).

24. A. Y. Nehru, University of London, Ph.D. Thesis (1962)

25. F. A. Champion and M. Whyte, J.I.M. 75, 737, (1949).

26. E. A. Gulbransen, Trans. E.C.S. 83, 301, (1943).

27. D. Cubiccioti, J. Am. Chem. Soc. 72, 4138, (1950).

28. J. Belle and M. W. Mallet J.E.C.S. 101, 339, (1954).

29. A. Charlesby, Acta Met. 1, 340, 348, (1953).

30. H. A. Porte, J. G. Schnizlein, R. C. Vogel and D. F. Fisher, J.E.C.S. 107, 506, (1960).

31. O. Kubaschewski and B. E. Hopkins. "Oxidation of Metals and Alloys". Butterworths - London (1953)

32. E. A. Gulbransen and K. F. Andrew. Trans. Am. Inst. Min (Met.) Engs. 212, 281, (1958).

33. K. Orthagon and P. Kofstad. J.E.C.S. 109, 204, (1962).

34. W. W. Smeltzer, R. R. Hoering and J. S. Kirkaldy. Acta Met., 9, 880, (1961).

35. J. S. L. Leach and A. Y. Nehru, "Corrosion of Reactor Materials". Vol. I, I.A.E.A. Vienna (1962)

36. R. K. Geary, U.S.A.E.C. Rept. Westinghouse Corps. WAPD - 127, Part I (1955)
M. W. Burkart Part III (1956)

37. J. E. Draley and W. E. Ruther, Corrosion 12, 441, 481, (1956).

38. J. E. Draley and W. E. Ruther, J.E.C.S. 104, 329, (1957).

39. D.E. Thomas and S. Kass, J.E.C.S. 104, 261, (1957).

40. J. N. Wanklyn and B. E. Hopkinson, J. App. Chem. 8, 496, (1958).

41. R. Cigna, J. S. L. Leach and A. Y. Nehru, J.E.C.S., 113, 105, (1966).

42. B. Lustman and F. Kerze. "The Metallurgy of Zirconium" McGraw-Hill (1955).

43. J. T. Waber, U.S.A.E.C. Rept. Los Alomos 2035 (1958).

44. J. T. Waber, Paper 699, Proc. 2nd Int. Conf. on Peaceful uses of A. Energy. Geneva (1958).

45. J. S. L. Leach, J.I.M. 88, 24, (1959).

46. C. Wagner, J. Chem. Phys. 21, 1819, (1953).

47. E. A. Gulbransen. Trans. E.C.S. 81, 327, (1942).

48. W. McKewan and W. M. Fassell, Jr. Trans. Amer. Inst. min (metall.) Engrs. 197, 1127, (1953).

49. C. N. Hinshelwood, Proc. Roy. Soc., 102-A, 318, (1922-23).

50. W. E. Campbell and U. B. Thomas, Trans. E.C.S. 91, 623, (1947).

51. U. R. Evans and L. C. Bannister, Proc. Roy. Soc. 125-A, 370, (1929).

52. W. E. Campbell and U. B. Thomas, Trans. E.C.S. 76, 303, (1939).

53. A. B. Winterbottom, Communication to Ref. No.52, Page 326.

54. R. H. Lambert and D. J. Trevoy, J.E.C.S. 105, 18, (1959).

55. K. Hauffe "Oxidation of Metals" Plenum Press - New York, 1965, Page 439.

56. L. Young, Trans. Faraday Soc. 51, 1250 (1955)

57. K. F. Lorking, J. App. Chem. 10, 449, (1960).

58. J. J. McMullen and N. Hackerman, J.E.C.S. 106, 341, (1959).

59. J. V. Petrocelli, J.E.C.S. 106, 566, (1959).

60. J. N. Wanklyn and D. R. Silvester, J.E.C.S. 105, 647, (1958).

61. J. N. Wanklyn and B. E. Hopkinson, J. App. Chem. 8, 496, (1958).

62. J. S. L. Leach J.I.M. 88, 24, (1959).

63. G. Tammann, Z. Anorg. Chem. 111, 78, (1920).
Reported by Ref. No. (64). Page (96).

64. U. R. Evans, "Metallic Corrosion, Passivity and Protection" 2nd Edition Arnold and Co. - London (1946) Page (97).

65. F. H. Constable Proc. Roy. Soc., 117-A, 376, (1927-28).

66. H. A. Miley, (i) Carnegie Scholarship Memoirs (Iron and Steel Institute), 25, 197, (1936), (ii) J. Am. Chem. Soc. 59, 2626, (1937).

67. L. E. Price and G. J. Thomas, J.I.M., 63, 29, (1938).

68. L. Tronstad, Trans. Faraday Soc. 29, 502, (1933).

69. A. B. Winterbottom

(a) Appendix in Ref. No. (64) Page (802).

(b) Trans. Faraday Soc. 42, 487, (1946).

(c) J. Op. Soc. Amer. 38, 1074, (1948).

70. O. S. Heavens, "Optical Properties of Thin Solid Films". Butterworths - London (1955) Chapter 4.

71. R. W. Ditchburn, "Light" 2nd Edition, Blackie - London (1963). Chapters 14 and 15.

72. P. A. Jaquet. Proc. 1st World Met. Cong. (1951).

73. W. J. M. Tegart, "The Electrolytic and Chemical Polishing of Metals in Research and Industry". Pergamon - London (1959).

74. M. Stern. J.E.C.S 102, 356, (1955).

75. A. E. Lorch, Trans. E.C.S., 74, 587, (1938).

76. C. Wagner and W. Traud, Z. Elektrochem. 44, 391, (1938).

77. J. A. V. Butler and G. Armstrong, J. Chem. Soc. 743, (1934).

78. A. Charlesby, Acta Met. 1, 340, (1953).

79. A. Guntherschulze and H. Betz, Z. Elektrochem. 37, 726, (1931) (reported by Ref. No. 78).

80. B. Cox, J.E.C.S., 108, 24, (1961).

81. P. A. Brook, Private Communications (1968).

82. K. Kiukkola and C. Wagner, J.E.C.S. 104, 379, (1957).

83. M. W. Mallet and W. M. Albrecht, J.E.C.S. 102, 407, (1955).

84. A. R. Bray, P. W. M. Jacobs and L. Young, J. Nuc. Mat. 1, 356, (1959).

85. D. L. Douglas "Corrosion of Reactor Materials". Vol II. I.A.E.A. Vienna, (1962).

86. J. S. L. Leach and A. Y. Nehru, J. Nuc. Mat. 13, 270, (1964).

87. S. J. Gregg and W. B. Jepson. J.I.M. 87, 187, (1958).

88. E. C. Potter and G. M. W. Mann. Proc. 1st Int. Cong. Met. Corrosion. Butterworth - London (1962).

89. D. E. Thomas U.S.A.E.C. Westinghouse WAPD-T 186 (1954).

90. D. E. Thomas and F. Forscher, J. Metals. 8, 640, (1956).

91 P. G. H. Draper Unpublished work. Reported by Ref. No. 41.

```
08/05/68   16.39.07
EDINBURGH UNIVERSITY ATLAS AUTOCODE   19/12/67


MET/ZAP/25
     2   BEGI
    67       ROUTINE ZAP
    88       END OF ROUTINE
    89   END OF PROGRAM

PROGRAM (*PERM) OCCUPIES 2784 WORDS
PROGRAM DUMPED
COMPILING TIME   21 SEC /  10 SEC
    1.5000000000*  1
    4.4000000000*  1    2.0000000000*-1    1.0000000000*-1
VALUE OF ORIGIN FOR POST-TRANSITION PERIOD
TO   45.000  X0    0.200
CORRECTED VALUES OF LOG(X) AND LOG(T)
 LOG(T)    LOG(X)
  2.190   -0.523
  2.781   -0.097
  3.333    0.255
  3.636    0.447
  3.872    0.580
  3.997    0.653
 0.0000*-40    4.5000000000*  1
    5.4000000000*  1    3.6000000000*-1    2.6000000000*-1
VALUE OF ORIGIN FOR POST-TRANSITION PERIOD
TO   55.000  X0    0.360
CORRECTED VALUES OF LOG(X) AND LOG(T)
 LOG(T)    LOG(X)
  2.290   -0.466
  2.736   -0.194
  3.159    0.057
  3.468    0.215
  3.694    0.330
  3.899    0.422
 0.0000*-40    9.0000000000*  1
    8.9000000000*  1    6.0000000000*-1    5.0000000000*-1    4.0000000000*-1
VALUE OF ORIGIN FOR POST-TRANSITION PERIOD
TO   90.000  X0    0.600
CORRECTED VALUES OF LOG(X) AND LOG(T)
 LOG(T)    LOG(X)
  2.000   -0.699
  2.462   -0.398
  2.880   -0.155
  3.280    0.041
  3.492    0.146
  3.949    0.342
 0.0000*-40    1.1000000000*  2
    1.0900000000*  2    8.6000000000*-1    7.6000000000*-1    6.6000000000*-1
VALUE OF ORIGIN FOR POST-TRANSITION PERIOD
TO  110.000  X0    0.860
CORRECTED VALUES OF LOG(X) AND LOG(T)
 LOG(T)    LOG(X)
  1.699   -0.854
  2.255   -0.468
  2.732   -0.131
  3.075    0.057




  3.460    0.241
  3.894    0.438
 0.0000*-40    9.0000000000*  1
    8.9000000000*  1    1.0000000000*  0    9.0000000000*-1    8.0000000000*-1
VALUE OF ORIGIN FOR POST-TRANSITION PERIOD
TO   90.000  X0    1.000
CORRECTED VALUES OF LOG(X) AND LOG(T)
 LOG(T)    LOG(X)
  1.699   -0.699
  2.361   -0.222
  2.748    0.000
  3.303    0.301
  3.690    0.477
  3.979    0.602
 0.0000*-40    1.0500000000*  2
    1.0400000000*  2    8.5000000000*-1    7.5000000000*-1    6.5000000000*-1
VALUE OF ORIGIN FOR POST-TRANSITION PERIOD
TO  105.000  X0    0.850
CORRECTED VALUES OF LOG(X) AND LOG(T)
 LOG(T)    LOG(X)
  1.977   -0.824
  2.389   -0.456
  2.694   -0.260
  3.277    0.061
  3.612    0.190
  3.897    0.332
 0.0000*-40    8.3000000000*  1
    8.2000000000*  1    4.0000000000*-1    3.0000000000*-1    2.0000000000*-1
VALUE OF ORIGIN FOR POST-TRANSITION PERIOD
TO   83.000  X0    0.400
CORRECTED VALUES OF LOG(X) AND LOG(T)
 LOG(T)    LOG(X)
  2.088   -0.699
  2.501   -0.398
  2.753   -0.222
  3.234    0.041
  3.520    0.204
  3.959    0.415
 0.0000*-40    8.5000000000*  1
    8.4000000000*  1    9.0000000000*-1    8.0000000000*-1
VALUE OF ORIGIN FOR POST-TRANSITION PERIOD
TO   85.000  X0    0.900
CORRECTED VALUES OF LOG(X) AND LOG(T)
 LOG(T)    LOG(X)
  1.398   -1.000
  2.060   -0.523
  2.498   -0.222
  2.936    0.041
  3.520    0.322
  3.914    0.491
 0.0000*-40    8.5000000000*  1
    8.4000000000*  1    1.1000000000*  0    1.0000000000*  0    9.0000000000*-1
VALUE OF ORIGIN FOR POST-TRANSITION PERIOD
TO   85.000  X0    1.100
CORRECTED VALUES OF LOG(X) AND LOG(T)
 LOG(T)    LOG(X)
  1.977   -0.523
  2.406   -0.222
  2.676   -0.046
  3.282    0.279
  3.691    0.462




  3.949    0.568
 0.0000*-40    7.5000000000*  1
    7.4000000000*  1    1.2000000000*  0    1.1000000000*  0    1.0000000000*  0
VALUE OF ORIGIN FOR POST-TRANSITION PERIOD
TO   75.000  X0    1.200
CORRECTED VALUES OF LOG(X) AND LOG(T)
 LOG(T)    LOG(X)
  1.875   -0.523
  2.484   -0.097
  2.860    0.114
  3.122    0.255
  3.521    0.447
  3.858    0.580
 0.0000*-40    1.0500000000*  2
    1.0400000000*  2    6.2000000000*-1    5.0000000000*-1
VALUE OF ORIGIN FOR POST-TRANSITION PERIOD
TO  105.000  X0    0.600
CORRECTED VALUES OF LOG(X) AND LOG(T)
 LOG(T)    LOG(X)
  2.021   -0.699
  2.439   -0.398
  2.951   -0.046
  3.277    0.146
  3.543    0.279
  3.723    0.380
 0.0000*-40    6.5000000000*  1
    6.4000000000*  1    1.0000000000*  0    9.0000000000*-1    8.0000000000*-1
VALUE OF ORIGIN FOR POST-TRANSITION PERIOD
TO   65.000  X0    1.000
CORRECTED VALUES OF LOG(X) AND LOG(T)
 LOG(T)    LOG(X)
  1.653   -0.699
  2.311   -0.222
  2.638    0.000
  3.239    0.301
  3.606    0.477
  3.925    0.602
 0.0000*-40    5.0000000000*  1
    4.9000000000*  1    1.0000000000*  0    9.0000000000*-1    8.0000000000*-1
VALUE OF ORIGIN FOR POST-TRANSITION PERIOD
TO   50.000  X0    1.000
CORRECTED VALUES OF LOG(X) AND LOG(T)
 LOG(T)    LOG(X)
  1.699   -0.523
  2.176   -0.222
  2.518    0.000
  3.096    0.301
  3.469    0.477
  3.774    0.602
 0.0000*-40    4.5000000000*  1
    4.4000000000*  1    1.1000000000*  0    1.0000000000*  0    9.0000000000*-1    9.0000000000*-1    4.4000000000*  1
    4.3000000000*  1    1.1000000000*  0    1.0000000000*  0    1.0000000000*  0    4.3000000000*  1
    4.2000000000*  1    1.1000000000*  0    1.0000000000*  0
VALUE OF ORIGIN FOR POST-TRANSITION PERIOD
TO   43.000  X0    1.000
CORRECTED VALUES OF LOG(X) AND LOG(T)
 LOG(T)    LOG(X)
  1.826   -0.301
  2.316    0.000
  2.906    0.301
  3.291    0.477




  3.597    0.602
  3.842    0.699
 0.0000*-40


STOPPED AT LINE  89
MET/ZAP/25
RUNNING TIME   15 SEC /  3 SEC
```

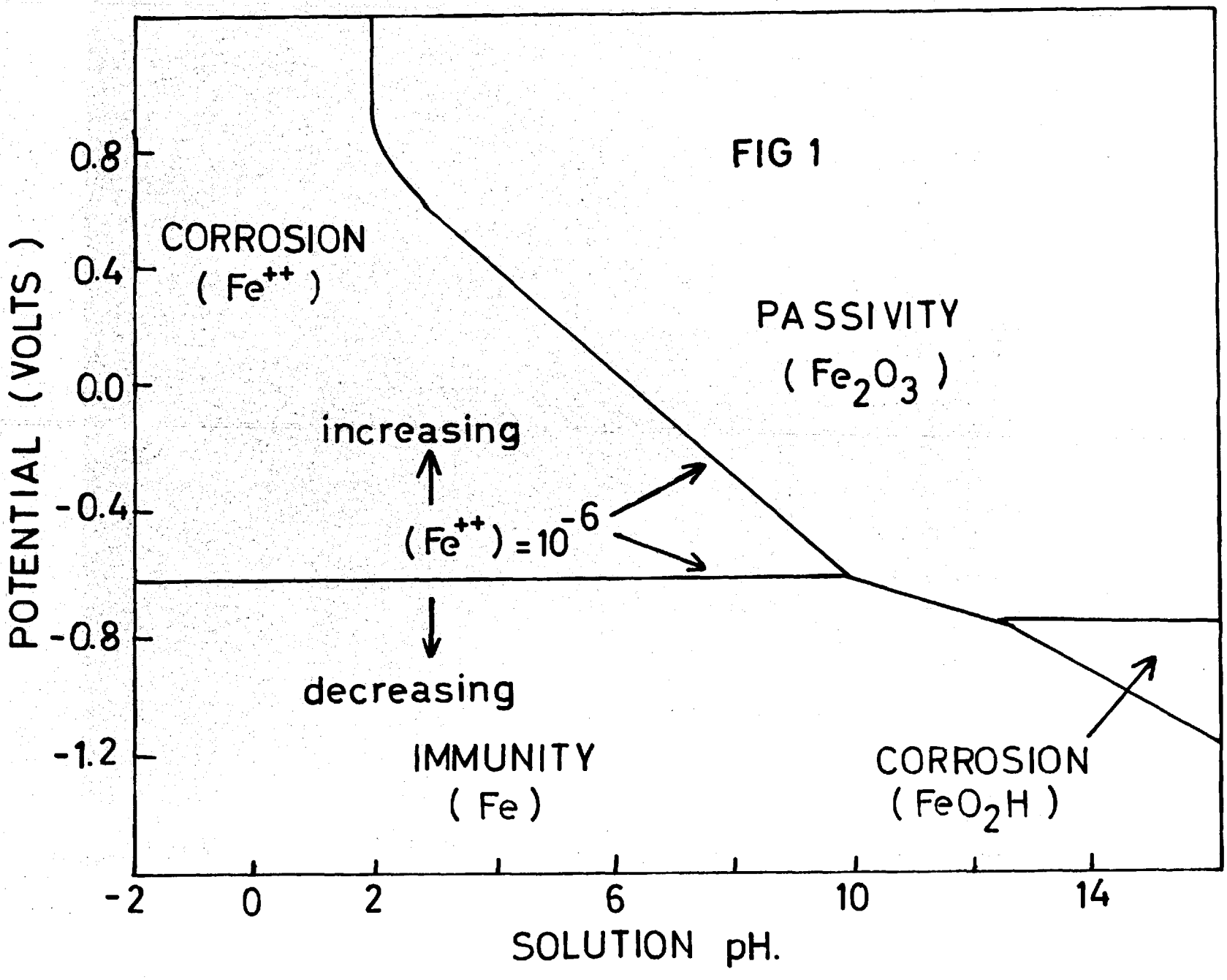
FIG 1
CORROSION
(Fe^{++})
PASSIVITY
(Fe_2O_3)
increasing
(Fe^{++}) = 10^{-6}
decreasing
IMMUNITY
(Fe)
CORROSION
(FeO_2H)
POTENTIAL (VOLTS)
0.8
0.4
0.0
-0.4
-0.8
-1.2
-2
0
2
6
10
14
SOLUTION pH.

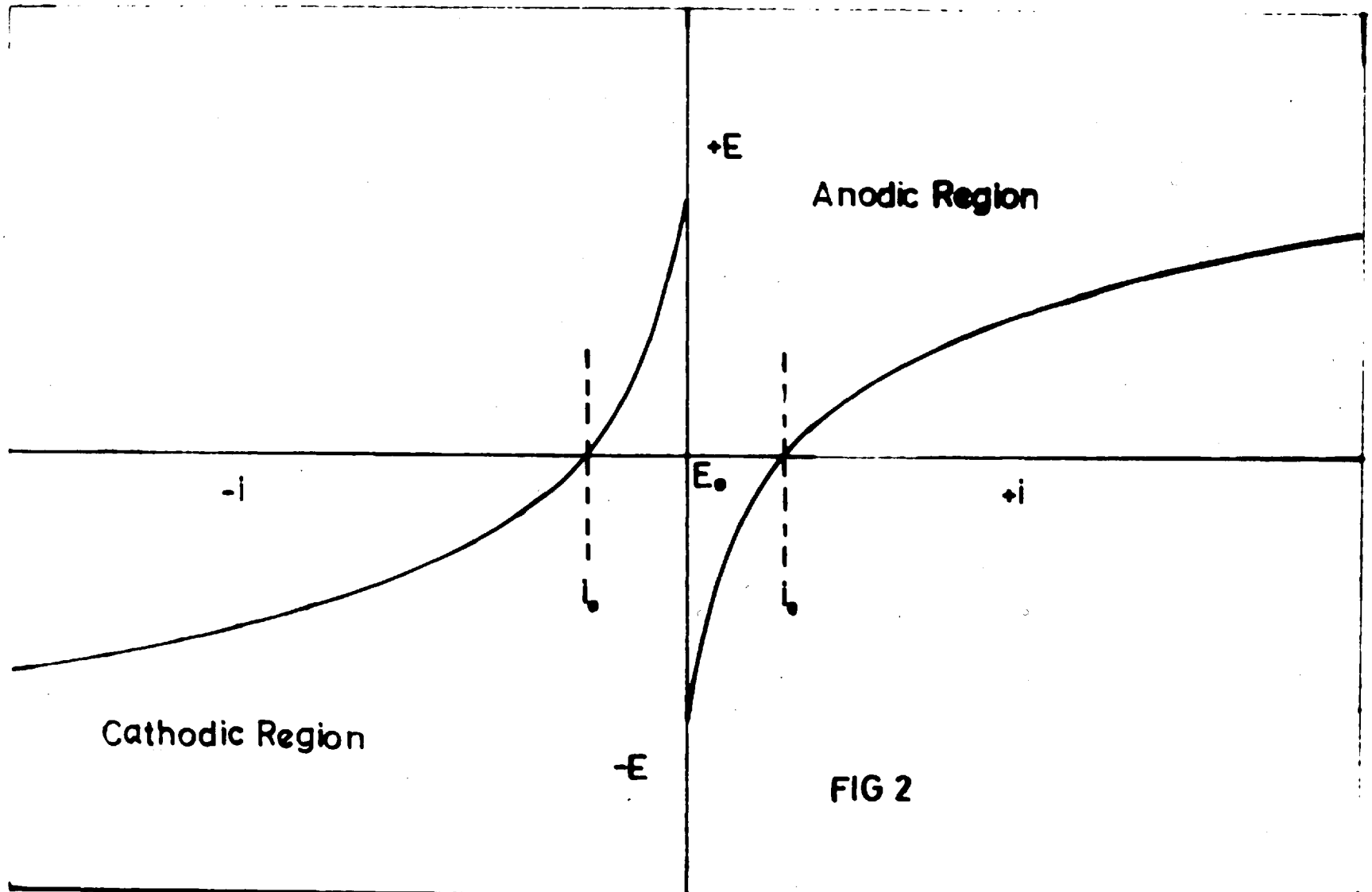

FIG 2

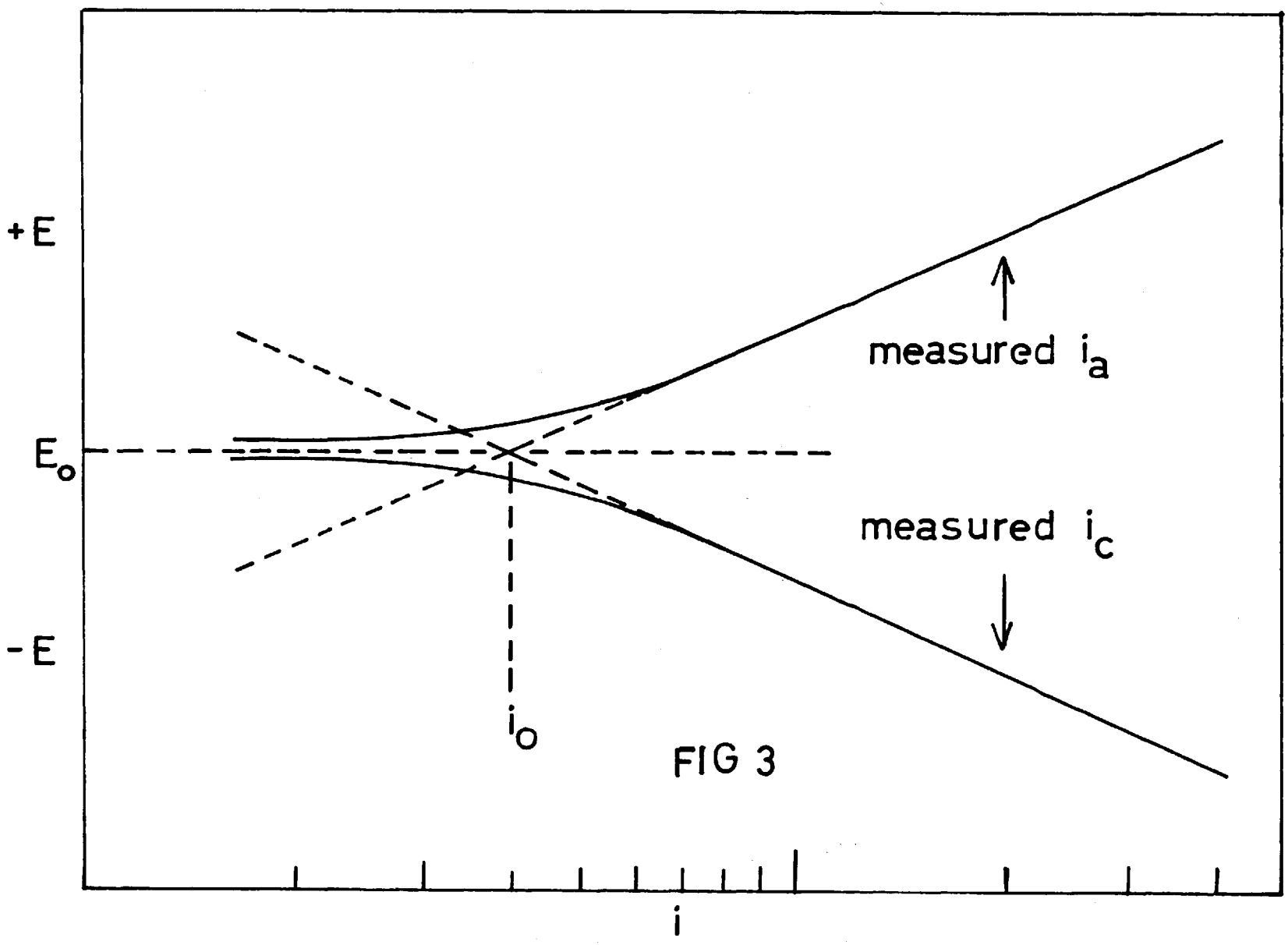

FIG 3

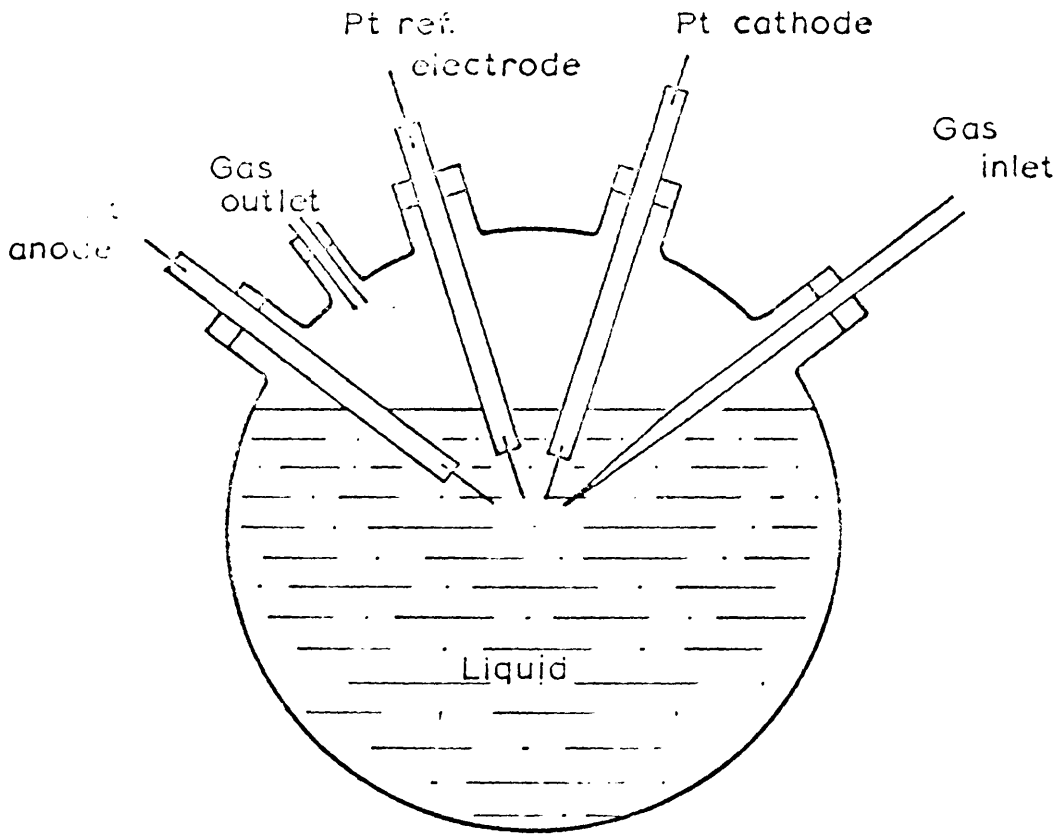

FIG. 4 GLASS CELL

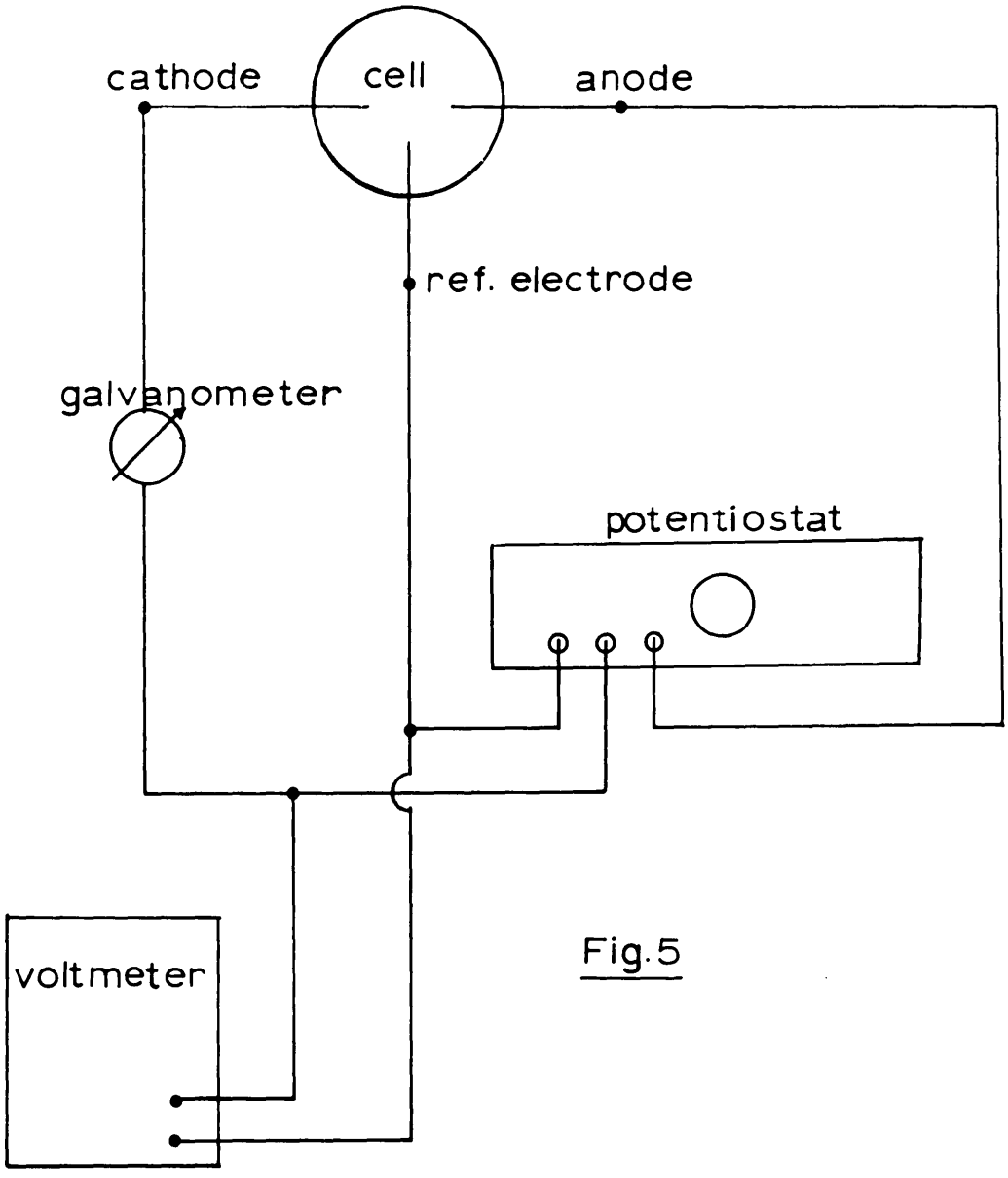

Fig.5

ELECTRICAL CIRCUIT FOR POLARIZATION MEASUREMENTS

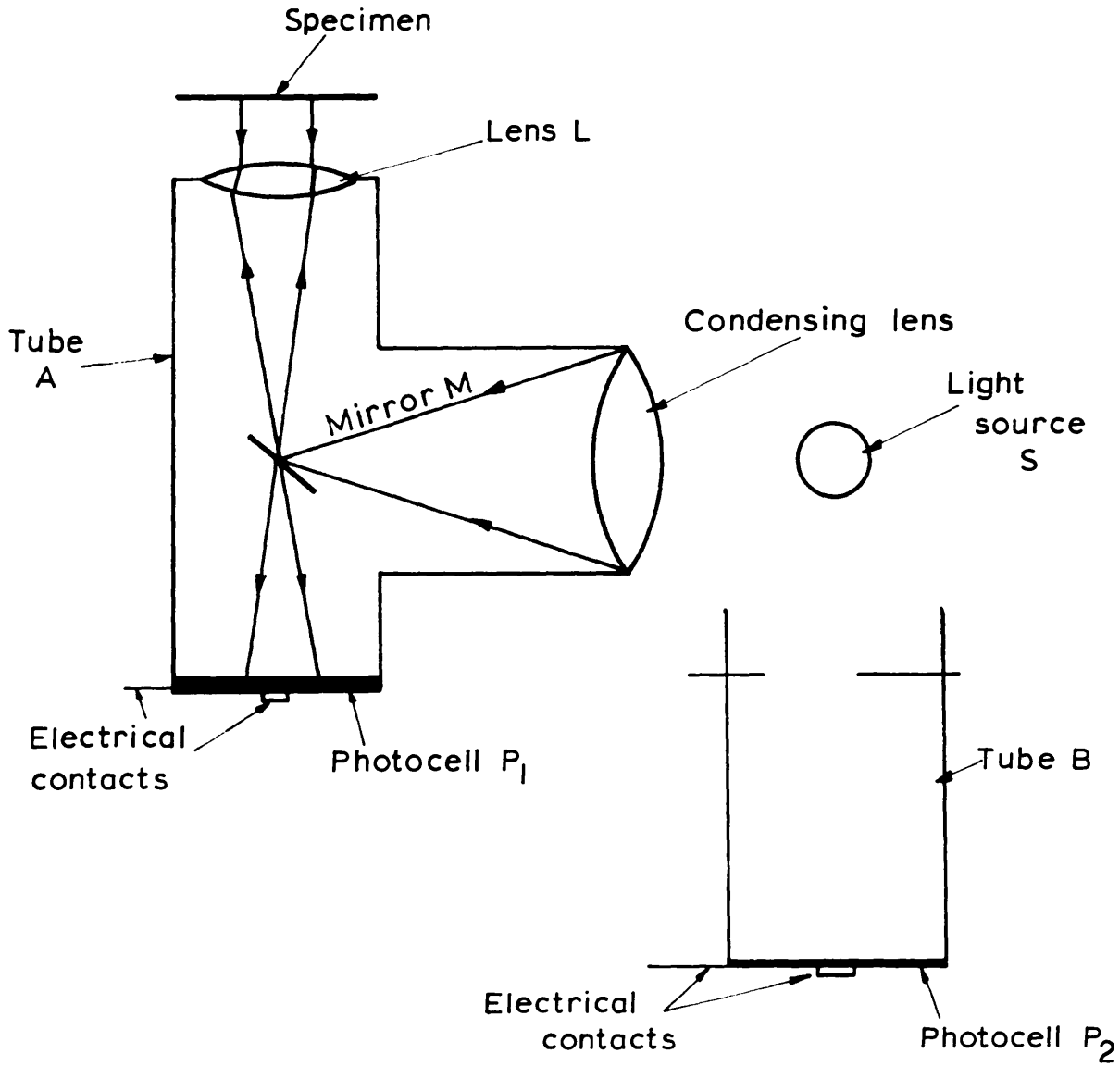

FIG. 6 OPTICAL ARRANGEMENT FOR RATE MEASUREMENTS

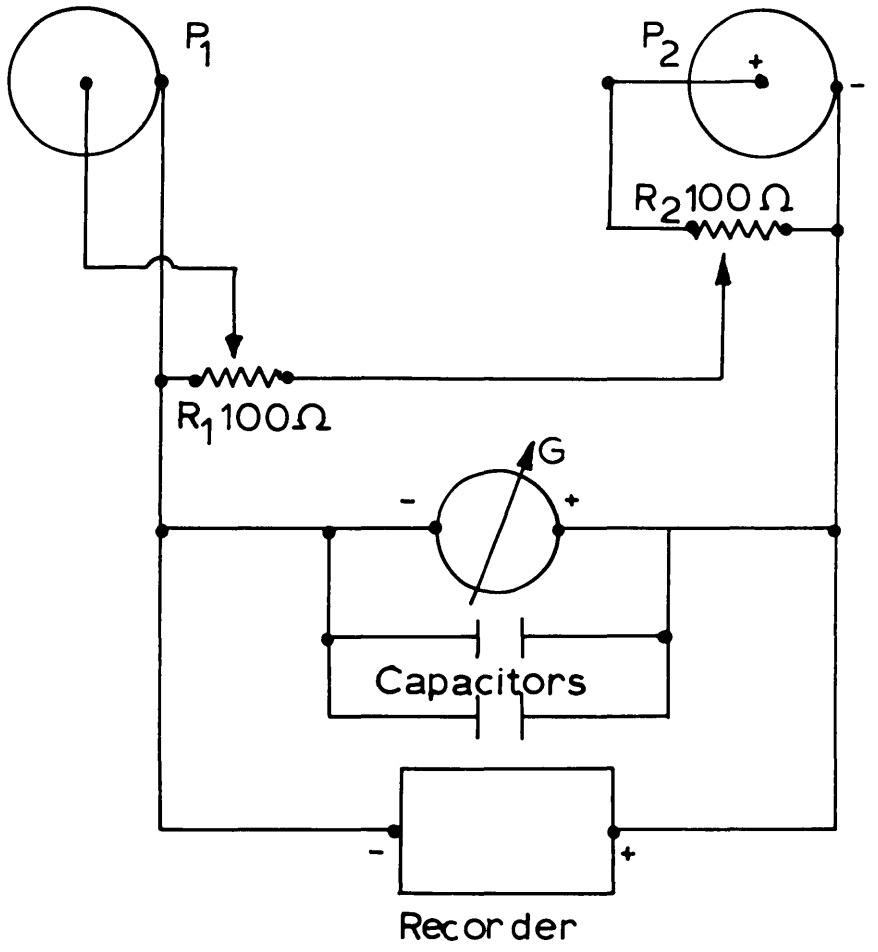

Fig.7

ELECTRICAL CIRCUITRY OF THE OPTICAL EQUIPMENT

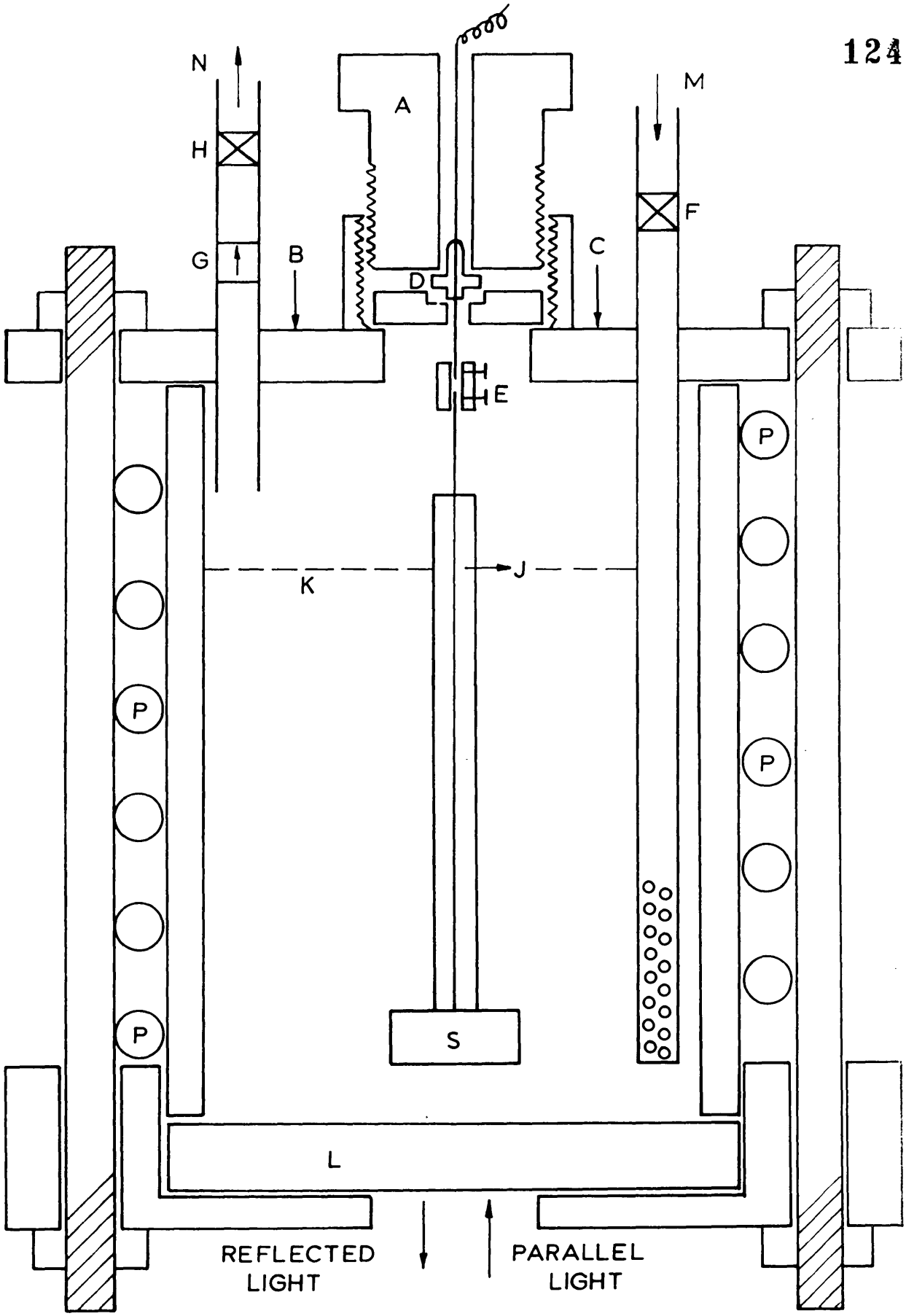

FIG. 8 AUTOCLAVE

AUTOCLAVE DETAILS

A B C	ARRANGEMENTS FOR INTRODUCING ELECTRODES
D	PRESSURE SEAL
E	S.S.CONNECTOR
F	VALVE
G	PRESSURE GAUGE
H	RELIEF VALVE
J	ARALDITE INSULATION
K	LIQUID LEVEL
L	TOUGHENED GLASS DISC
M	GAS INLET
N	GAS OUTLET
S	SPECIMEN
P	HEATING COIL

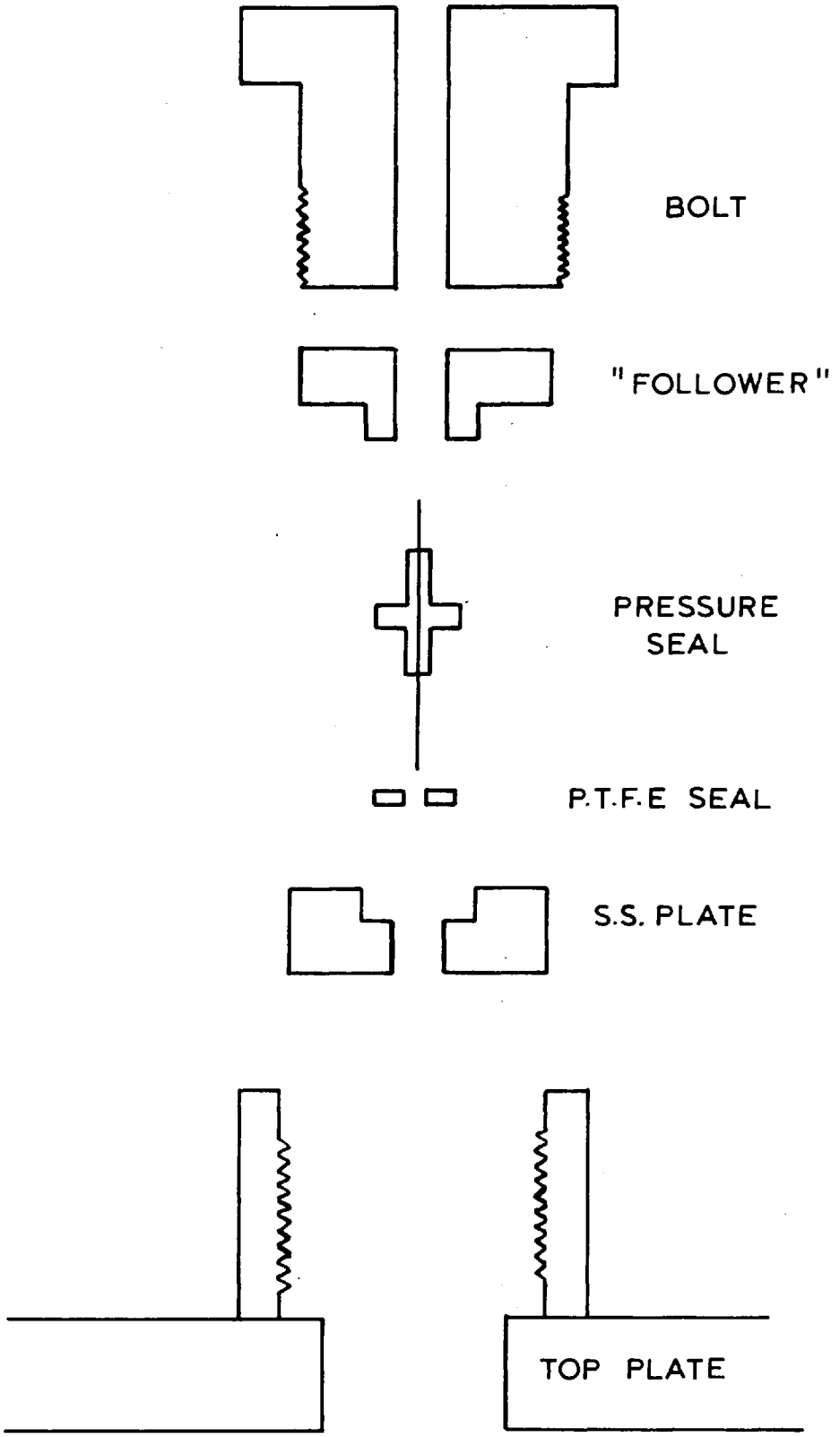

FIG.9 ARRANGEMENT FOR INTRODUCING SPECIMEN INTO AUTOCLAVE

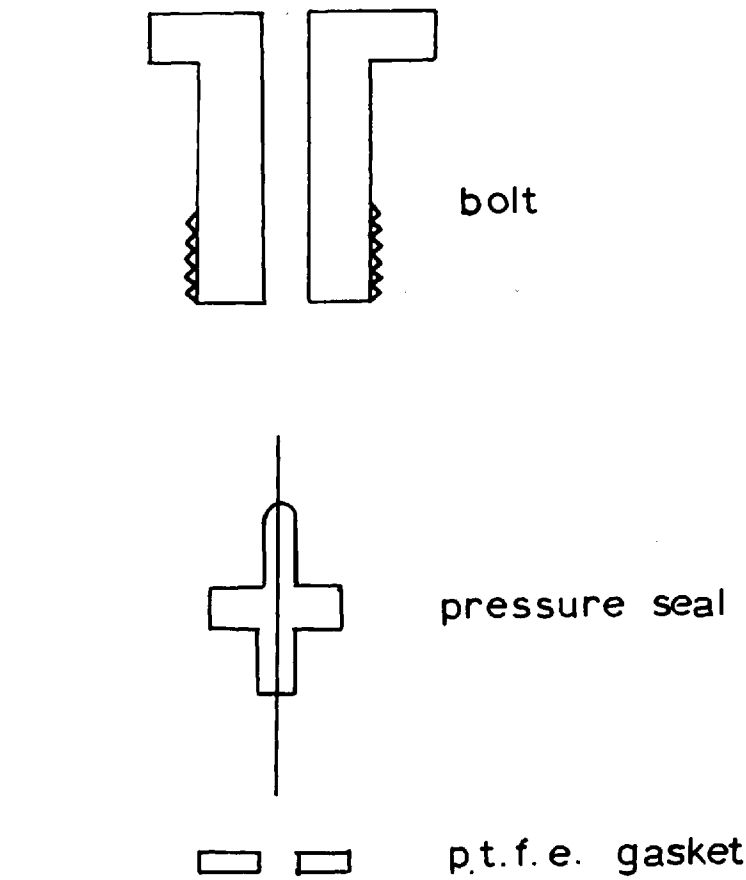

Fig.10

ARRANGEMENT FOR PERMANENT ELECTRODES

FIG. II

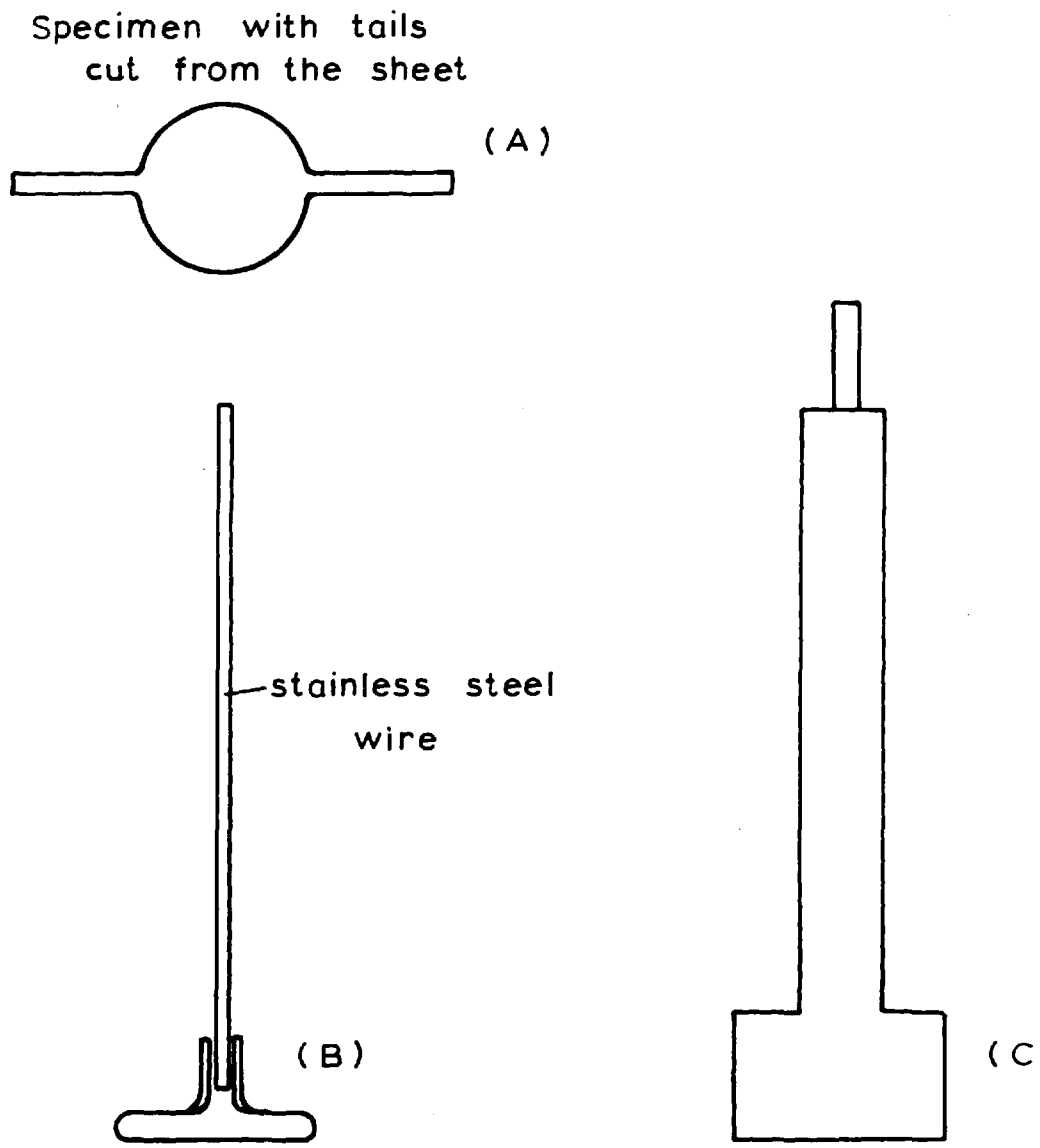

tails bent backwards and stainless steel wire attached

Araldite insulated specimen after breaking the glass moulds.

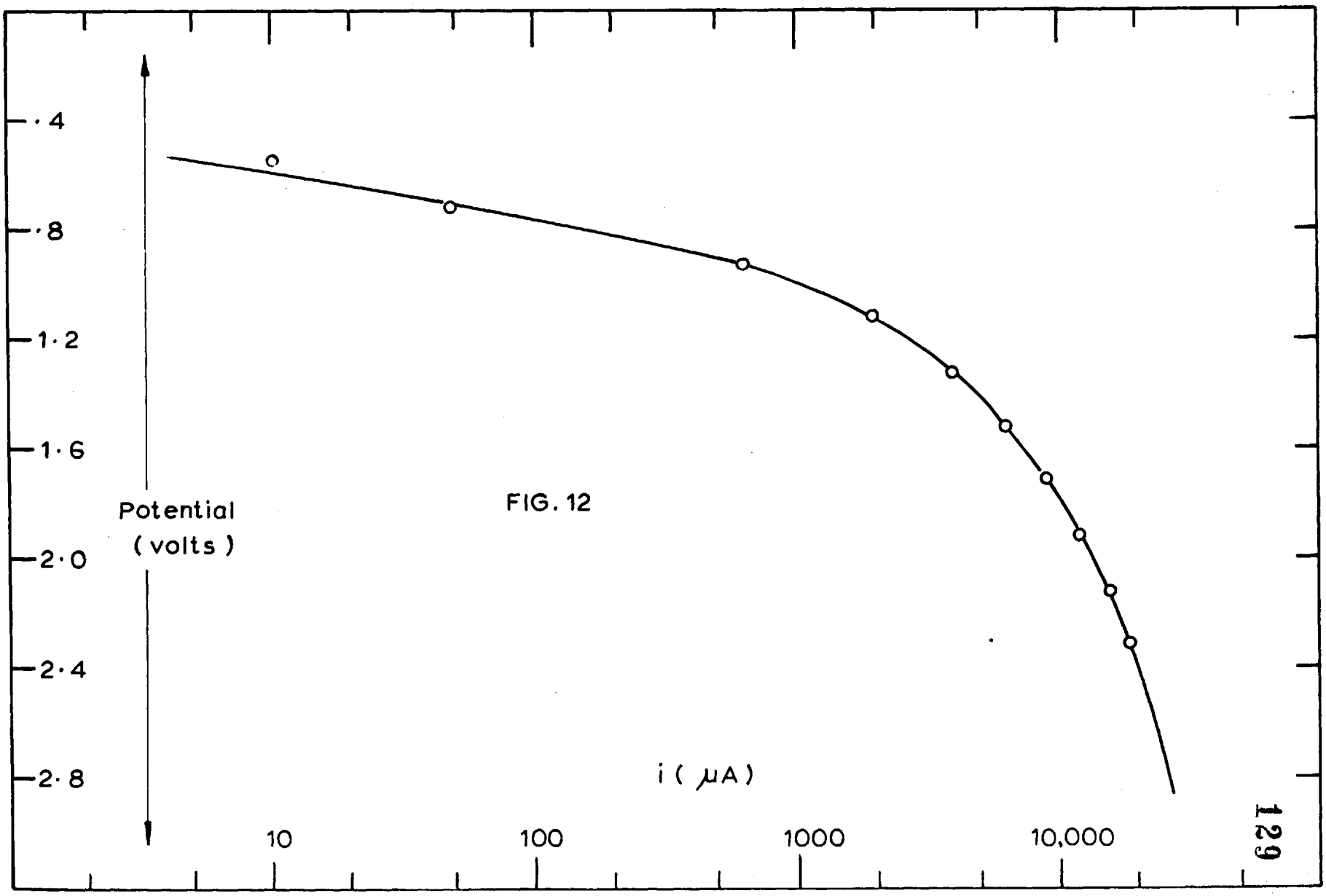

FIG. 12

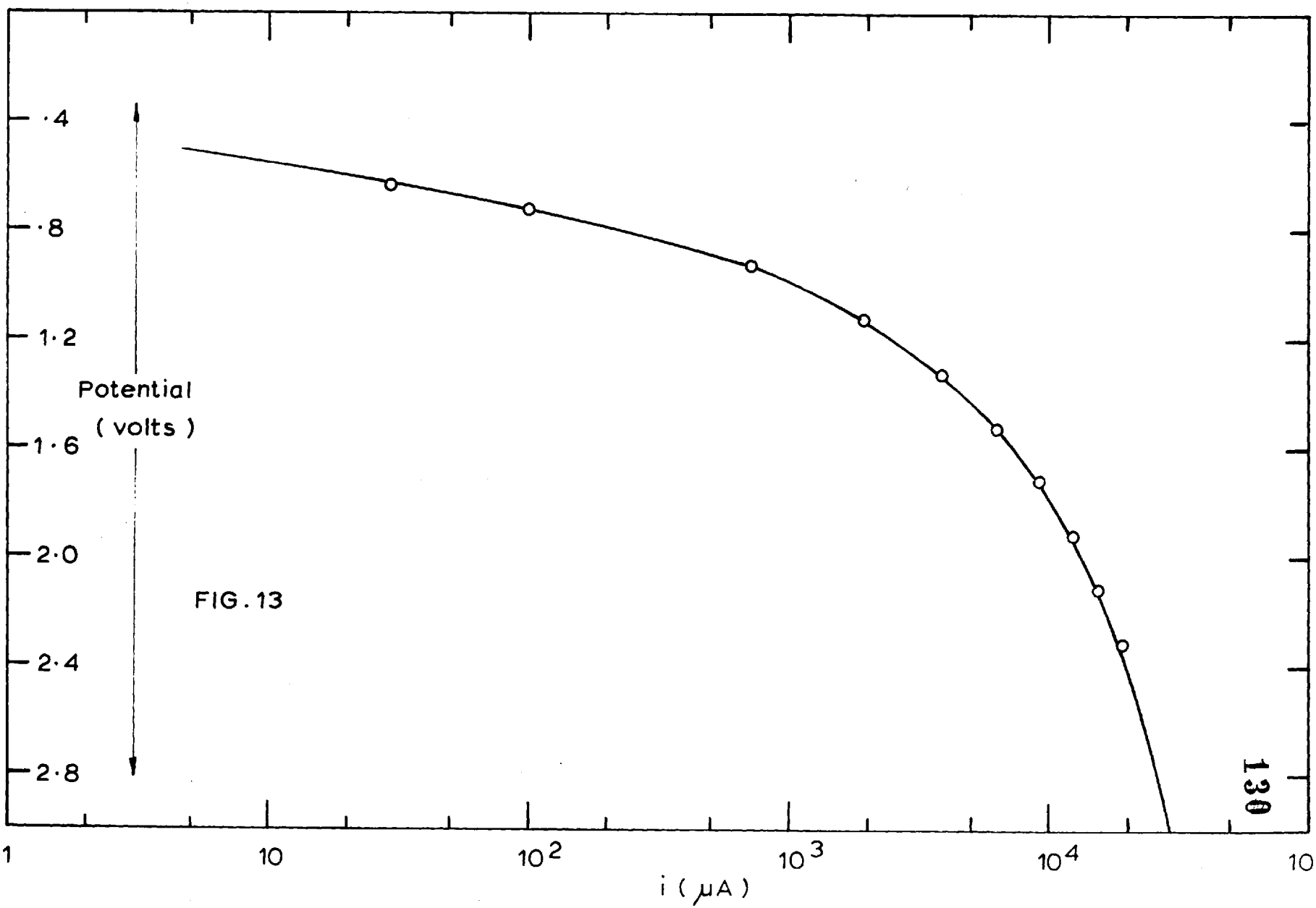

FIG. 13

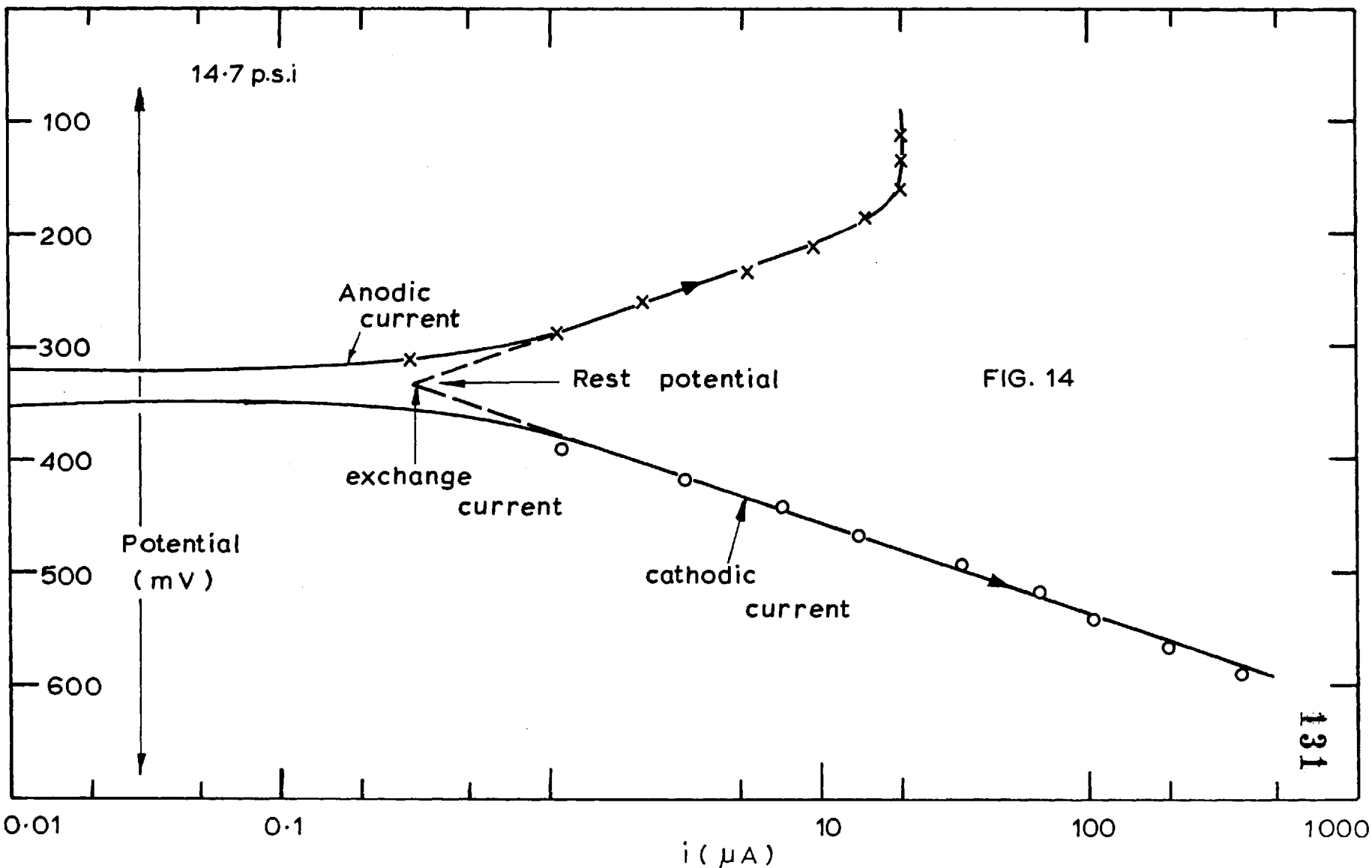
14·7 p.s.i
100
200
300
400
500
600
Potential
(mV)
Anodic
current
Rest potential
exchange
current
cathodic
current
0·01
0·1
10
100
1000
i (μA)

FIG. 14

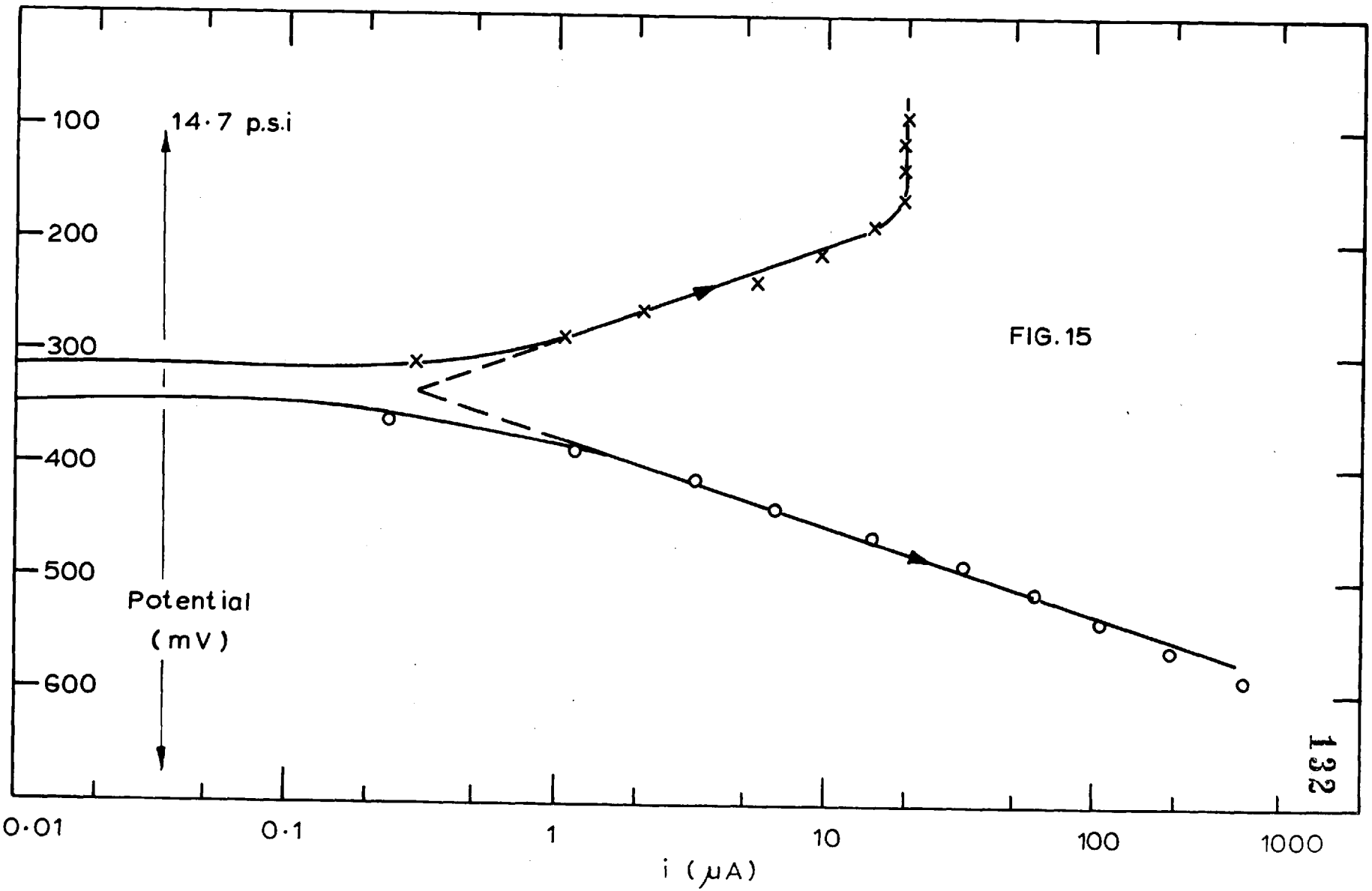
14·7 p.s.i
100
200
300
400
500
600
Potential
(mV)
0·01
0·1
1
10
100
1000
i (μA)

FIG. 15

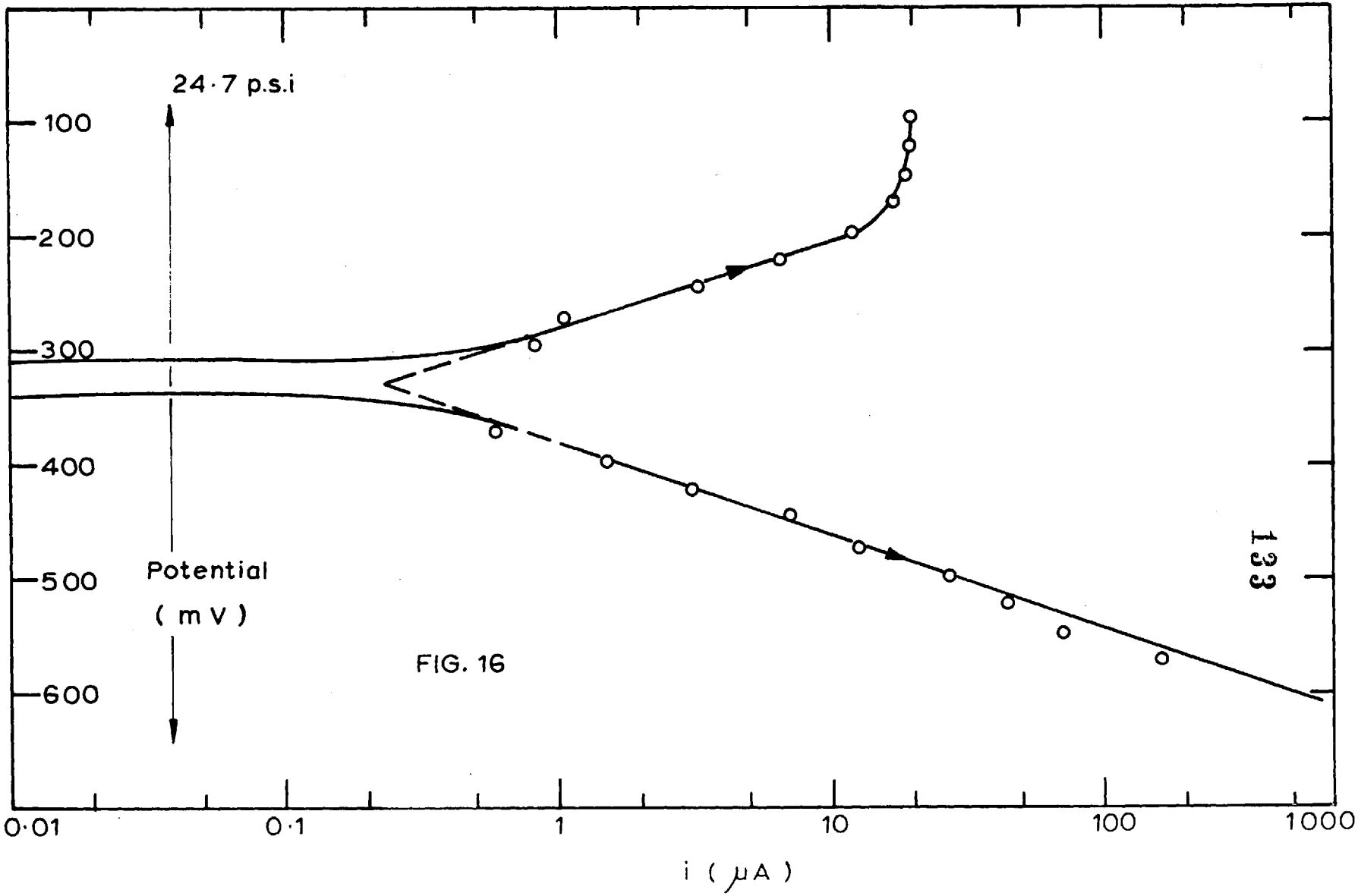
24·7 p.s.i
100
200
300
400
500
600
Potential
(m V)
0·01
0·1
1
10
100
1000
i (μA)

FIG. 16

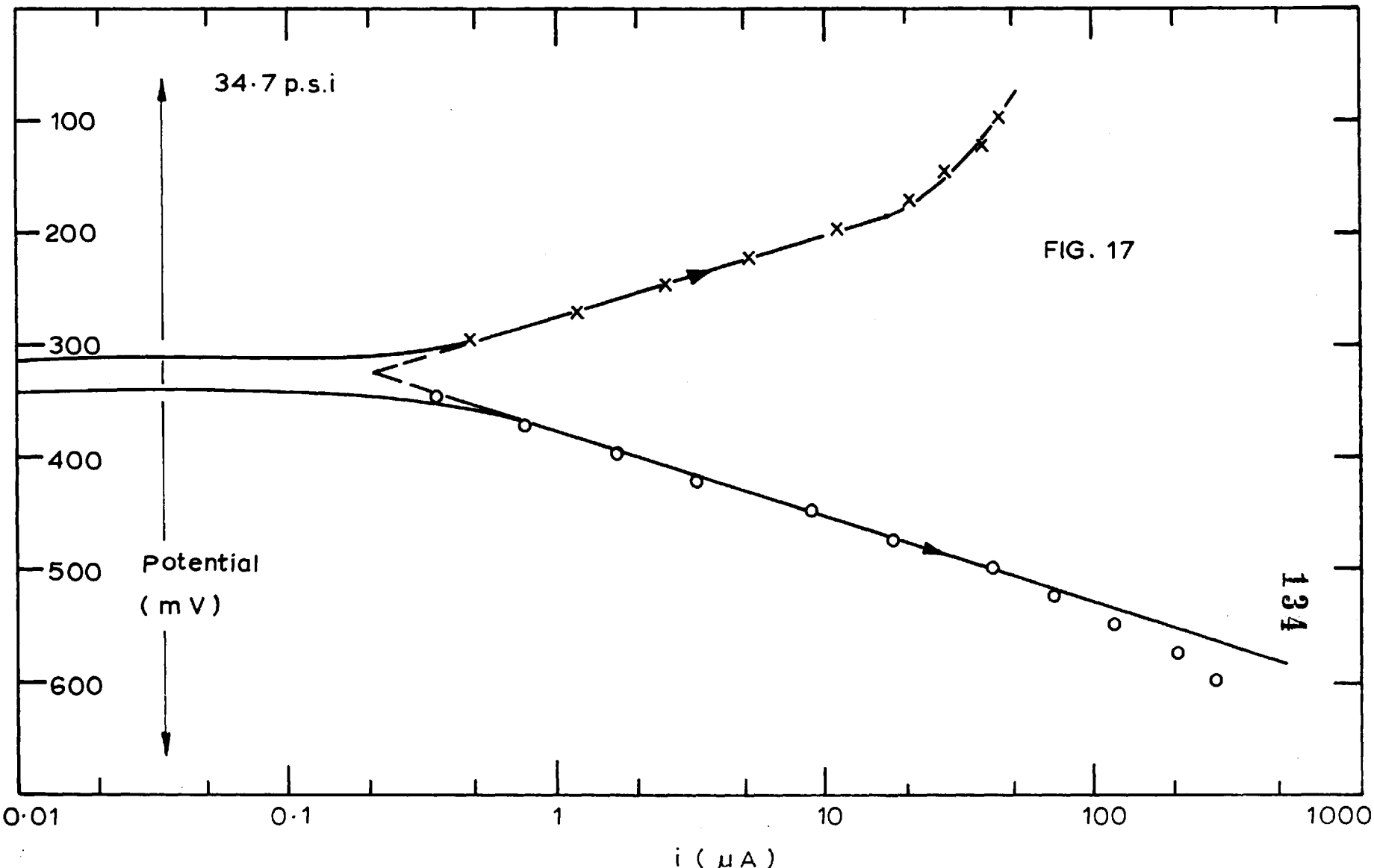
34·7 p.s.i
100
200
300
400
500
600
Potential
(m V)
0·01
0·1
1
10
100
1000
i (μA)

FIG. 17

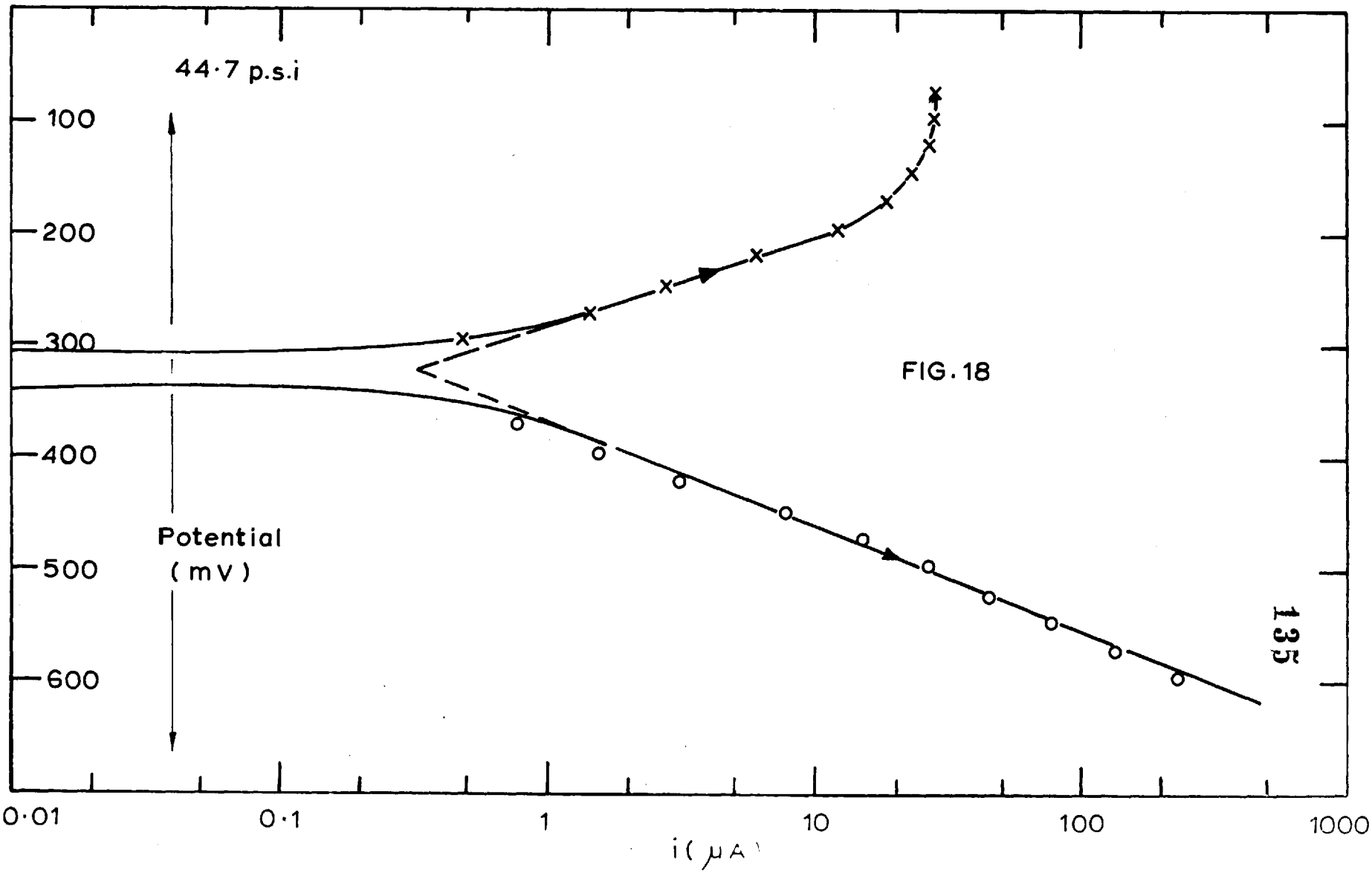
44·7 p.s.i
100
200
300
400
500
600
Potential
(mV)
0·01
0·1
1
10
100
1000
i (μA)

FIG. 18

FIG. 19

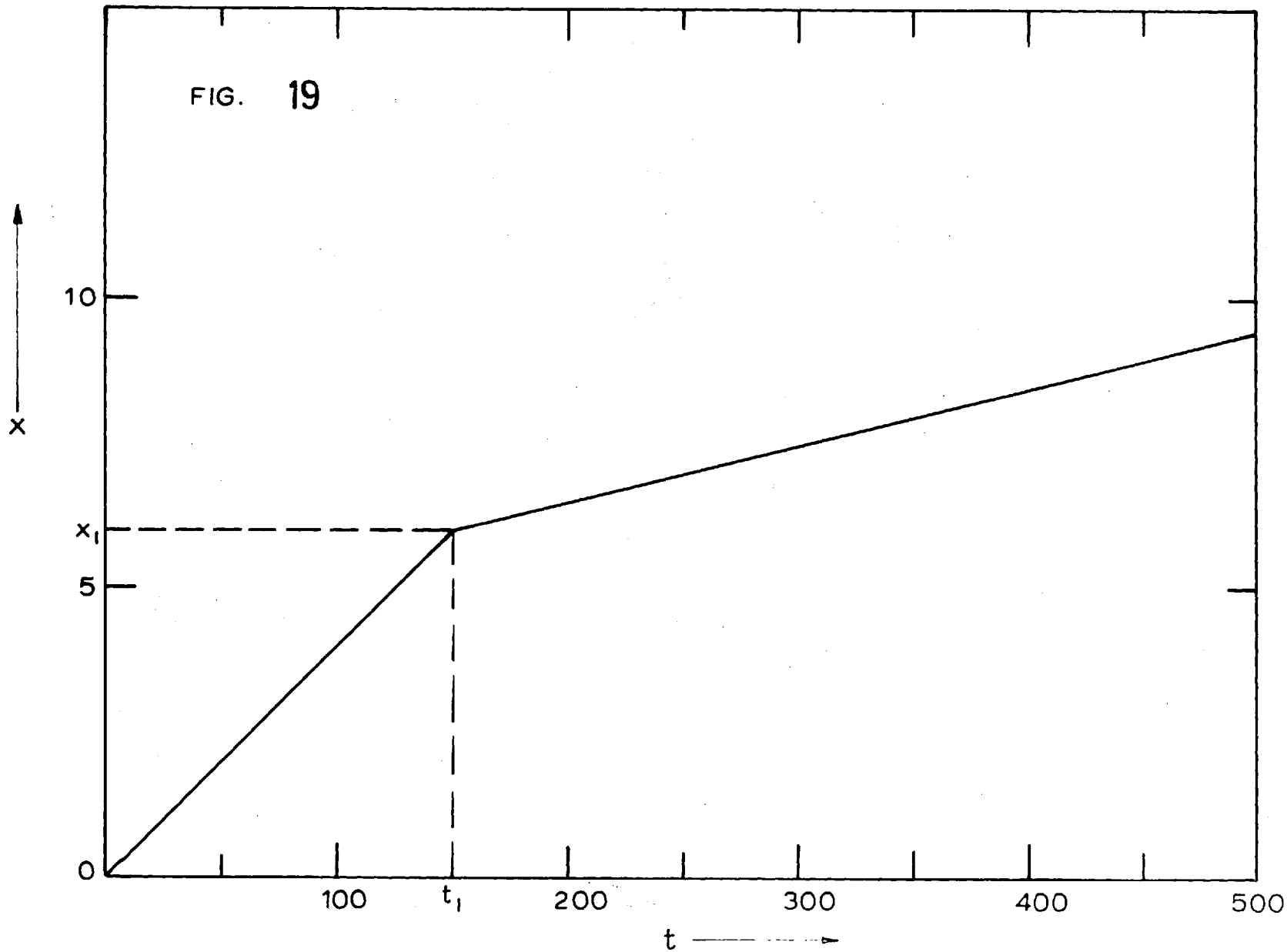

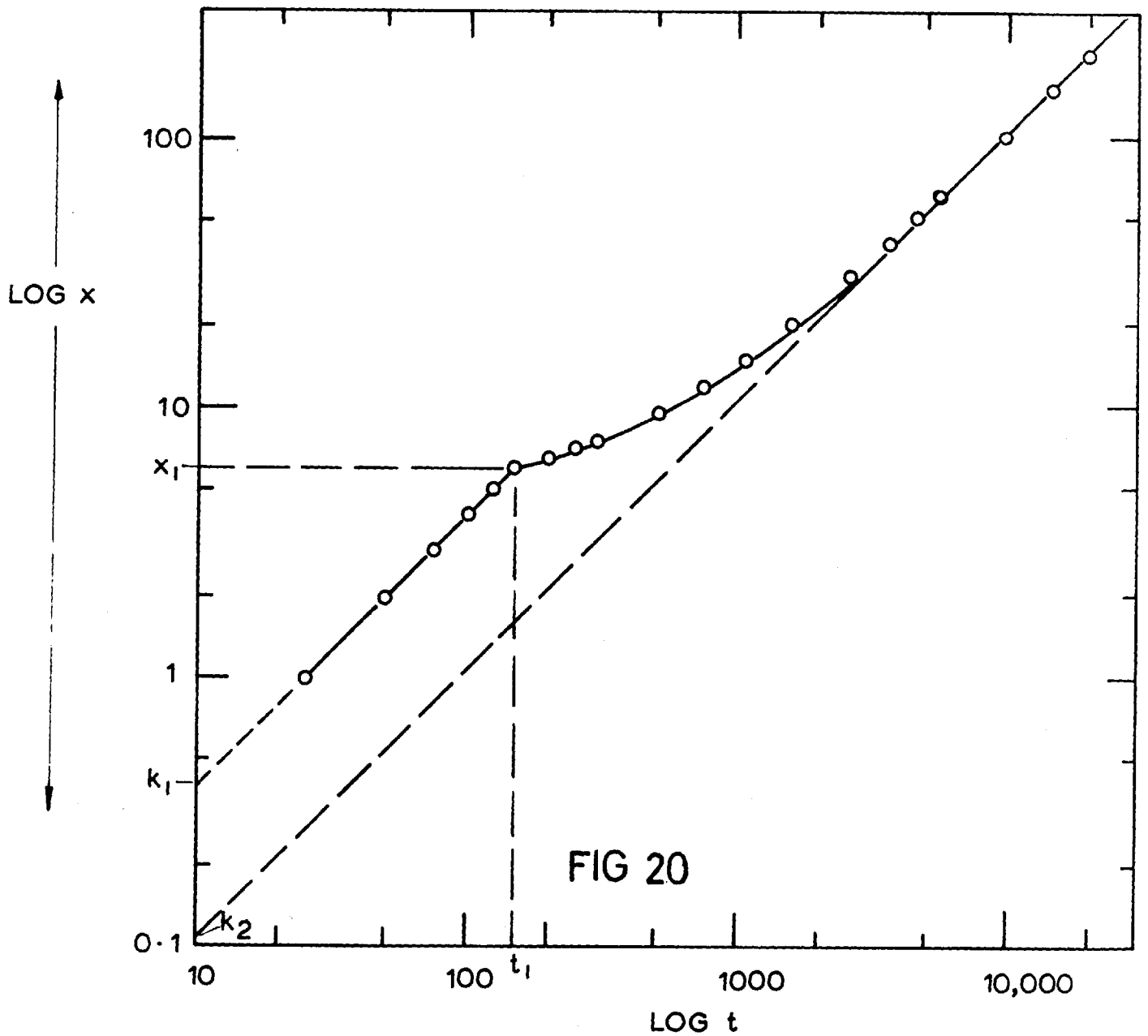

FIG 20

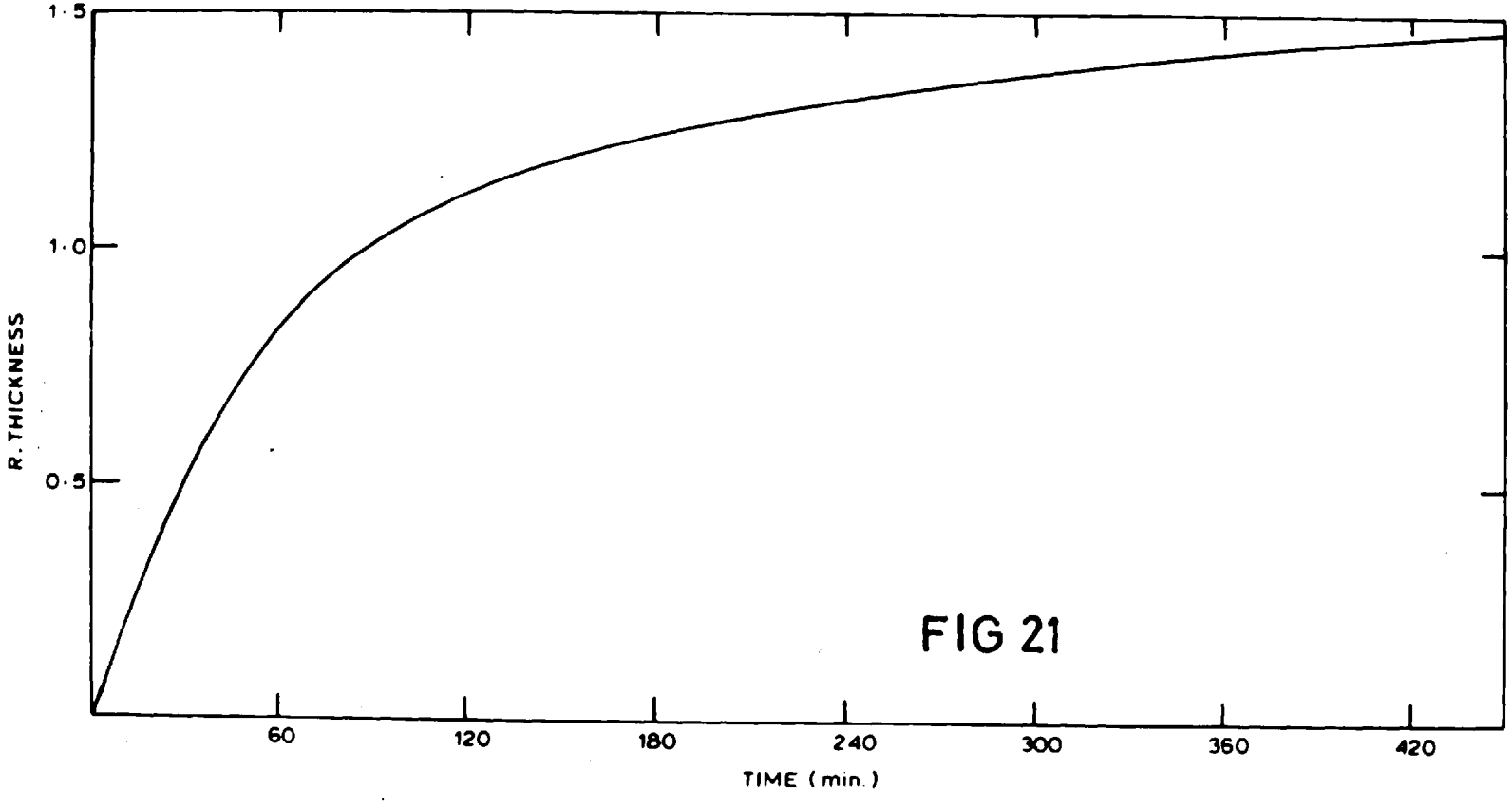

FIG 21

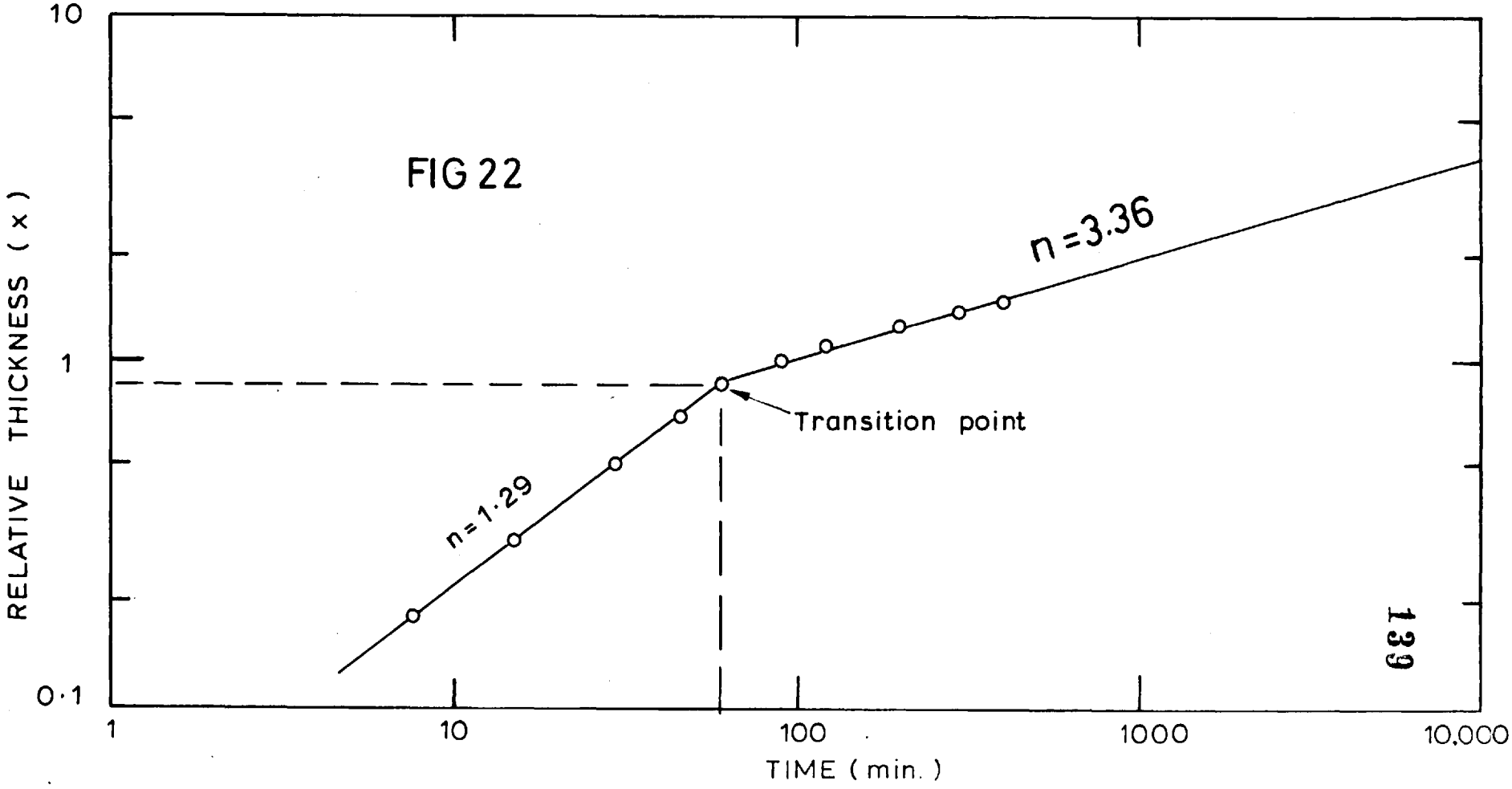
FIG 22
10
1
0·1
RELATIVE THICKNESS (x)
n=3.36
n=1·29
Transition point
1
10
100
1000
10,000
TIME (min.)
139

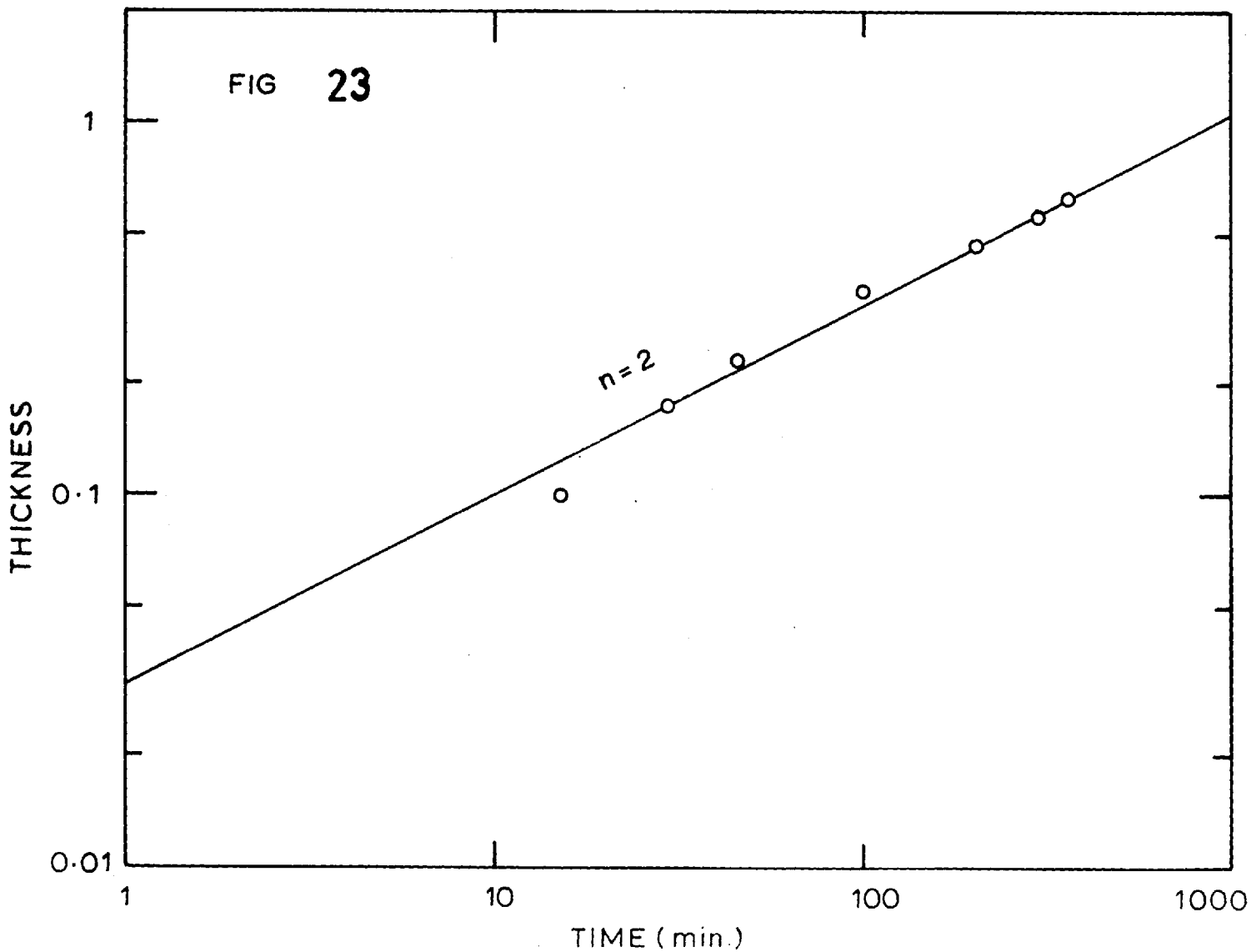
FIG 23
THICKNESS
1
0·1
0·01
1
10
100
1000
TIME (min.)
n=2

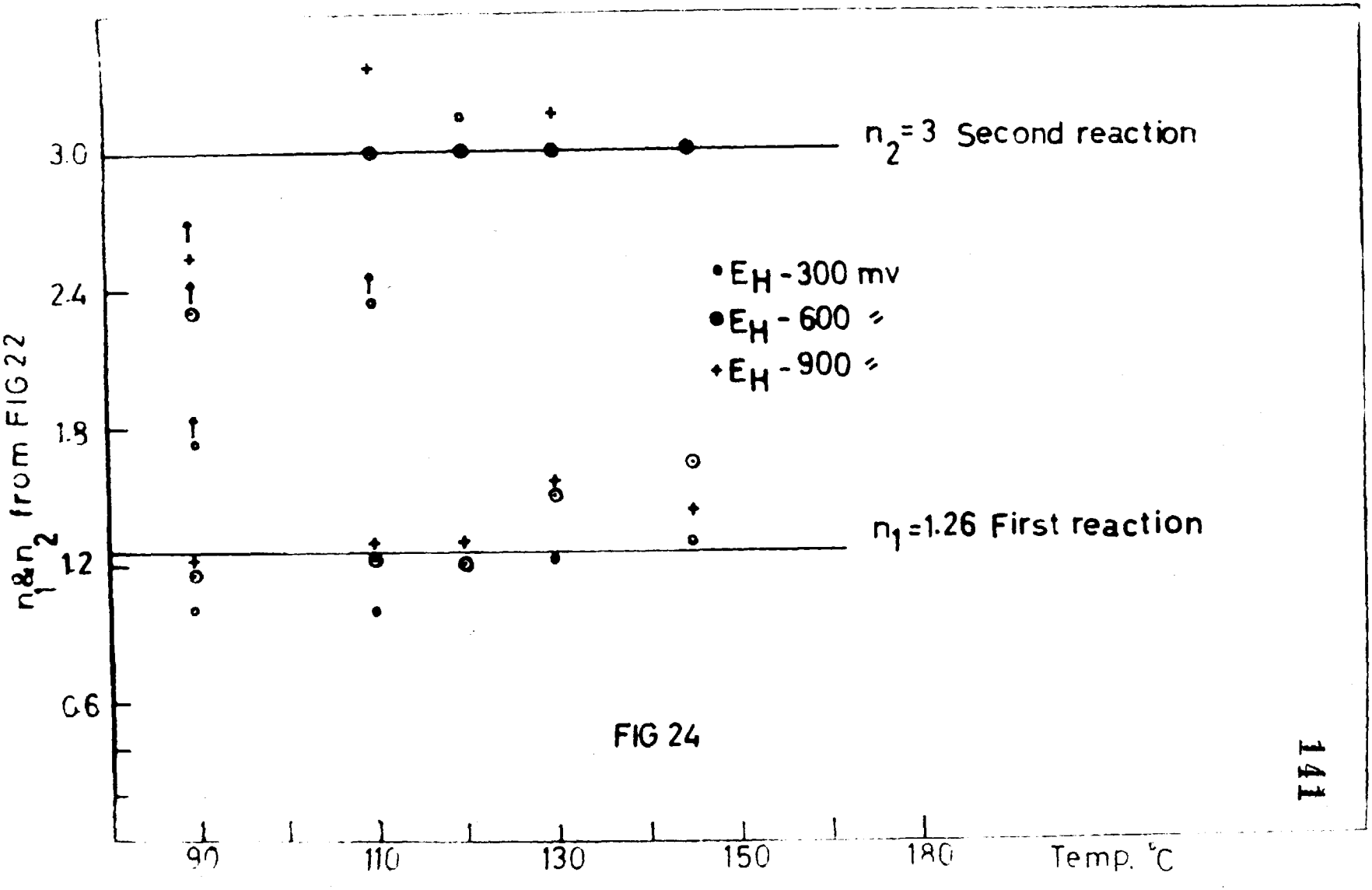
3.0
2.4
1.8
1.2
0.6
n_1&n_2 from FIG 22
n_2=3 Second reaction
n_1=1.26 First reaction
•E_H -300 mv
•E_H -600 "
+E_H -900 "
90
110
130
150
180
Temp. °C

FIG 24

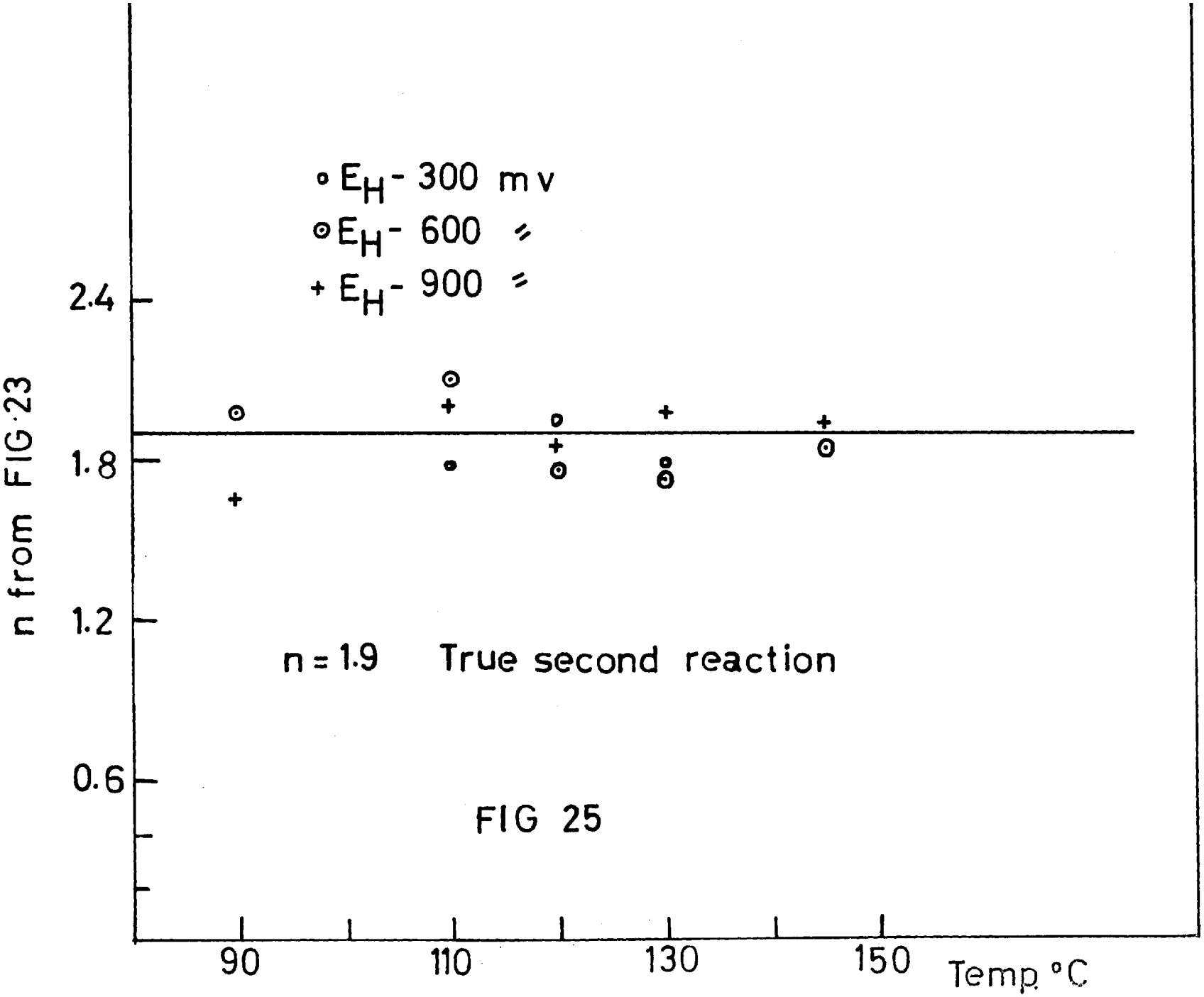
o E_H - 300 mv
⊙ E_H - 600 "
+ E_H - 900 "
2.4
1.8
1.2
0.6
n from FIG 23
n = 1.9 True second reaction
90
110
130
150
Temp °C

FIG 25

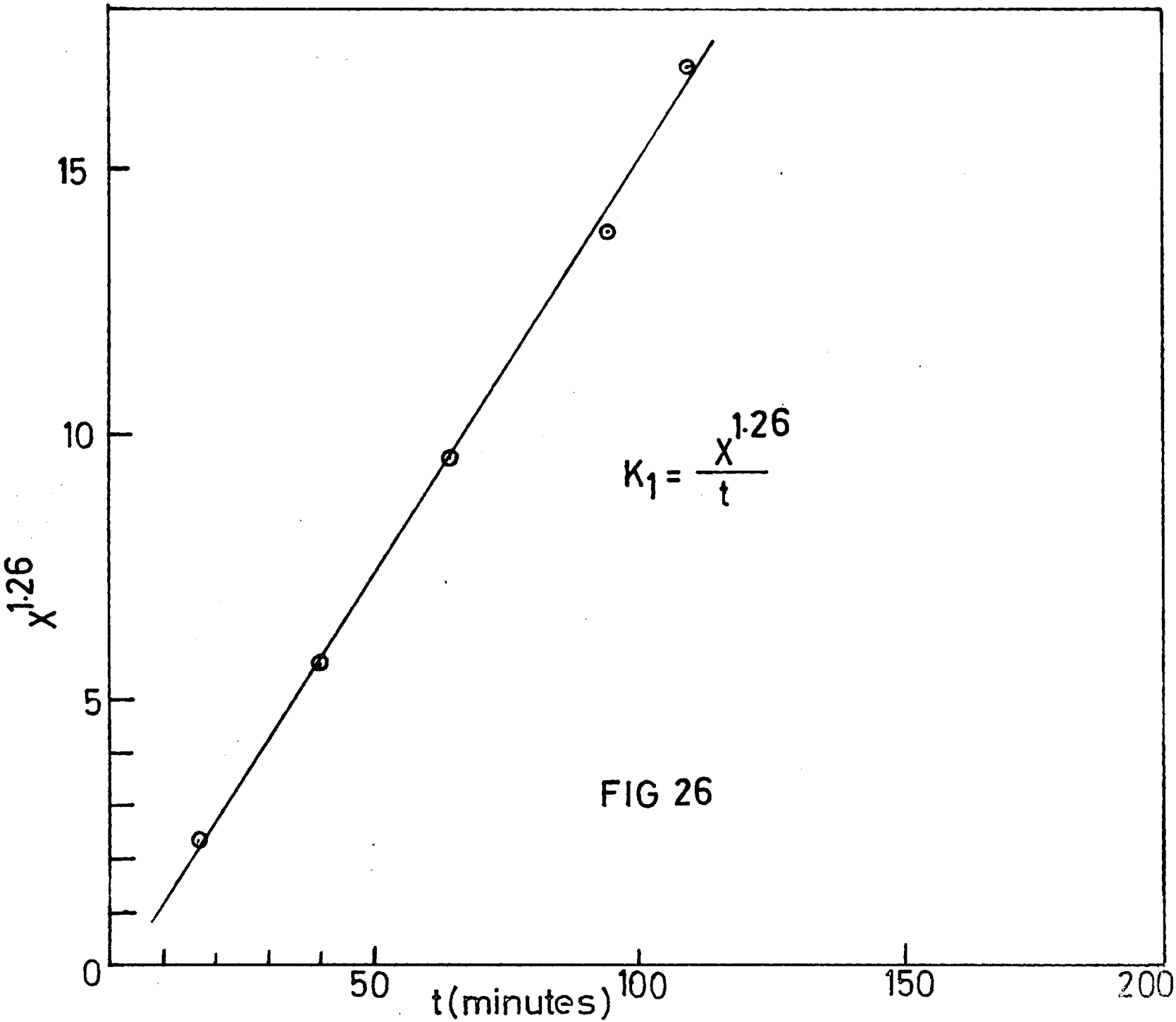

FIG 26

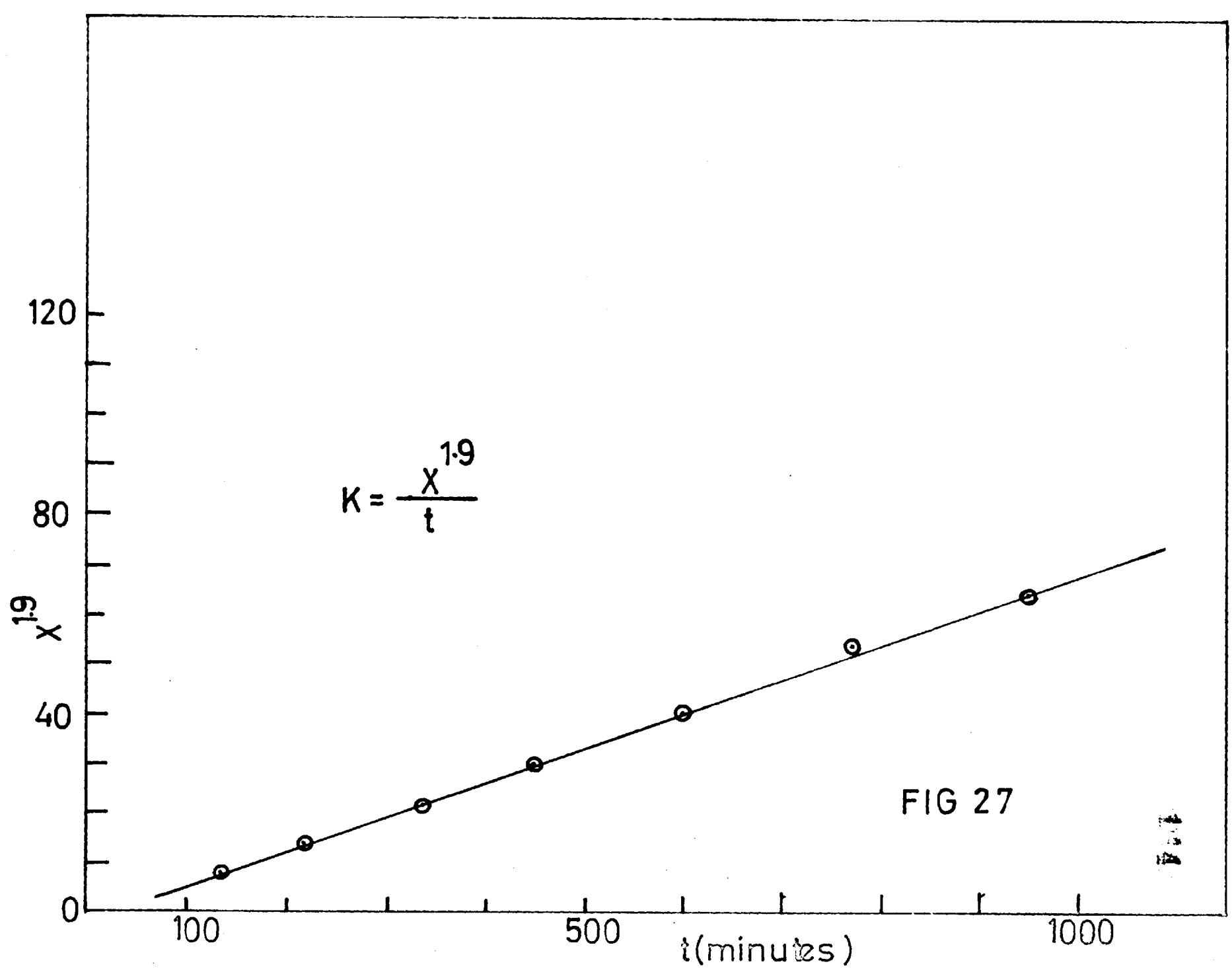

FIG 27

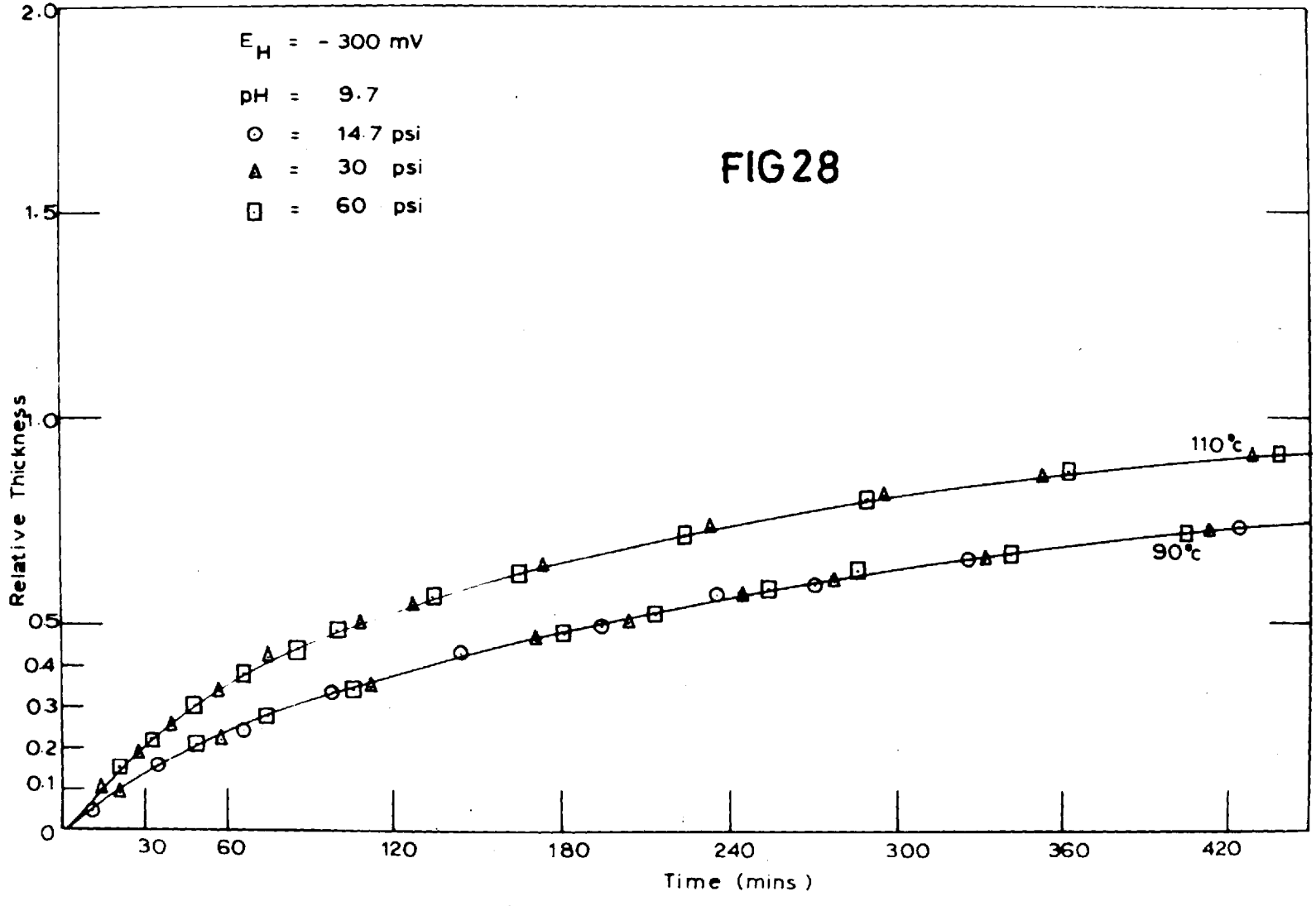
E_H = - 300 mV
pH = 9.7
⊙ = 14.7 psi
△ = 30 psi
□ = 60 psi
110°c
90°c
Relative Thickness
Time (mins)
2.0
1.5
1.0
0.5
0.4
0.3
0.2
0.1
0
30
60
120
180
240
300
360
420

FIG28

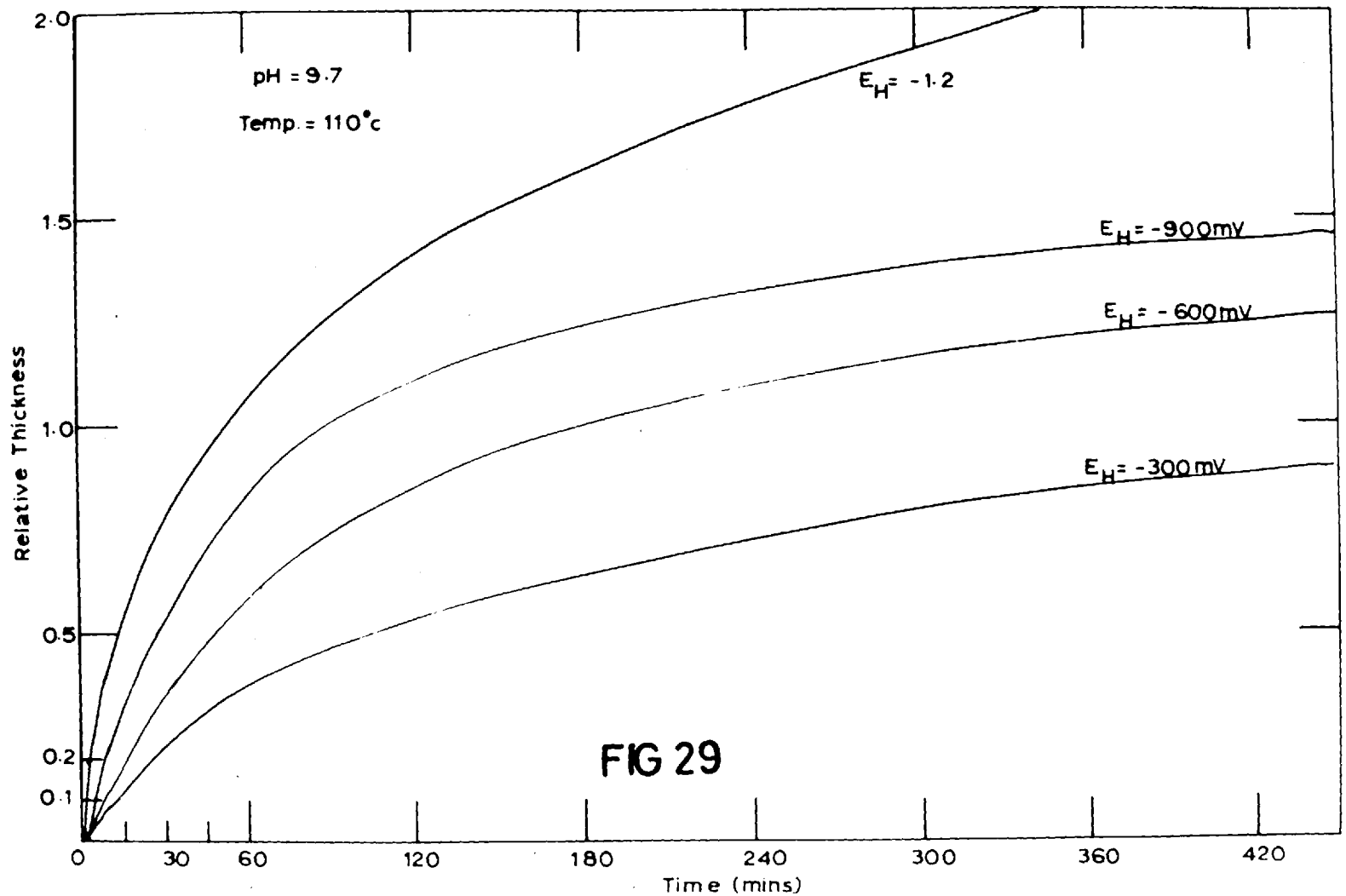
pH = 9.7
Temp. = 110°c
E_H = -1.2
E_H = -900mV
E_H = -600mV
E_H = -300mV
Relative Thickness
2·0
1·5
1·0
0·5
0·2
0·1
0
30
60
120
180
240
300
360
420
Time (mins)

FIG 29

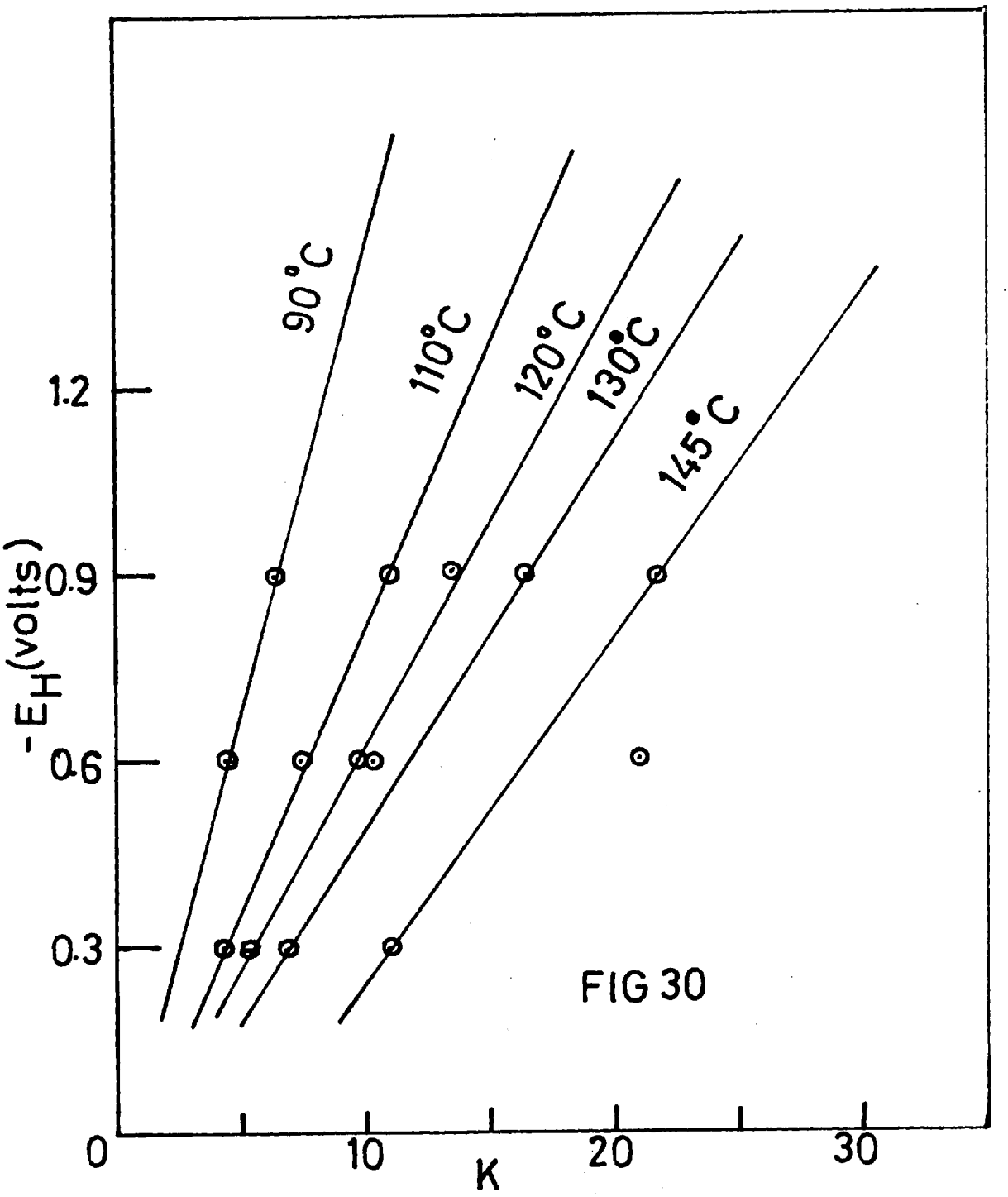

FIG 30

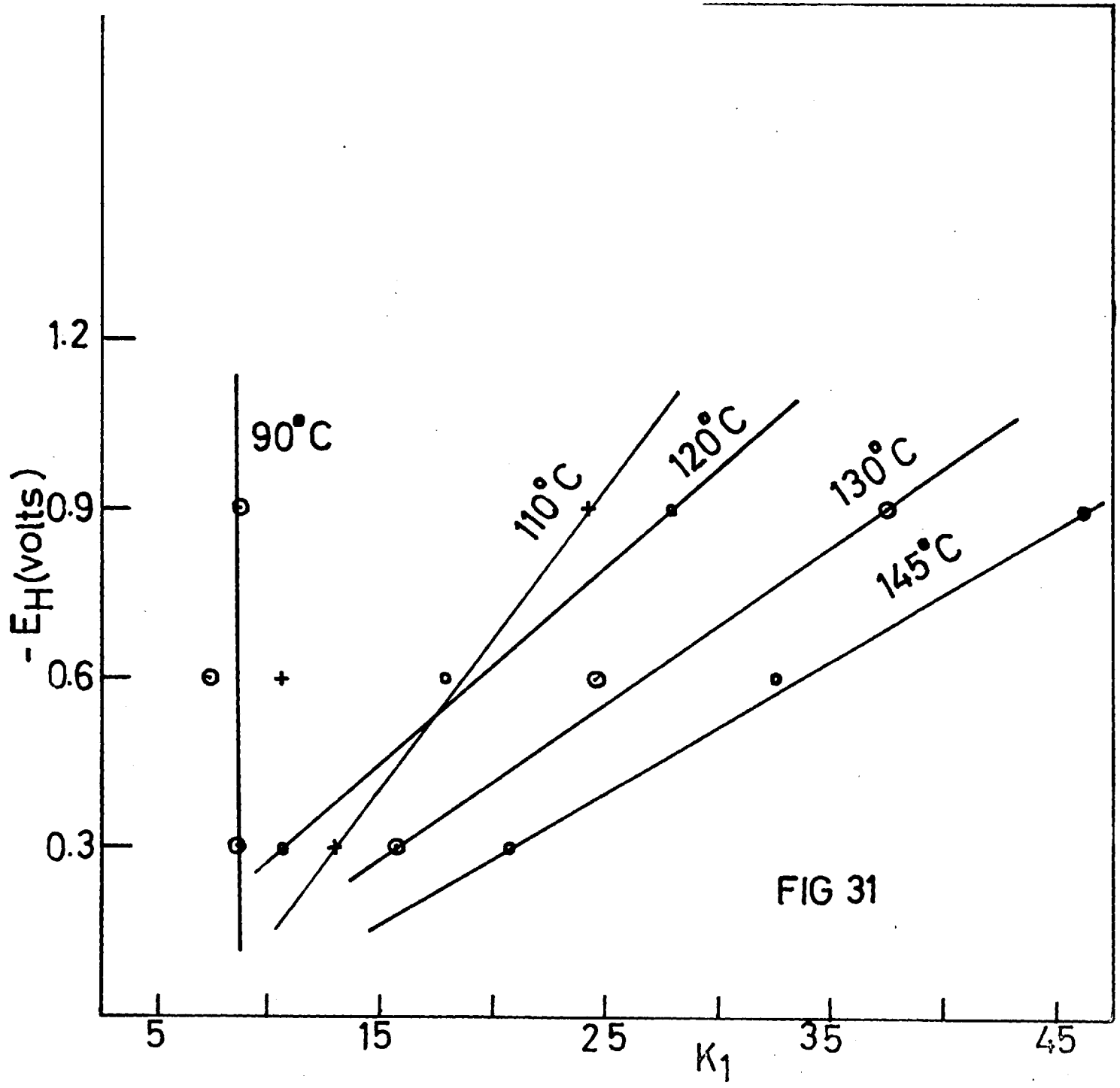

FIG 31

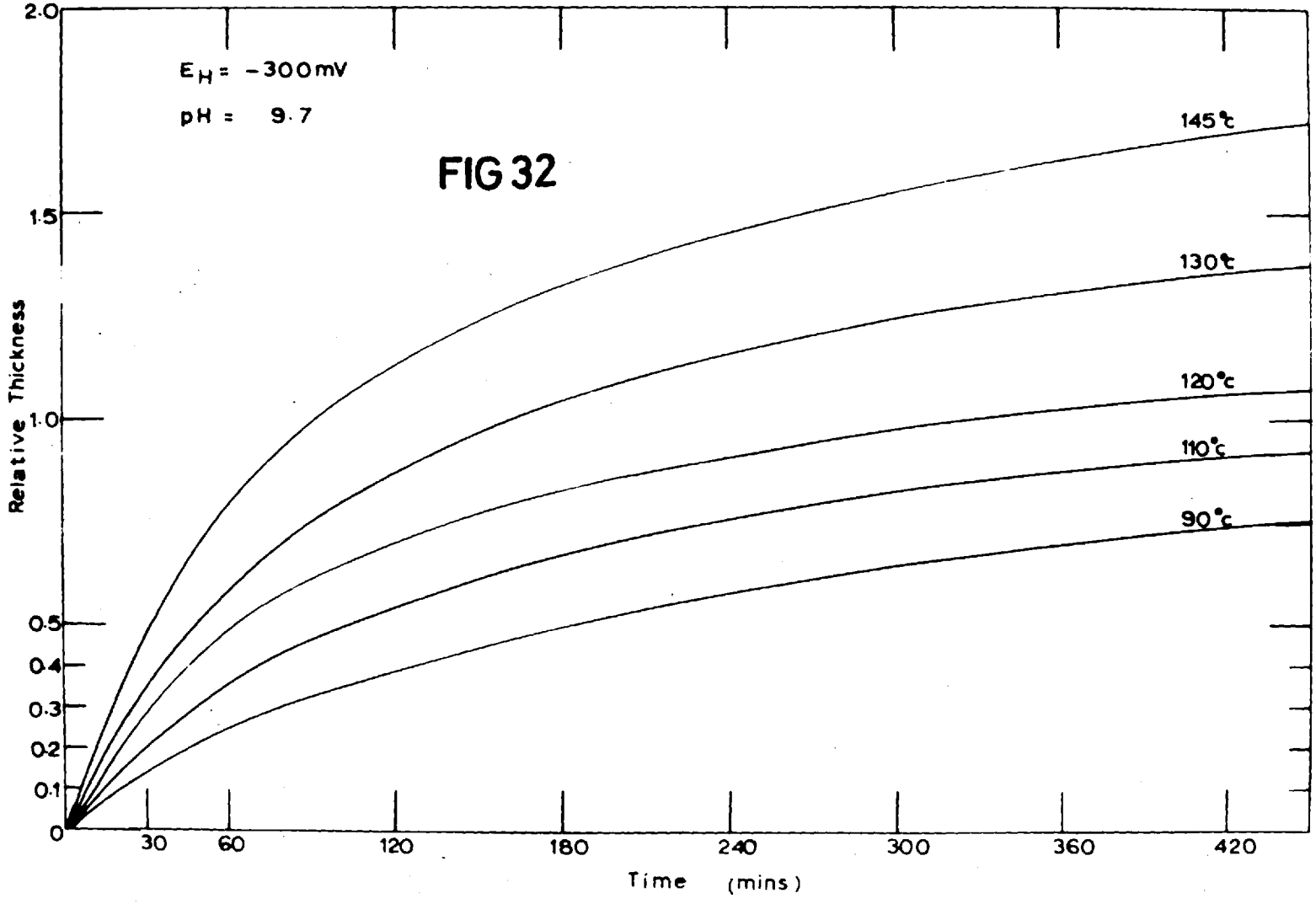
E_H = -300mV
pH = 9.7
145°c
130°c
120°c
110°c
90°c
Relative Thickness
2.0
1.5
1.0
0.5
0.4
0.3
0.2
0.1
0
30
60
120
180
240
300
360
420
Time (mins)

FIG 32

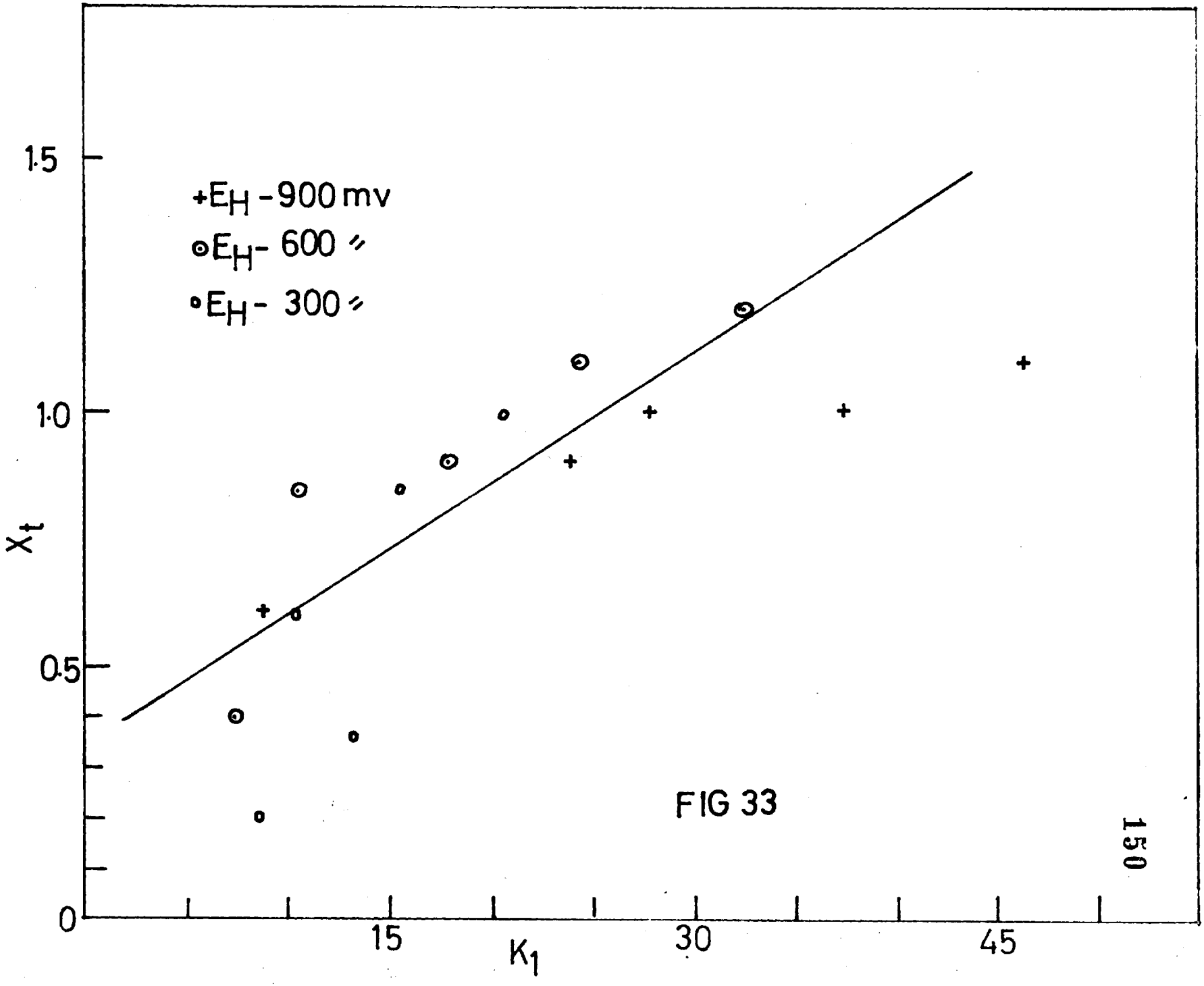

FIG 33

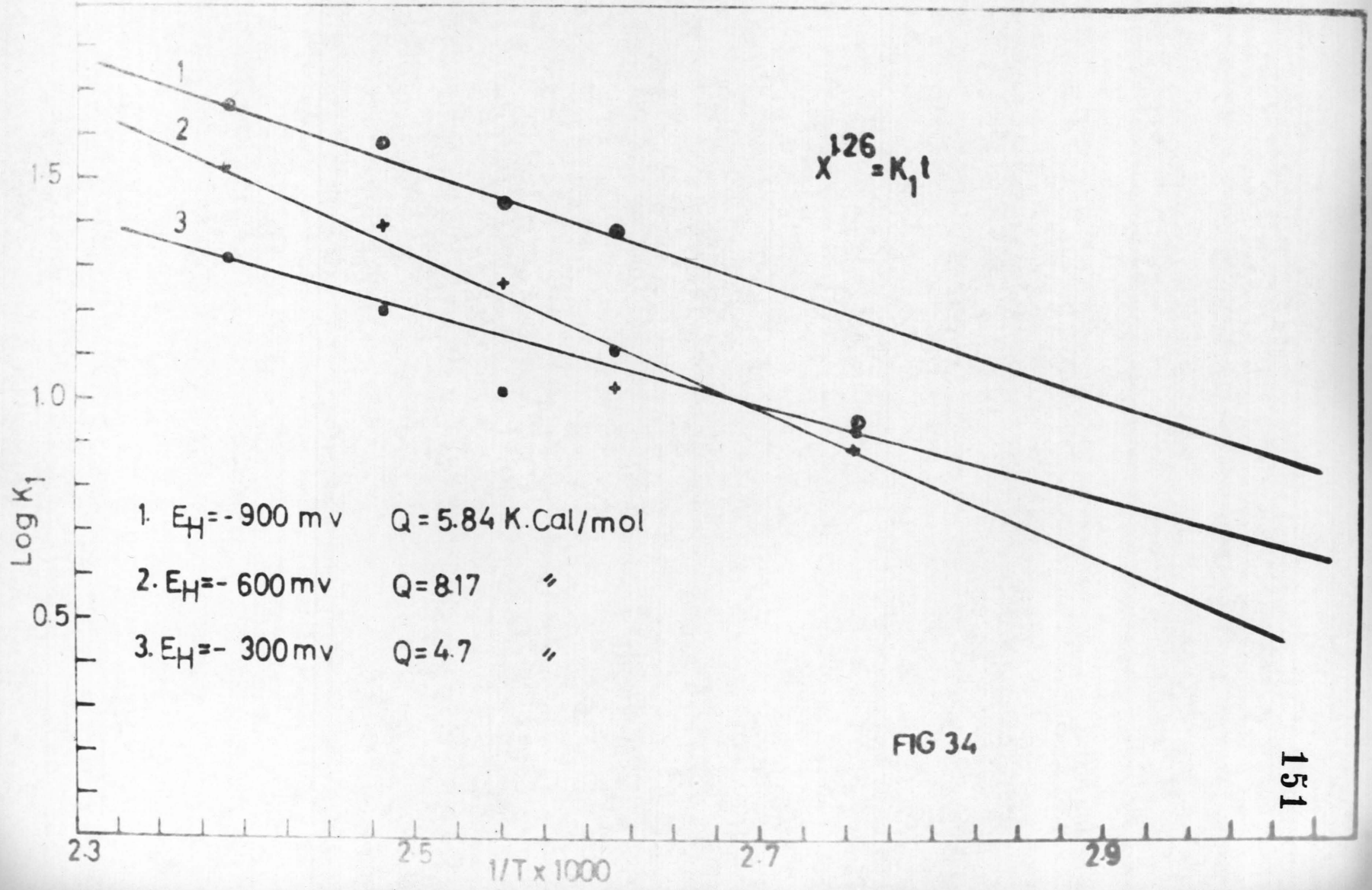
1
2
3
$X^{126} = K_1 t$
1.5
1.0
0.5
Log K_1
1. E_H = - 900 mv Q = 5.84 K.Cal/mol
2. E_H = - 600 mv Q = 8.17 "
3. E_H = - 300 mv Q = 4.7 "
2.3
2.5
2.7
2.9
1/T x 1000

FIG 34

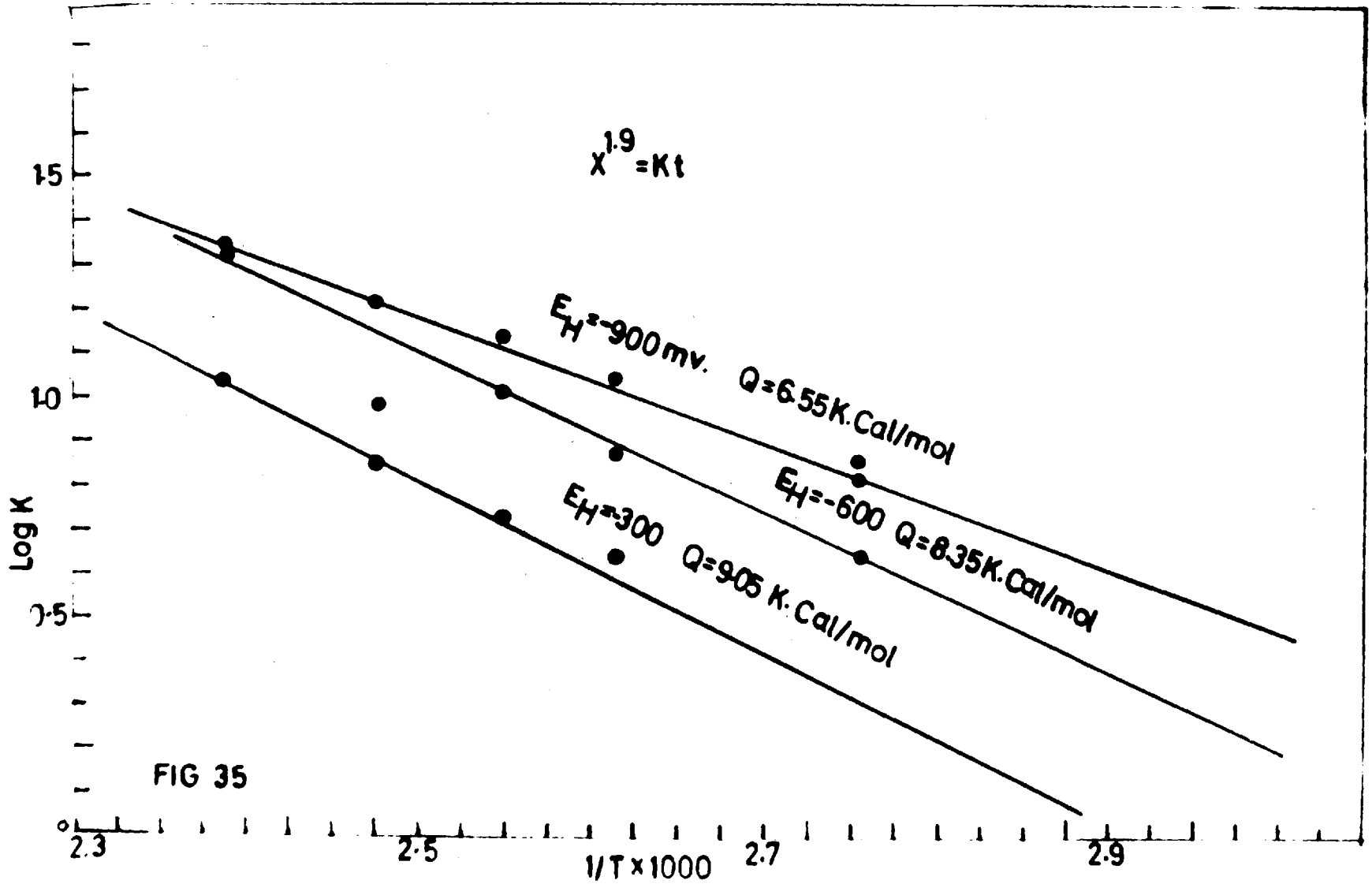
$X^{1.9} = Kt$
E_H=-900mv. Q=6.55K.Cal/mol
E_H=-600 Q=8.35K.Cal/mol
E_H=300 Q=9.05 K.Cal/mol
Log K
1·5
1·0
0·5
0
2.3
2.5
2.7
2.9
1/T x 1000

FIG 35

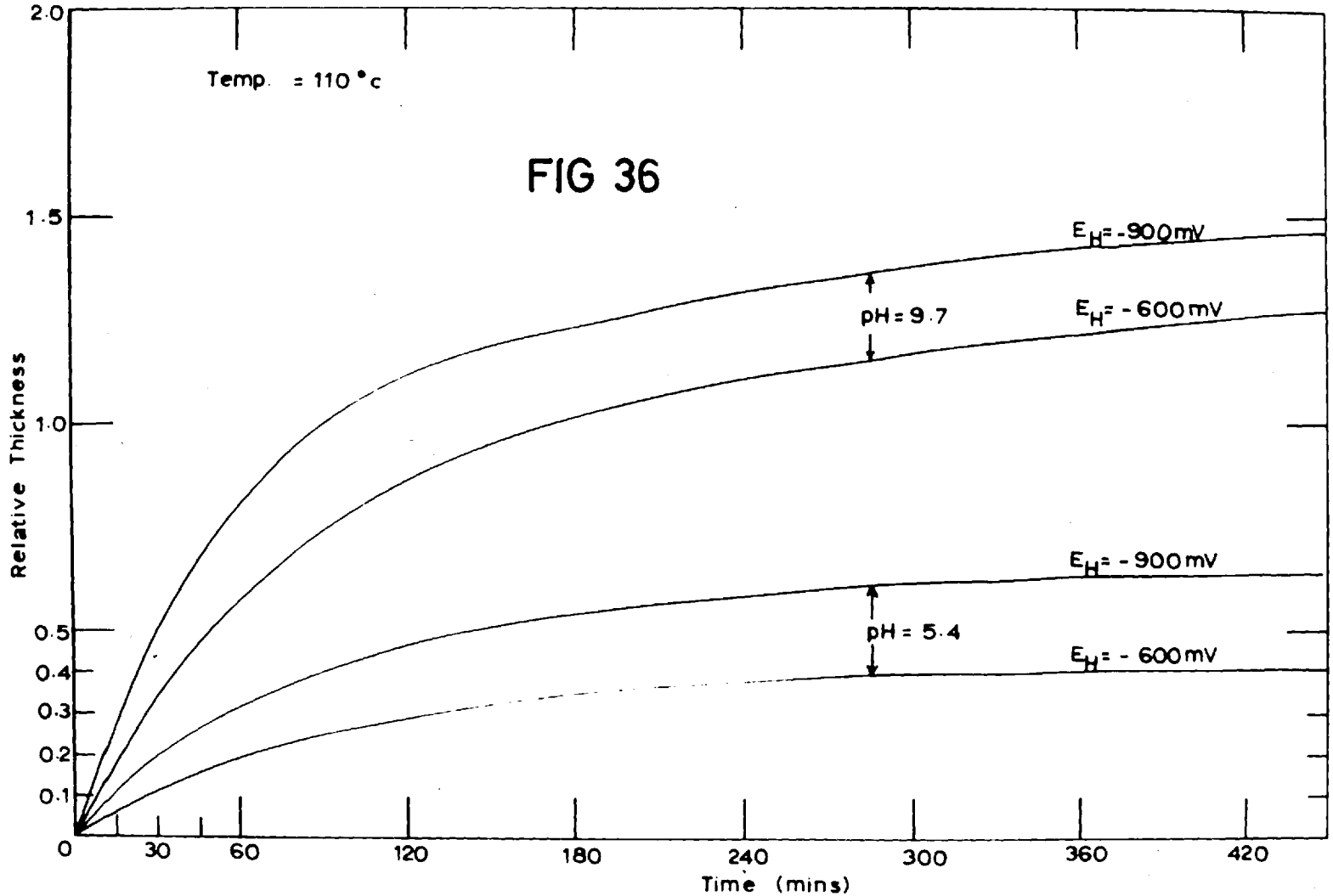
Temp. = 110 °c
FIG 36
Relative Thickness
2·0
1·5
1·0
0·5
0·4
0·3
0·2
0·1
0
30
60
120
180
240
300
360
420
Time (mins)
E_H = -900mV
pH = 9·7
E_H = -600mV
E_H = -900mV
pH = 5·4
E_H = -600mV

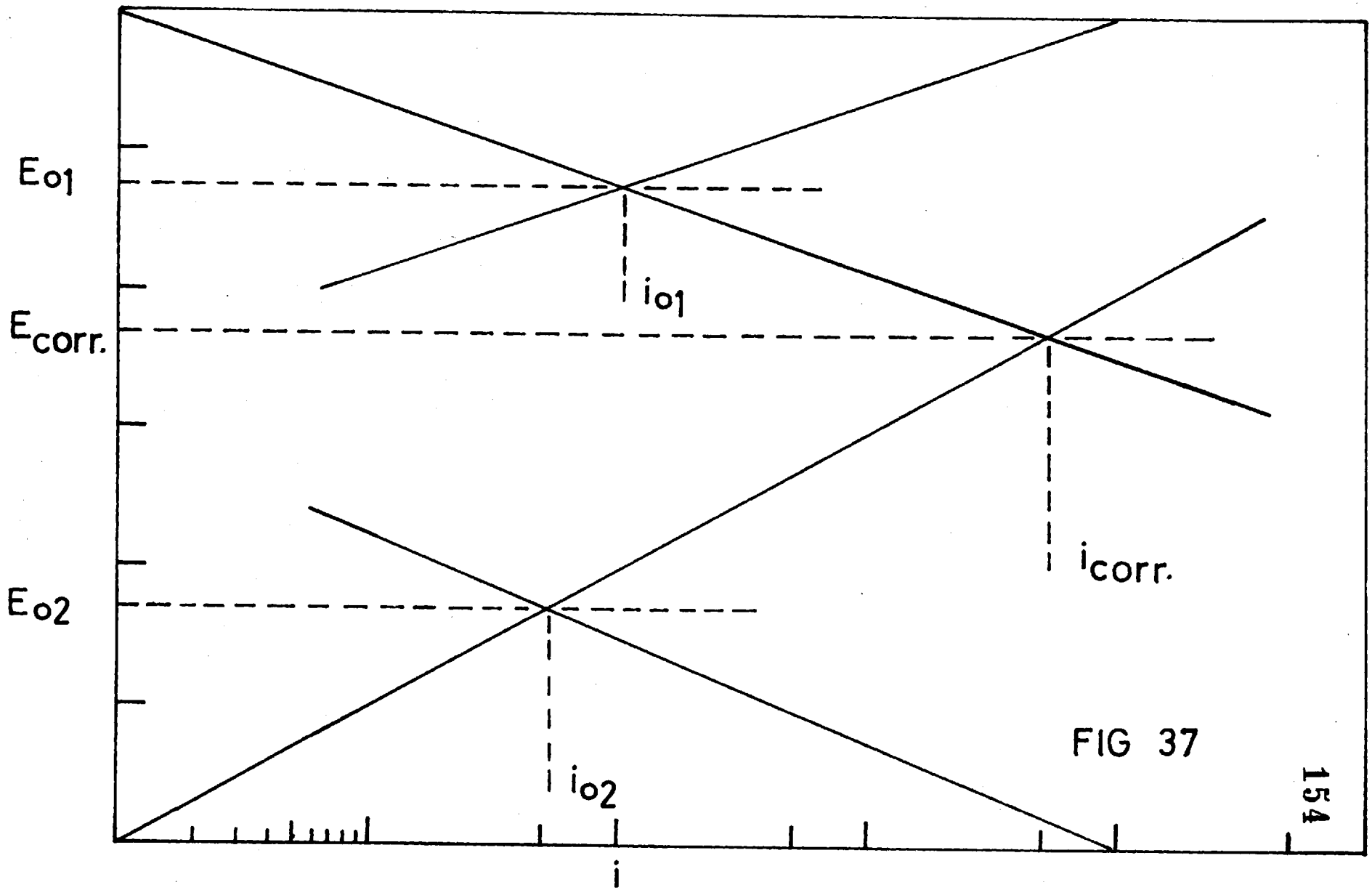

FIG 37

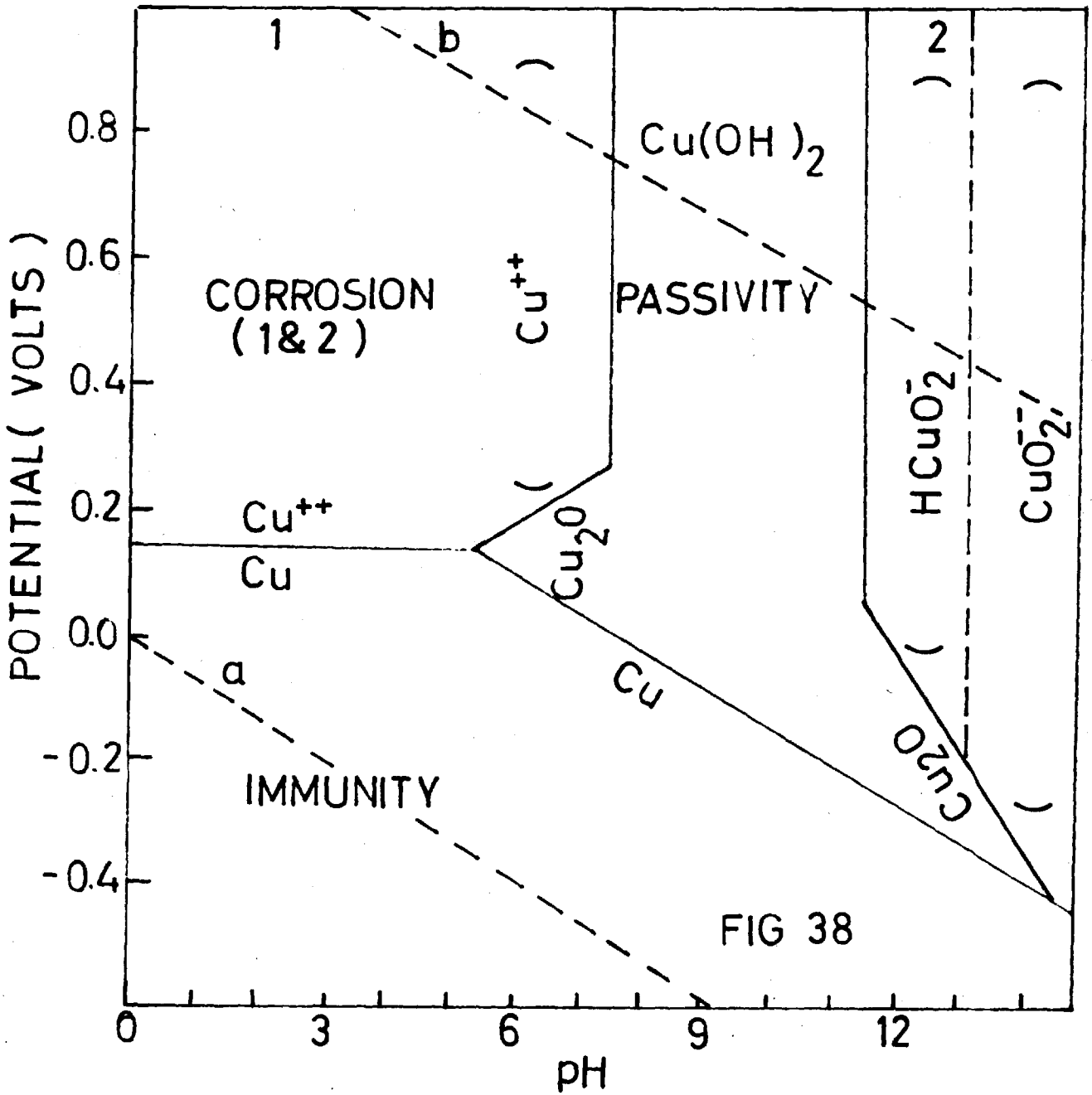
1
b
2
0.8
0.6
0.4
0.2
0.0
-0.2
-0.4
POTENTIAL (VOLTS)
CORROSION
(1& 2)
Cu++
Cu(OH)2
PASSIVITY
HCuO2-
CuO2--
Cu++
Cu
Cu2O
Cu
Cu2O
a
IMMUNITY
0
3
6
9
12
pH

FIG 38

```
***A
JOB
MET/ZAF/20
COMPILER AA

begin
integer i,n
routine spec zaf (realname jmb,arrayname yi,xi,real y0,x0,k,integer n)
read(n)
cycle i=1,1,n
real p1,k1,grad1,x0,t0,p2,k2,k3,bates1,bates2,t01,t02,x01,x02,storebates,storet,storex
integer j,abs, count
read(p1,p2,k1,x0,t0)
read (abs)
count = 0
array x, t(1:abs)
cycle j=1,1,abs
read (x(j),t(j))
repeat
grad 1 = k1/(p1*exp((p1 - 1)* log(x0)))
k2 = grad 1* p2* exp((p2 - 1) log(x0))
zaf (bates 1,x,t,x0,t0,k2,abs)
      store bates = bates 1; store x = x0; store t = t0
t01 = t0 2
1: newline;  t01=t01 - 1 2
    if t01<0 then -> 4
x01 = x0 2
2: x01 = x01 - 0.1 2 ; count = count + 1; newline if fracpt(count/50)=0;print(count,4,0) if fracpt (count/50) = 0
if x01 < 0 then -> 5
k2 = grad 1* p2* exp ((p2 - 1) log (x0 -x01))
zaf (bates 2,x,t,x01,t01,k2, abs)
comment check bates 1 v. bates 2
if bates 1 > bates 2 then  -> 3
-> 7
3: bates 1 = bates 2
-> 2
7:
if store bates < bates 2 then -> 8
store bates = bates 2
store x = x01 2
store t = t01 2
-> 1
8:
newline
caption value ¢ of ¢ origin ¢ for ¢ post - transition ¢ period
newline
caption t0; print (store t, 4, 3 ) ; spaces ( 2 )
caption x0; print ( store x, 4, 3 )
cycle j = 1, 1, abs
x(j) = x(j) - store x
x(j) = log (x(j)) / 2.303
t(j) = t(j) - store t
t(j) = log (t(j)) / 2.303
repeat
newline
caption corrected ¢ values ¢ of ¢ log (x)¢ and ¢ log(t)
newline
caption ¢ log(t) ¢¢¢¢ log(x)
cycle j = 1, 1, abs
newline
print (t(j), 1 , 3); spaces (2); print (x(j), 1, 3)
repeat
newline
-> 10
caption value ¢ of ¢ pre-expon. ¢ term ¢ in post-transition ¢ period
k3 = grad 1* p2* exp((p2 - 1) log(x0 - store x))
10 :
printfl(k3, 4)
-> 6
4: caption no ¢ solution ¢ for ¢ t ¢ greater ¢ than ¢ zero; ->6
5: caption no ¢ solution ¢ for ¢ x ¢ greater ¢ than ¢ zero
6: repeat
routine zaf(realname jmb, arrayname yi, xi, real y0, x0, k, integer n)
comment k is the pre-exponential after the post-transition period
integer i ; array yci(1:n)
real ssq, ssr, a, b
ssq = 0
ssr = 0
a = 0
b = 0
cycle i = 1, 1, n
a = a + (log(yi(i) - y0))²
b = b + log(yi(i) - y0)
repeat
b =(b*b)/n
ssq = a - b
cycle i = 1, 1, n
yci(i) = exp (log(k*(xi(i) - x0))/p2)
repeat
cycle i = 1, 1, n
ssr = ssr + (log(mod(yi(i) -yci(i))))²
repeat
jmb = ssr/ssq
end
end of program
14
1.0
1.65
2.34
0.2
45
6
0.5 200
1.0 650
2.0 2000
3.0 4400
4.0 7500
4.7 10000
1.5
1.2
12.0
0.56
55
6
0.5 250
1.0 600
1.5 1500
2.0 3000
2.5 5000
3.0 8000
1.34
1.43
10.1
0.6
[illegible]
6
0.8 150
1.0 280
1.5 850
1.7 2000
2.0 [illegible]
2.5 [illegible]
[illegible]
1.2
[illegible]
[illegible]
[illegible]
6
1.0 160
1.5 300
1.8 600
2.0 1300
2.6 3000
3.5 8000
1.5
1.34
20.7
1.0
60
6
1.2 140
1.6 320
2.0 650
3.0 2100
4.0 5000
5.0 9500
1.43
2.11
10.3
0.23
105
6
[illegible]
[illegible]
[illegible]
[illegible]
[illegible]
[illegible]
1.2
1.75
0.4
85
6
0.6 200
0.8 400
1.0 650
1.5 1800
2.0 3400
3.0 9000
1.33
1.73
17.0
0.3
85
6
1.0 110
1.2 200
1.5 400
2.0 950
3.0 3400
4.0 8300
1.52
1.73
24.1
1.1
35
6
1.4 180
1.7 340
2.0 500
3.0 2000
4.0 5000
4.8 9000
1.65
1.83
[illegible]
.2
75
6
1.5 150
2.0 280
2.3 340
3.0 1400
4.0 3400
5.0 7500
1.33
1.54
9.0
0.2
105
6
0.8 210
1.0 380
1.5 [illegible]
2.0 [illegible]
[illegible]
3.0 [illegible]
1.33
1.86
27
1.0
65
6
1.2 110
1.6 270
2.0 500
3.0 1800
4.0 4100
5.0 8500
1.55
1.97
37.5
1.0
50
6
1.2 100
1.5 200
2.0 380
3.0 1500
4.0 [illegible]
5.0 [illegible]
[illegible]
[illegible]
4[illegible].2
1.1
45
1.5 110
2.0 250
3.0 850
4.0 2000
5.0 4000
6.0 7000
***Z
```